

**CHEMICALLY MODIFIED GLASSY CARBON ELECTRODE AS  
SENSORS FOR VARIOUS PHARMACEUTICALS**

*Thesis submitted to  
Cochin University of Science and Technology  
in partial fulfilment of the requirements for  
the award of the degree of  
Doctor of Philosophy  
in  
Chemistry*

*by*

**LEENA R**



**Department of Applied Chemistry  
Cochin University of Science and Technology  
Kochi - 682 022**

**October 2012**

**Chemically Modified Glassy Carbon Electrode as Sensors for  
Various Pharmaceuticals**

GI 886

*Ph. D. Thesis under the Faculty of Science*

***Author:***

**LEENA R**

Research Fellow, Department of Applied Chemistry

Cochin University of Science and Technology

Kochi, India 682 022

E mail: leenarajith@gmail.com

***Research Guide:***

**Dr. K. GIRISH KUMAR**

Professor of Analytical Chemistry

Department of Applied Chemistry

Cochin University of Science and Technology

Kochi, India 682 022

Email: giri@cusat.ac.in

Department of Applied Chemistry

Cochin University of Science and Technology

Kochi, India 682 022

October 2012

**DEPARTMENT OF APPLIED CHEMISTRY  
COCHIN UNIVERSITY OF SCIENCE AND TECHNOLOGY  
KOCHI - 682 022, INDIA**



---

**Dr. K. Girish Kumar**  
Professor of Analytical Chemistry

Tel: 0484-2575804  
E-mail: chem@cusat.ac.in

---

Date: 31<sup>st</sup> October 2012

## **Certificate**

Certified that the present work entitled “**Chemically Modified Glassy Carbon Electrode as Sensors for Various Pharmaceuticals**”, submitted by Mrs. Leena R., in partial fulfilment of the requirements for the degree of Doctor of Philosophy in Chemistry to Cochin University of Science and Technology, is an authentic and bonafide record of the original research work carried out by her under my supervision in the Department of Applied Chemistry. Further, the results embodied in this thesis, in full or in part, have not been submitted previously for the award of any other degree.

  
**K. Girish Kumar**  
(Supervising Guide)

## *Declaration*

I hereby declare that the work presented in this thesis entitled “**Chemically Modified Glassy Carbon Electrode as Sensors for Various Pharmaceuticals**” is based on the original work carried out by me under the guidance of Dr. K. Girish Kumar, Professor of Analytical Chemistry, Department of Applied Chemistry, Cochin University of Science and Technology and has not been included in any other thesis submitted previously for the award of any degree.

Kochi-22  
31<sup>st</sup> October 2012

  
**Leena R.**

# Acknowledgements

---

*This thesis is the culmination of more than five years of research during the course of which, I have received help, support and encouragement from many teachers, friends, well wishers and my family. It is a divine pleasure to render a special mention of those who have rendered help in fructifying my research work to its expected goals.*

*First and foremost my sincere thanks and reverence to my guide Dr. K. Girish Kumar, Professor of Analytical Chemistry, Department of Applied Chemistry, Cochin University of Science and Technology for having rendered an opportunity to carry out research under his esteemed guidance. Through out the course of the research he has been an avid inspirer and motivator. I am indebted to him for his faith in me and without his constructive criticism I would not have been able to achieve this goal.*

*My profound gratitude and thanks to Dr. K. Sreekumar, Head of the Department and the doctoral committee member for his continuous help and encouragement to pursue my research. I am also indebted to the support and help of all the teachers of the department who with their keen insight and acumen has been a consistent source of support for me.*

*The non-teaching staff of the department has always been cooperative and obliging to my requests and I thank them for their support.*

*Dr. Anita I, of Maharajas College, Ernakulam, the latter half of my guide has been extending moral encouragement.*

*My lab mates have been very encouraging and together all of us have worked as a single team to overcome any setback and I sincerely thank these labmates right from my seniors - Dr. Remalakshmy Poduval, Dr. Pearl, Dr. Sareena, Dr. Beena and Dr. Sindhu for their help and encouragement. A special mention of my friends Dr. Renjini, Litha, Theresa, Sobhana Teacher, Ajilesh, Sajitha chichi, Laina, Divya, Soumya, Jesny chechi, Zafna, Rajitha, Anuja, Ajith, Shinu, Sreejith, Sruthi and Meera for their*

*camaraderie, support, help and care. Our friendship had indeed made the lab lively and vibrant. My thanks to the friends from other labs in the department for the help and support rendered.*

*A portion of the work with respect to computational studies was conducted at Indian Institute of Science Education and Research(IISER), Trivandrum under the able guidance of Dr. Ayan Datta and under the companionship of Jissy and I am extremely thankful to them for their patience and endurance to guide me through this work. Also, special thanks to Deepthi, Nijamudheen, Vidya and Priya who have helped me at IISER.*

*It is my pleasure to put in a word of gratitude to the Cochin University of Science and Technology and UGC for the BSR fellowship. My thanks also goes to the Directorate of Extramural Research and Property Rights, DRDO, New Delhi for their funding assistance. I pay my gratitude to Dr. G. Devala Rao, Principal, KVSRCollege of Pharmacy, Vijayawada for providing pure drug samples. Also I thank IIT, Chennai and STIC, CUSAT for the characterization of compounds.*

*The brunt of my research work had to be born by my family. But still all of them have given full support to my endeavor. My father, mother and grand mothers have provided consistent support and encouragement through out my life and they have shown that persistent hard work and respecting the dignity of fellow beings is the road to success. My sister Lisha who also has chosen my path has been a great support to me with her ideas and help.*

*I would like to admire the patient support of my husband Rajith and my daughter Gayatri to pass through the testing times and who without any grim on their face would suffer my absence at home. There are no words to convey my love for them. Rajith has been a true and great supporter and has been instrumental in instilling confidence in me even when he was passing through testing times in the family. These years have not been an easy ride. I truly thank them for sticking by my side, even when I was irritable and depressed. All three of us learned a lot about life and strengthened our commitment and determination to each other. I also have to put in a*

*word of respect to my mother in law who was called to her heavenly abode during the course of my research work.*

*I thank my friends Mini, Vineesh, Sheena, Misha, Ambili and Dhanya for their true friendship and I cherish the wonderful moments I had with them. A special thanks to Mini who has always supported me, guided me in the right path and has given valuable suggestions in the crucial stages of life.*

*Jessy Madam, Antony sir and Kumari madam of Rubber Research Institute of India had given their full support and encouragement during the final stages of the thesis work. I extend my heartfelt gratitude to them. My sincere thanks to Binoop Kumar of Indu Photos for the compilation of the thesis.*

*Before concluding I would wish to bow in reverence before all the teachers who taught me both in school and college, who have nurtured my talents and who inspired me.*

*My sincere thanks go to all other individuals who have supported me in these years of research. Anybody left out is not deliberate.*

*My acknowledgments end with a prayer to the almighty who has showered his blessings on me in completing the research with out any major hiccup.*

*Leena R*

## *Preface*

Voltammetric methods are applicable for the determination of a wide variety of both organic and inorganic species. Its features are compact equipment, simple sample preparation, short analysis time, high accuracy and sensitivity. Voltammetry is especially suitable for laboratories in which only a few parameters have to be monitored with a moderate sample throughput. Of various electrode materials, glassy carbon electrode is particularly useful because of its high electrical conductivity, impermeability to gases, high chemical resistance, reasonable mechanical and dimensional stability and widest potential range of all carbonaceous electrodes. Electrode modification is a vigorous research area by which the electrochemical determination of various analyte species is facilitated. The scope of pharmaceutical analysis includes the analytical investigation of pure drug, drug formulations, impurities and degradation products of drugs, biological samples containing the drugs and their metabolites with the aim of obtaining data that can contribute to the maximal efficacy and maximal safety of drug therapy.

This thesis presents the modification of glassy carbon electrode using metalloporphyrin and dyes and subsequently using these modified electrodes for the determination of various pharmaceuticals. The thesis consists of 9 chapters.

Chapter 1 outlines a general introduction of electrochemistry and electroanalytical techniques, especially voltammetry. Various types of electrodes, in particular glassy carbon electrode and the need for modification of electrodes are discussed. The chapter also includes literature review based on modification of electrode using metalloporphyrin and dyes.

Chapter 2 is devoted to the description of reagents used, cleaning of glassy carbon electrode and preparation of various buffer solutions. Instruments used in the work are also discussed.

Chapter 3 deals with the voltammetric determination of trimethoprim (TMP) using metalloporphyrin modified glassy carbon electrode. [5,10,15,20-tetrakis (4-methoxyphenyl)porphyrinato]manganese(III)chloride (TMOPPMn(III)Cl) was synthesised and used for the modification of glassy carbon electrode. Electrochemical parameters were optimised. The method is applied for the determination of TMP in urine sample.

Chapter 4 focuses on TMOPPMn(III)Cl modified glassy carbon electrode (TMOPPMn(III)Cl/GCE) for the determination of ambroxol (AMX). The electrocatalytic nature of TMOPPMn(III)Cl/GCE for the determination of AMX is evident from the favorable reduction in oxidation overpotential of AMX. The optimized conditions for the determination of AMX were probed for. The developed sensor was used for the determination of AMX in human urine and pharmaceutical product.

Chapter 5 deals with the fabrication of poly(malachite green) modified glassy carbon electrode (PMG/GCE) and determination of sulfamethoxazole (SMX). Optimisation of various electrochemical parameters for the determination of SMX was carried out. Determination of SMX in commercial sample and spiked urine samples were carried out.

Chapter 6 describes the voltammetric determination of domperidone (DOM) on poly(methyl red) modified glassy carbon electrode (PMRE/GCE). Different voltammetric studies were carried out for the determination of DOM in pure form. Analysis of DOM in pharmaceutical formulations and spiked urine sample were performed.

Chapter 7 discusses the voltammetric determination of tinidazole (TNZ) on poly(eriochrome black T) modified glassy carbon electrode (PEBT/GCE). Electroreduction of TNZ on PEBT/GCE was studied and the method was used for the determination of TNZ in pharmaceutical formulation and urine sample.

Chapter 8 deals with the quantum mechanical calculations which explain the role of manganese porphyrin in the easy oxidation of trimethoprim. Atoms in molecules analysis and natural bond analysis were carried out. The facile oxidation of trimethoprim in the presence of TMOPPMn(III)Cl is attributed to the interaction between the metal ion and deprotonated trimethoprim, which assists the transfer of electron and hence catalyses the reaction.

Chapter 9 gives the summary of the work done and future outlook. References are given as separate section.

# Contents

## Chapter 1

### INTRODUCTION ..... 01 - 45

|             |   |    |
|-------------|---|----|
| 1.1         | Electrodics   | 01 |
| 1.2         | Electroanalytical techniques  | 04 |
| 1.2.1       | Electrogravimetry   | 05 |
| 1.2.2       | Coulometry  | 05 |
| 1.2.3       | Potentiometry   | 05 |
| 1.2.4       | Voltammetry   | 06 |
| 1.2.4.1     | Modes of mass transfer in voltammetry   | 08 |
| 1.2.4.1.1   | Migration   | 09 |
| 1.2.4.1.2   | Convection  | 09 |
| 1.2.4.1.3   | Diffusion   | 10 |
| 1.2.4.2     | Voltammetric cell set up  | 11 |
| 1.2.4.3     | Working electrodes  | 12 |
| 1.2.4.3.1   | Dropping Mercury Electrode (DME)  | 12 |
| 1.2.4.3.2   | Solid electrodes  | 12 |
| 1.2.4.3.3   | Glassy carbon electrode (GCE)   | 13 |
| 1.2.4.4     | Reference electrodes  | 14 |
| 1.2.4.5     | Auxiliary electrode   | 15 |
| 1.2.4.6     | Various voltammetric techniques   | 15 |
| 1.2.4.6.1   | Cyclic Voltammetry (CV)   | 16 |
| 1.2.4.6.2   | Linear Sweep Voltammetry (LSV)  | 17 |
| 1.2.4.6.3   | Step and pulse techniques   | 18 |
| 1.2.4.6.3.1 | Normal Pulse Voltammetry (NPV)  | 18 |
| 1.2.4.6.3.2 | Differential Pulse Voltammetry (DPV)  | 19 |
| 1.2.4.6.3.3 | Square Wave Voltammetry (SWV)   | 19 |
| 1.2.4.6.4   | Stripping methods   | 20 |
| 1.3         | Sensors   | 21 |
| 1.4         | Modified electrodes   | 22 |
| 1.4.1       | Metalloporphyrin  | 25 |
| 1.4.2       | Conducting polymers   | 26 |
| 1.5         | A brief overview of the reported works on metalloporphyrin and dye modified electrodes for the voltammetric /amperometric determination of pharmaceutical compounds | 28 |
| 1.6         | Scope of the present investigation  | 42 |

## Chapter 2

### MATERIALS AND METHODS..... 47 - 51

|     |                  |    |
|-----|------------------|----|
| 2.1 | Reagents         | 47 |
| 2.2 | Instruments used | 48 |

|       |   |    |
|-------|---|----|
| 2.3   | Cleaning of glassy carbon electrode-----                          | 48 |
| 2.4   | Preparation of buffer solutions -----                             | 49 |
| 2.4.1 | Preparation of Phosphate Buffer Solution (PBS) of various pH----- | 49 |
| 2.4.2 | Preparation of Acetate Buffer Solution (ABS) of various pH-----   | 49 |
| 2.4.3 | Preparation of Citrate Buffer Solution (CBS) of various pH-----   | 49 |

### *Chapter 3*

## **METALLOPORPHYRIN MODIFIED ELECTRODE FOR THE VOLTAMMETRIC DETERMINATION OF TRIMETHOPRIM ..... 53 - 71**

|         |   |    |
|---------|---|----|
| 3.1     | Introduction-----   | 53 |
| 3.2     | Experimental-----   | 54 |
| 3.2.1   | Synthesis of 5,10,15,20-tetrakis(4-methoxyphenyl) porphyrin(TMOPP)-----                                       | 54 |
| 3.2.2   | Synthesis of [5,10,15,20-tetrakis(4-methoxyphenyl) porphyrinato] manganese(III)chloride (TMOPPMn(III)Cl)----- | 55 |
| 3.2.3   | Preparation of TMOPPMn(III)Cl modified glassy carbon electrode -----  | 56 |
| 3.2.4   | Preparation of analyte sample-----  | 56 |
| 3.2.5   | Analysis of sample-----   | 56 |
| 3.3     | Results and Discussion-----   | 57 |
| 3.3.1   | Surface studies of TMOPPMn(III)Cl/GCE-----  | 57 |
| 3.3.2   | Investigation of the electrochemical activity of TMOPPMn(III)Cl/GCE -----                                     | 58 |
| 3.3.3   | Electrochemical behaviour of TMP and the optimization of the developed method-----                            | 58 |
| 3.3.3.1 | Comparison of the electrochemical behaviour of TMP at bare GCE and TMOPPMn(III)Cl/GCE-----                    | 58 |
| 3.3.3.2 | Effect of various supporting electrolyte -----  | 59 |
| 3.3.3.3 | Effect of pH of the medium -----  | 59 |
| 3.3.3.4 | Effect of the volume of TMOPPMn(III)Cl solution drop casted on GCE-----                                       | 59 |
| 3.3.3.5 | Effect of accumulation of TMP-----  | 60 |
| 3.3.3.6 | Effect of scan rate and nature of electrochemical process -----   | 60 |
| 3.3.3.7 | Investigation of the possible mechanistic pathway for the electrooxidation of TMP-----                        | 60 |
| 3.3.3.8 | Estimation of limit of detection of TMP-----  | 61 |
| 3.3.3.9 | Reproducibility and stability of TMOPPMn(III)Cl /GCE -----  | 62 |
| 3.3.4   | Influence of foreign species on the oxidation of TMP-----   | 62 |

|  |    |
|--|----|
| 3.3.5 Application of the developed method in urine sample----- | 62 |
| 3.3.6 Comparison with the reported works-----                  | 63 |
| 3.4 Conclusions -----  | 63 |

**Chapter 4**

**METALLOPORPHYRIN MODIFIED ELECTRODE FOR THE VOLTAMMETRIC DETERMINATION OF AMBROXOL..... 73 - 88**

|  |    |
|--|----|
| 4.1 Introduction-----  | 73 |
| 4.2 Experimental-----  | 75 |
| 4.2.1 Fabrication of TMOPPMn(III)Cl modified GCE (TMOPPMn(III) Cl /GCE) -----                                | 75 |
| 4.2.2 Preparation of analyte sample -----  | 75 |
| 4.2.3 Electrochemical measurements of AMX -----  | 75 |
| 4.3 Results and discussion-----  | 76 |
| 4.3.1 Electrocatalytic oxidation of AMX on TMOPPMn (III)Cl/GCE and optimization of the developed method----- | 76 |
| 4.3.1.1 Comparison of the electrochemical behaviour of AMX at bare GCE and TMOPPMn(III)Cl/GCE-----           | 76 |
| 4.3.1.2 Influence of various supporting electrolyte-----   | 76 |
| 4.3.1.3 Effect of pH of the medium -----   | 77 |
| 4.3.1.4 Effect of volume of TMOPPMn(III)Cl solution dropped on GCE-----                                      | 77 |
| 4.3.1.5 Effect of preconcentration of AMX-----   | 77 |
| 4.3.1.6 Effect of scan rate on the oxidation of AMX -----  | 77 |
| 4.3.1.7 Investigation of the possible mechanistic pathway for the electrooxidation of AMX-----               | 78 |
| 4.3.1.8 Quantification of AMX-----   | 78 |
| 4.3.1.9 Reproducibility and stability-----   | 79 |
| 4.3.2 Selectivity -----  | 79 |
| 4.3.3 Application potential of the sensor -----  | 79 |
| 4.3.4 Comparison with the reported works-----  | 80 |
| 4.4 Conclusions-----   | 80 |

**Chapter 5**

**POLY(MALACHITE GREEN) MODIFIED GLASSY CARBON ELECTRODE FOR THE VOLTAMMETRIC DETERMINATION OF SULFAMETHOXAZOLE..... 89 - 107**

|                       |    |
|-----------------------|----|
| 5.1 Introduction----- | 89 |
|-----------------------|----|

|         |  |    |
|---------|--|----|
| 5.2     | Experimental-----  | 91 |
| 5.2.1   | Fabrication of poly(malachite green) modified glassy carbon electrode (PMG/GCE)----- | 91 |
| 5.2.2   | Preparation of analyte sample-----   | 91 |
| 5.2.3   | Voltammetric measurements of SMX-----  | 92 |
| 5.3     | Results and Discussion-----  | 92 |
| 5.3.1   | Surface studies of PMG/GCE-----  | 92 |
| 5.3.2   | Investigation of the electrochemical activity of PMG/GCE-----                        | 93 |
| 5.3.3   | Electrochemical behavior of SMX and optimization of the developed method-----        | 93 |
| 5.3.3.1 | Comparison of the electrochemical behavior of SMX at bare GCE and PMG/GCE-----       | 93 |
| 5.3.3.2 | Influence of various supporting electrolyte-----                                     | 94 |
| 5.3.3.3 | Effect of pH of the medium-----  | 94 |
| 5.3.3.4 | Effect of accumulation of SMX-----   | 94 |
| 5.3.3.5 | Effect of scan rate-----   | 95 |
| 5.3.3.6 | Probe for the possible mechanism of electrooxidation of SMX-----                     | 95 |
| 5.3.3.7 | Estimation of lower detection limit of SMX-----                                      | 96 |
| 5.3.3.8 | Reproducibility and stability of PMG/GCE-----  | 96 |
| 5.3.4   | Selectivity of PMG/GCE towards SMX-----  | 96 |
| 5.3.5   | Application of the sensor in real samples-----                                       | 97 |
| 5.3.6   | Comparison with the reported works-----  | 97 |
| 5.4     | Conclusions-----   | 98 |

## *Chapter 6*

### **POLY(METHYL RED) MODIFIED GLASSY CARBON ELECTRODE FOR THE VOLTAMMETRIC DETERMINATION OF DOMPERIDONE .....**

**109 - 126**

|       |  |     |
|-------|--|-----|
| 6.1   | Introduction-----  | 109 |
| 6.2   | Experimental-----  | 111 |
| 6.2.1 | Fabrication of poly(methyl red) modified glassy carbon electrode (PMRE/GCE)-----   | 111 |
| 6.2.2 | Preparation of analyte sample-----   | 111 |
| 6.2.3 | Analysis of sample-----  | 111 |
| 6.3   | Results and Discussion-----  | 112 |
| 6.3.1 | Surface studies of PMRE/GCE-----   | 112 |
| 6.3.2 | Investigation of the electrochemical activity of PMRE/GCE-----                     | 112 |
| 6.3.3 | Electrochemical behaviour of DOM and the optimization of the developed method----- | 113 |

|         |   |     |
|---------|---|-----|
| 6.3.3.1 | Comparison of the electrochemical behaviour of DOM at bare GCE and PMRE/GCE       | 113 |
| 6.3.3.2 | Effect of various supporting electrolyte  | 113 |
| 6.3.3.3 | Effect of pH of the medium  | 114 |
| 6.3.3.4 | Effect of accumulation of DOM   | 114 |
| 6.3.3.5 | Effect of scan rate and nature of electrochemical process                         | 114 |
| 6.3.3.6 | Investigation of the possible mechanistic pathway for the electrooxidation of DOM | 114 |
| 6.3.3.7 | Estimation of limit of detection of DOM   | 115 |
| 6.3.3.8 | Reproducibility and stability of PMRE/GCE   | 115 |
| 6.3.4   | Influence of foreign species on the oxidation of DOM                              | 115 |
| 6.3.5   | Application of the developed method   | 116 |
| 6.3.6   | Comparison with the reported works  | 116 |
| 6.4     | Conclusions   | 116 |

## *Chapter 7*

### **POLY (ERIOCHROME BLACK T) MODIFIED ELECTRODE FOR THE VOLTAMMETRIC DETERMINATION OF TINIDAZOLE.....127 - 145**

|         |  |     |
|---------|--|-----|
| 7.1     | Introduction   | 127 |
| 7.2     | Experimental   | 128 |
| 7.2.1   | Fabrication of poly(eriochrome black T) modified glassy carbon electrode (PEBT/GCE)    | 128 |
| 7.2.2   | Preparation of analyte sample  | 129 |
| 7.2.3   | Electrochemical measurements of TNZ  | 129 |
| 7.3     | Results and discussion   | 129 |
| 7.3.1   | Surface studies of PEBT/GCE  | 129 |
| 7.3.2   | Investigation of the electrochemical activity of PEBT/GCE                              | 130 |
| 7.3.3   | Electrocatalytic reduction of TNZ on PEBT/GCE and optimization of the developed method | 130 |
| 7.3.3.1 | Comparison of the electrochemical behaviour of TNZ at bare GCE and PEBT/GCE            | 130 |
| 7.3.3.2 | Influence of various supporting electrolyte  | 131 |
| 7.3.3.3 | Effect of pH of the medium   | 131 |
| 7.3.3.4 | Effect of preconcentration of TNZ  | 132 |
| 7.3.3.5 | Effect of scan rate on the reduction of TNZ  | 132 |
| 7.3.3.6 | Investigation of the possible mechanistic pathway for the electroreduction of TNZ      | 132 |
| 7.3.3.7 | Quantification of TNZ  | 133 |
| 7.3.3.8 | Reproducibility and stability  | 133 |
| 7.3.4   | Selectivity  | 133 |
| 7.3.5   | Application potential of the sensor  | 134 |
| 7.3.6   | Comparison with the reported works   | 134 |
| 7.4     | Conclusions  | 135 |

*Chapter 8*

**COMPUTATIONAL STUDIES OF THE ELECTROOXIDATION OF TRIMETHOPRIM ..... 147 - 164**

- 8.1 Introduction-----147
  - 8.1.1 Density functional theory ----- 149
- 8.2 Computational method -----154
- 8.3 Results and Discussion -----154
- 8.4 Conclusions-----157

*Chapter 9*

**CONCLUSIONS.....165 - 167**

- 9.1 Objectives of the work----- 165
- 9.2 Summary of the work done ----- 166
- 9.3 Future outlook ----- 166

**REFERENCES..... 169 - 185**

**LIST OF PUBLICATIONS ..... 187 - 188**

- RESEARCH PAPERS PUBLISHED IN INTERNATIONAL JOURNALS ..... 187**
- PAPERS PRESENTED IN NATIONAL/ INTERNATIONAL CONFERENCES..... 188**

## *List of Tables*

|            |   |     |
|------------|---|-----|
| Table 2.1. | Preparation of PBS of different pH-----   | 50  |
| Table 2.2. | Preparation of ABS of different pH -----  | 50  |
| Table 2.3. | Preparation of CBS of different pH -----  | 51  |
| Table 3.1. | Influence of $1 \times 10^{-1}$ M of foreign species on the oxidation peak<br>current of $10^{-3}$ M TMP -----  | 64  |
| Table 3.2. | Determination of TMP in urine sample-----   | 64  |
| Table 3.3. | Comparison of the developed method with other reported<br>works for the determination of TMP-----   | 64  |
| Table 4.1. | Influence of $10^{-1}$ M of foreign species on the anodic peak<br>current of $10^{-3}$ M AMX -----  | 81  |
| Table 4.2. | Determination of AMX in tablet-----   | 81  |
| Table 4.3. | Determination of AMX in urine sample -----  | 81  |
| Table 4.4. | Comparison of the developed method with other reported<br>works for the determination of AMX -----  | 82  |
| Table 5.1. | Influence of $10^{-1}$ M of foreign species on the anodic peak<br>current of $10^{-3}$ M SMX-----   | 99  |
| Table 5.2. | Determination of SMX in tablet -----  | 99  |
| Table 5.3. | Determination of SMX in urine sample -----  | 99  |
| Table 5.4. | Comparison of the present work with some of the reported<br>works -----   | 100 |
| Table 6.1. | Influence of $10^{-1}$ M of foreign species on the anodic peak<br>current of $10^{-3}$ M DOM -----  | 118 |
| Table 6.2. | Determination of DOM in commercial formulation -----  | 118 |
| Table 6.3. | Determination of DOM in urine sample -----  | 118 |
| Table 6.4. | Comparison of the present work with some of the reported works-----   | 119 |
| Table 7.1. | Influence of $10^{-1}$ M of foreign species on the cathodic peak<br>current of $10^{-3}$ M TNZ-----   | 136 |
| Table 7.2. | Determination of TNZ in commercial formulation -----  | 136 |
| Table 7.3. | Determination of TNZ in urine sample -----  | 136 |
| Table 7.4. | Comparison of the developed method with other reported<br>works for the determination of TNZ -----  | 137 |
| Table 8.1. | Selected bond lengths of [Mn(III)porphyrin]Cl $\cdots$ trimethoprim<br>and [Mn(III)porphyrin]Cl $\cdots$ trimethoprim anion computed at<br>B3LYP/6-31+G(d), CEP-31G level of theory ----- | 158 |

## List of Figures

|  |    |
|--|----|
| Figure 3.1. Structure of TMP -----   | 65 |
| Figure 3.2. Structure of TMOPPMn(III)Cl-----   | 65 |
| Figure 3.3. SEM images of a) bare GCE and b) TMOPPMn(III)Cl/GCE-----   | 66 |
| Figure 3.4. Differential pulse voltammogram of $1 \times 10^{-3}$ TMP at (a) bare GCE (b) TMOPPMn(III)Cl/GCE -----   | 66 |
| Figure 3.5. Relationship between anodic peak current and pH of the medium-----   | 67 |
| Figure 3.6. Relationship between anodic peak current and volume of the modifier -----  | 67 |
| Figure 3.7. Effect of accumulation time of TMP on the anodic peak current -----  | 68 |
| Figure 3.8. Differential pulse voltammograms of $10^{-6}$ M TMP at scan rates 20, 30, 40, 50, 60, 70, 80 $\text{mVs}^{-1}$ -----                                 | 68 |
| Figure 3.9. Variance of anodic peak current of TMP with scan rate in the range 20 $\text{mVs}^{-1}$ – 60 $\text{mVs}^{-1}$ -----                                 | 69 |
| Figure 3.10. Plot of $\ln$ scan rate versus anodic potential-----  | 69 |
| Figure 3.11. Differential pulse voltammograms of oxidation of TMP of concentrations $10^{-3}$ , $10^{-4}$ , $10^{-5}$ , $10^{-6}$ , $10^{-7}$ , $10^{-8}$ M----- | 70 |
| Figure 3.12. Dependence of peak current on the concentrations of TMP in the range $6 \times 10^{-8}$ - $1 \times 10^{-6}$ M -----                                | 70 |
| Figure 4.1. Structure of AMX-----  | 83 |
| Figure 4.2. Differential pulse voltammograms of the oxidation of $10^{-3}$ M AMX at a) bare GCE b) TMOPPMn(III)Cl/GCE -----                                      | 83 |
| Figure 4.3. Differential pulse voltammograms of the oxidation of $10^{-3}$ M of (a) TMP and (b)AMX at TMOPPMn(III)Cl/GCE-----                                    | 84 |
| Figure 4.4. Variation of anodic peak current with pH of the medium-----  | 84 |
| Figure 4.5. Relationship between anodic peak current and volume of the modifier -----  | 85 |
| Figure 4.6. Effect of accumulation time of AMX on the anodic peak current -----  | 85 |
| Figure 4.7. Plot of square root of scan rate versus anodic peak current of $10^{-3}$ M AMX -----   | 86 |

|   |     |
|---|-----|
| Figure 4.8. Variation of ln scan rate versus anodic potential-----  | 86  |
| Figure 4.9. Differential pulse voltammograms of the oxidation of $10^{-3}$ , $10^{-4}$ ,<br>$10^{-5}$ , $10^{-6}$ , $10^{-7}$ , $10^{-8}$ M AMX -----   | 87  |
| Figure 4.10. Nature of dependence of anodic peak current with concentration<br>in the range $3 \times 10^{-8}$ M - $3 \times 10^{-7}$ M-----  | 87  |
| Figure 5.1. Structure of malachite green -----  | 101 |
| Figure 5.2. Structure of SMX -----  | 101 |
| Figure 5.3. Cyclic voltammograms of polymerisation of malachite green<br>on GCE at a scan rate of $100 \text{ mVs}^{-1}$ -----  | 102 |
| Figure 5.4. SEM images of (a) bare GCE at $500 \times$ magnification (b)<br>PMG/GCE at $500 \times$ magnification (c) PMG/GCE at $20000 \times$<br>magnification -----  | 103 |
| Figure 5.5. Square wave voltammograms of electrochemical oxidation of<br>$1 \times 10^{-3}$ M SMX on (a) bare GCE and (b) PMG/GCE-----  | 104 |
| Figure 5.6. Variation of anodic peak current with pH-----   | 104 |
| Figure. 5.7. Effect of accumulation time of SMX on the anodic peak current-----   | 105 |
| Figure 5.8. Variation of the anodic peak current of SMX as a function of<br>square root of scan rate-----   | 105 |
| Figure 5.9. Variation of ln scan rate versus anodic potential-----  | 106 |
| Figure 5.10. Dependence of concentration of SMX on peak current -----   | 106 |
| Figure 6.1. Structure of Domperidone-----   | 120 |
| Figure 6.2. Structure of methyl red-----  | 120 |
| Figure 6.3. Cyclic voltammograms of polymerisation of methyl red on<br>GCE at a scan rate of $100 \text{ mVs}^{-1}$ -----   | 121 |
| Figure 6.4. SEM images of (a) bare GCE at $500 \times$ magnification (b)<br>PMRE/GCE at $500 \times$ magnification (c) PMRE/GCE at $1000 \times$<br>magnification (d) PMRE/GCE at $3000 \times$ magnification ----- | 122 |
| Figure 6.5. Square wave voltammograms of electrochemical oxidation of<br>$1 \times 10^{-3}$ M DOM on (a) bare GCE and (b) PMRE/GCE -----  | 123 |
| Figure 6.6. Variation of anodic peak current with pH-----   | 123 |
| Figure 6.7. Effect of accumulation time of DOM on the anodic peak<br>current-----   | 124 |
| Figure 6.8. Linear sweep voltammograms of $10^{-3}$ M DOM at scan rates 20,<br>30, 40, 50, 60, 70, 80, 90, $100 \text{ mVs}^{-1}$ -----   | 124 |

|  |     |
|--|-----|
| Figure 6.9. Variation of the anodic peak current of DOM as a function of square root of scan rate-----   | 125 |
| Figure 6.10. Variation of ln scan rate versus anodic potential-----  | 125 |
| Figure 6.11. Square wave voltammograms of concentrations $10^{-3}$ , $10^{-4}$ , $10^{-5}$ , $10^{-6}$ , $10^{-7}$ M of DOM-----   | 126 |
| Figure 6.12. Dependence of concentration of DOM on peak current-----   | 126 |
| Figure 7.1. Structure of TNZ-----  | 138 |
| Figure 7.2. Structure of EBT-----  | 138 |
| Figure 7.3. Cyclic voltammograms of polymerisation of eriochrome black T on GCE at a scan rate of $100 \text{ mVs}^{-1}$ -----   | 139 |
| Figure 7.4. SEM images of (a) bare GCE at $500\times$ magnification (b) PEBT/GCE at $500\times$ magnification (c) PEBT/GCE at $1000\times$ magnification (d) PEBT/GCE at $3000\times$ magnification----- | 140 |
| Figure 7.5. Differential pulse voltammograms of the reduction of $10^{-3}$ M TNZ at a) bare GCE b) PEBT/GCE-----   | 141 |
| Figure 7.6. Plot of pH versus potential-----   | 141 |
| Figure 7.7. Plot of pH versus current-----   | 142 |
| Figure 7.8. Relationship between cathodic peak current and accumulation time-----  | 142 |
| Figure 7.9. Linear sweep voltammograms of $10^{-3}$ M of TNZ at scan rates 20, 30, 40, 50, 60, 70, 80 $\text{mVs}^{-1}$ -----  | 143 |
| Figure 7.10. Variance of cathodic peak current of $10^{-3}$ M of TNZ with square root of scan rate-----  | 143 |
| Figure 7.11. Plot of ln scan rate versus cathodic potential-----   | 144 |
| Figure 7.12. Differential pulse voltammograms of reduction of TNZ of concentrations $10^{-3}$ , $10^{-4}$ , $10^{-5}$ , $10^{-6}$ , $10^{-7}$ , $10^{-8}$ M-----   | 144 |
| Figure 7.13. Dependence of peak current on the concentrations of TNZ in the range $1\times 10^{-8}$ - $8\times 10^{-7}$ M-----   | 145 |
| Figure 8.1. Variation of anodic peak potential of $10^{-3}$ M of Trimethoprim with pH-----   | 159 |
| Figure 8.2. Optimised structure of Trimethoprim-----   | 159 |
| Figure 8.3. Deprotonation of Trimethoprim-----   | 160 |
| Figure 8.4. Optimised structure of $[\text{Mn(III)porphyrin}]\text{Cl}$ -----  | 160 |
| Figure 8.5. Deprotonation in $[\text{Mn(III)porphyrin}]\text{Cl}\dots$ trimethoprim-----   | 161 |

Figure 8.6. HOMO-LUMO of (A) [Mn(II)porphyrin]Cl···trimethoprim  
and (B) [Mn(III)porphyrin]Cl···trimethoprim anion ----- 162

Figure 8.7. Plots of the gradient of charge density in (A) [Mn(III)porphyrin]  
Cl···trimethoprim and (B) [Mn(II)porphyrin]Cl···trimethoprim  
anion----- 163

## ***List of Schemes***

|  |     |
|--|-----|
| Scheme 3.1. Mechanism of oxidation of TMP -----                      | 71  |
| Scheme 4.1. Suggested Mechanism of electrooxidation of AMX -----     | 88  |
| Scheme 5.1. Probable mechanism for the electrooxidation of SMX ----- | 107 |
| Scheme 7.1. Mechanism of electroreduction of TNZ-----                | 145 |
| Scheme 8.1. Detailed mechanism of oxidation of TMP-----              | 164 |

.....*SC*.....

## INTRODUCTION

- 1.1. *Electrodeics*
- 1.2. *Electroanalytical techniques*
- 1.3. *Sensors*
- 1.4. *Modified electrodes*
- 1.5. *A brief overview of the reported works on metalloporphyrin and dye modified electrodes for the voltammetric/amperometric determination of pharmaceutical compounds*
- 1.6. *Scope of the present investigation*

Electrochemistry is an offshoot of a synthesis between biochemistry and electricity and is conceived as an essential discipline among the chemical sciences needed to equip society for the near future. The two main types of electrochemistry are ionics, which deals with the physical chemistry of ionically conducting solution and electrodeics, which deals with the physical chemistry of electrically charged interfaces. While ionics concerns with ion-solvent interactions, ion-ion interactions, ion transport in solution, electrodeics concerns with the region between an electronic and an ionic conductor and the transfer of electric charge across it.<sup>1</sup>

### 1.1 Electrodeics

When an electronically conducting surface is in contact with a solution and a stream of electrons is passed into the electronic conductor, randomly moving ions in the solution get caught up in the gradient of concentration thus created and this gradient acts on the ions forcing them onward towards the electrode. The ion and its hydration sheath are aligned against the electrode,

separated from it by only a single water layer. There exists a special property of the region between an electrode in contact with a solution and the layer of ions that collide with it in their wandering and stay there awhile. This property is the strong electric field of about  $10^9 \text{ Vm}^{-1}$  between the electrode and the layer and extends only 0.5 nm into the solution.<sup>2</sup>

Two types of processes occur at electrodes. One kind comprises of transfer of charges across the electrode solution interface. This electron transfer causes oxidation or reduction to occur. Since these reactions are governed by Faraday's law, they are called Faradaic processes. Under certain conditions, a given electrode-solution interface will show a range of potentials where no charge transfer reactions occur because such reactions are thermodynamically or kinetically unfavourable. But adsorption and desorption processes can occur and the structure of electrode solution interface can change with changing potential or solution composition. These processes are called non faradaic processes. Although charge does not cross the interface under these conditions, external currents can flow when the potential, electrode area or solution composition changes. Both Faradaic and non Faradaic processes occur when electrode reaction takes place. Faradaic processes are of primary interest in the investigation of an electrode reaction, whereas the effects of non Faradaic processes must be taken into account in using the electrochemical data to obtain information about charge transfer and associated reactions.

The whole array of charged species and oriented dipoles existing at the metal solution interface is called the electrical double layer. At a given potential, the electrode solution interface is characterized by a double layer capacitance,  $C_d$  typically in the range of 10 to 40  $\mu\text{Fcm}^{-2}$ . Unlike real capacitors whose capacitances are independent of the voltage across them,  $C_d$  is often a function of potential. The solution side of the double layer is thought

to be made up of several layers. The layer closest to the electrode, the inner layer called the Helmholtz or Stern layer contains solvent molecules and sometimes other species that are specifically adsorbed. The locus of the electrical centres of the specifically adsorbed ions is called the inner Helmholtz plane (IHP) which is at a distance of  $x_1$ . Solvated ions can only approach the electrode to a distance  $x_2$ . The locus of centres of these nearest solvated ions is called the outer Helmholtz plane (OHP). The interaction of the solvated ions with the charged electrode involves only long range electrostatic forces, so that their interaction is independent of the chemical properties of the ions. These ions are said to be nonspecifically adsorbed. The nonspecifically adsorbed ions are distributed in a three dimensional region called the diffuse layer, which extends from the OHP into the bulk of the solution. The thickness of the diffuse layer depends on the total ionic concentration in the solution. For concentration greater than  $10^{-2}$  M, the thickness is less than  $300 \text{ \AA}$ .

The structure of the double layer can affect the rates of electrode processes. The existence of the double layer capacitance or the presence of a charging current can seldom be neglected in electrochemical experiments. During electrode reactions involving very low concentrations of electroactive species, the charging current can be much larger than the faradaic current for the reduction or oxidation reaction.<sup>3</sup>

Information about an electrode reaction is often gathered by determining current as a function of potential. The departure of the electrode potential from the reversible value upon passage of faradaic current is termed polarization. Ideal polarized electrode shows a very large change in potential upon the passage of an infinitesimal current. A substance that tends to cause the potential of an electrode to be nearer to its equilibrium value by virtue of it being oxidized or reduced is called a depolarizer. An ideal non polarizable

electrode is an electrode of fixed potential whose potential does not change upon passage of current. The extent of polarization is measured by overpotential,  $\eta$ , which is the deviation of the potential from the equilibrium value.

$$\eta = E - E_{eq}$$

The simplest electrode reactions are those in which the kinetics of all electron transfer and associated chemical reactions are very rapid compared to those of the mass transfer processes.

In order to avoid the difficulty arising due to the effect of impurity adsorption onto the electrode from the solution that ruin the reproducibility of the measurements, the idea of making electrode kinetic measurements at short times called transients was introduced by Bowden and Rideal in 1928. Their aim was less to overcome undesired surface changes and more to make use of certain properties of potential-time transients to measure the real surface area of the electrode. Transient techniques can be classified into two – galvanostatic and potentiostatic in which current or potential, respectively, is kept constant during the observed variation of the other.<sup>2</sup>

## 1.2 Electroanalytical techniques

Electroanalysis can be ascribed as the science of carrying out analytical chemistry by the use of electrochemistry.<sup>4</sup> Direct electroanalytical techniques can determine an ion/molecule by direct measurements. There are essentially four types of direct electroanalytical measurements that can be performed:

- a) Electrogravimetry
- b) Coulometry
- c) Potentiometry
- d) Voltammetry/Amperometry

### **1.2.1 Electrogravimetry**

In this type of analytical measurements, the analyte element is weighed after it has been electrolytically deposited upon a suitable electrode. Electrodeposition is governed by Ohm's law and by Faraday's two laws of electrolysis. Electrogravimetric procedures require the use of carefully controlled experimental conditions to deposit an element electrolytically upon a suitable electrode. Electrogravimetry is carried out in an electrolytic cell. This consists of two electrodes with an external electrical energy supply. The electrodes are made of platinum gauze as the open construction assists the circulation of the solution.<sup>5</sup>

### **1.2.2 Coulometry**

Coulometric methods of analysis are based on the measurement of quantity of electrical charge that passes through a solution during an electrochemical reaction. It is an application of Faraday's first law of electrolysis as per which the extent of chemical reaction is proportional to the quantity of electricity passed through the electrode. The fundamental requirement of a coulometric analysis is that the electrode reaction used for the determination must proceed with 100% efficiency. Coulometry may be achieved in two ways, viz., with controlled potential of the working electrode and with constant current.<sup>5</sup>

### **1.2.3 Potentiometry**

This is a type of analytical measurement in which the function of the controlling device is primarily to ensure that no significant current is drawn from the cell. In order to obtain meaningful analytical measurements in potentiometry, one of the electrodes should be of constant potential without changing from experiment to experiment. An electrode fulfilling this condition

is called a reference electrode. Because of the invariance of the reference electrode, any change in the cell potential is due to the contribution of the other electrode called the indicator or working electrode. The current path between the two electrodes is highly resistive.<sup>4,6</sup>

### 1.2.4 Voltammetry

Electroanalytical methods that depend on the measurement of current as a function of applied potential are called voltammetric techniques. This method employs conditions that encourage polarization of indicator working electrode. To enhance polarization, working electrodes in voltammetry are relatively small. In amperometry, a fixed potential is applied to the electrode, which causes the species to be determined to react and a current to pass. If this potential is conveniently chosen, then the magnitude of the current is directly proportional to concentration. Historically, the field of voltammetry was developed from polarography, which was invented by Czechoslovakian chemist, Jaroslav Heyrovsky in the early 1920's. Polarography differs from other types of voltammetry in that the working electrode is the unique dropping mercury electrode. Earlier polarography was an important tool used by chemists for the determination of inorganic ions and certain organic species in aqueous solutions. In the late 1950's and in the early 1960's, however many of these analytical applications were replaced by various spectroscopic methods and polarography was considered having a least significance. In the mid 1960's, several major modifications of classical voltammetric techniques were developed that enhanced significantly the sensitivity and selectivity of the method. The result was a resurgence of interest in applying polarographic and voltammetric methods for the determination of a host of species, particularly those of pharmaceutical, environmental and biological interest. Modern voltammetry also continues to be an excellent tool in diverse areas of

chemistry, biochemistry, materials science and engineering and the environmental sciences for studying oxidation, reduction and adsorption processes.<sup>6,7</sup>

Voltammetry is based on the measurement of current under conditions of complete concentration polarization in which the rate of oxidation/reduction of the analyte is limited by the rate of mass transfer of the analyte to the electrode surface. In voltammetry, the current that flows across the electrode-solution interface arises from two sources - one is the Faradaic current which arises from the reduction or oxidation of the species in solution. However, due to double layer that forms at the electrode-solution interface, a significant capacitive current is observed on current-potential plots, which is called the non Faradaic current which forms the second source. The double layer is caused by the electrostatic attraction or repulsion of cations and anions respectively, near the electrode surface to balance the charge on the electrode.<sup>8</sup>

Ronald Gurney was the first physical electrochemist to apply the ideas of quantum mechanics to explain how electrons were emitted from or accepted by electrodes. He related electric currents across the electrode solution interface to the tunneling of electrons through energy barriers formed between the electrode and the ions or molecules in the first layer next to the electrode possessing electronic states. The electrochemical potential can be correlated to the Fermi energy of the electron in solution because, if one expels an electron into a vacuum, the electrons come overwhelmingly, if not entirely from the Fermi level of electrons in the metal electrode. Correspondingly, the concept is that the electrons (carried about in the outermost electron levels of ions) in solution exchange with electronic states in the most available states in the metal electrode, the topmost occupied state called the Fermi level. Because the electrons in solution are in equilibrium with the electrons in the Fermi level of the metal electrode, electrochemists have referred to this as the Fermi energy

of electrons in solution. The electrons in the Fermi level in a metal electrode are those that undergo the Fermi distribution law and are mobile. The electrons in solution are, in fact, in the bound level of ions. The electrochemical potential of the electron corresponds to the energy of the ground state of the electronic ions in the solution concerned. It is simple to vary the energy of electrons in an electrode over wide energy ranges by means of outside electronic circuitry. However electron transfer occurs when the energies of the state of the electrons in the metal electrode overlap with those of the energy of the electronic state in solution. Electronic states in solution must be available over the applied potential range if there is to be electron transfer from electrode to solution or solution to electrode. The number of states available in the solution at each energy level will play a major role in determining the rate of an electrode reaction and how it varies with the electrode potential.<sup>2</sup>

#### 1.2.4.1 Modes of mass transfer in voltammetry

Electron transfer can be limited by the mass transfer of ions to or from the electrode or by the rate of electron transfer at the electrode-solution interface. It is assumed that the rate of electron transfer at the electrode-solution interface is fast compared with the rate of mass transfer. A limiting current results whenever the rate of the electrode reaction is governed by the rate of supply of the electroactive species to the electrode surface by a process whose rate is more or less independent of the electrode potential. There are three general mass transfer processes by which a reacting species may be brought to an electrode surface –

- a) migration of charged ions in an electric field
- b) convection due to motion of the solution of the electrode
- c) diffusion under the influence of a concentration gradient

Hence there are three contributions to the limiting current  $i_{\text{limit}} = i_d + i_c + i_m$  where  $i_d$  is the diffusion current,  $i_c$  is the convection current and  $i_m$  is the migration current.

#### 1.2.4.1.1 Migration

Electrical migration is restricted to ionic substances or dipolar molecules capable of undergoing directed movement in an electrical field. Electrical migration may augment or oppose diffusion depending on whether the electroactive species is a cation or an anion. In voltammetry, the effect of electrical migration can be eliminated by adding supporting electrolyte in a concentration of at least hundred fold greater than the concentration of the substance being determined. The cations of the supporting electrolyte cannot be discharged at the cathode until the impressed potential becomes quite negative. Large number of them remains as a cloud around the electrode. This positively charged cloud restricts the potential gradient to a region close to the electrode surface. In the presence of a supporting electrolyte, the transference number of the electroactive species is decreased practically to zero thus making the potential (IR) gradient through it desirably small. Under this condition, the limiting current in a quiescent solution is controlled entirely by the diffusional rate of the mass transfer.<sup>8</sup>

#### 1.2.4.1.2 Convection

Electroactive species may either be moved by thermal currents or by density gradients and also whenever the solution is stirred into the path of the electrode. These processes can be grouped under the general term convection. If ions are transported toward the electrode surface by mechanical means such as stirring the solution, this will affect the limiting current. Convection can be minimized by using quiescent solutions.<sup>5,8</sup>

### 1.2.4.1.3 Diffusion

The movement of a chemical species under the influence of a gradient of chemical potential, i.e. a concentration gradient, is of paramount concern in voltammetric techniques. Concentration gradients at the electrode surface are dependent on time. In transient or dynamic methods, the system is intentionally disturbed from equilibrium by excitation signals consisting of variable potentials or currents. When either a potential or current is impressed upon the system, the other variable is a function of both the concentration of the electroactive species and time. When the potential reaches a value at which the faradaic process occurs, current flows. The current is the rate at which charge passes through the electrode-solution interface. Current that arises from a faradaic process is a direct measure of the rate of the process and if the rate is proportional to concentration, it is also a measure of the concentration of electroactive species in the bulk solution.<sup>8</sup>

According to Fick's first law, the net rate of diffusion of a species to a unit area of electrode surface  $A$  at any time  $t$  is proportional to the magnitude of the concentration gradient.

$$flux = \frac{-D(c - c_0)}{\delta}$$

where  $\delta$  is the thickness of the hypothetical diffusion layer about the microelectrode. Once the reaction potential has been reached, the concentration of the electro active species of interest changes from the bulk concentration value,  $c$ , observed at positions far removed from the electrode surface, to the concentration,  $c_0$ , at the electrode surface. As  $c_0$  approaches zero, the rate of diffusion becomes proportional to the concentration in the bulk of the solution.

The rate of diffusion of an ion to an electrode surface is given by Fick's second law as

$$\frac{\delta c}{\delta t} = D \frac{\partial^2 c}{\partial x^2}$$

where  $D$  is the diffusion coefficient,  $c$  is the concentration,  $t$  is time and  $x$  is distance from the electrode surface. For classical polarography or voltammetry, using an unstirred solution which contains an excess of supporting electrolyte, both  $i_m$  and  $i_c$  tend to zero and the only mechanism for transporting ions to the electrode surface is the normal diffusion of ions in solution. Thus, in polarography or voltammetry, the limiting current is identical to the diffusion current.<sup>5</sup>

The concentration in the thin diffusion layer is approximately a linear function of distance from the electrode, so that as a first approximation<sup>8</sup>

$$\frac{dc}{dx} = \frac{c - c_0}{\delta}$$

#### 1.2.4.2 Voltammetric cell set up

Voltammetric cell is made up of three electrodes – working, reference and counter or auxiliary, immersed in a solution containing the analyte and also an excess of a non reactive electrolyte called supporting electrolyte. Supporting electrolyte is an inert electrolyte that contributes to the transport of electricity by the solution, but is faradaically inactive. It increases the conductivity of the solution, hence diminishing IR voltage drops. It makes certain that the double layer is established in a reproducible manner, maintains a constant ionic strength and thereby ensures that the activity coefficient of the species under study does not change as the charge transfer reaction proceeds

and it swamps out the migration current. If no supporting electrolyte were present, migration would transport a considerable fraction of the ionic active species across the solution to the electrode. This would change the concentration profiles as defined by diffusion and thus alter the current.<sup>9</sup> If the concentration of the supporting electrolytes is very low, they can form a space charge near the surface and the space charge potential can influence the charge transfer kinetics.

#### 1.2.4.3 Working electrodes

In voltammetry, different working electrodes can be used. The most commonly employed are the following:

##### 1.2.4.3.1 Dropping Mercury Electrode (DME)

In classical polarography the dropping mercury electrode is used as a micro working electrode. The mercury drop is formed at the end of a glass capillary as the capillary is connected by flexible tube to a reservoir about 50 cms in height. The mercury droplets are of highly reproducible diameter and of a life time ranging from 2 to 6 seconds. The advantages of DME include reproducible current potential data due to the constant renewal of the electrode surface that eliminates the contamination of the electrode surface. The charge transfer overvoltage of hydrogen ions present in the aqueous solution is high on Hg, thus its reduction does not disturb the study of the reduction processes of the electroactive species having more negative potential than the reversible potential of the proton discharge.

##### 1.2.4.3.2 Solid electrodes

For the determination of oxidizable components, solid electrodes are generally used. Among the different electrodes, Pt, Au and C, graphite electrodes and glassy carbon electrodes have gained wide application in

analytical voltammetry. Carbon, in many respects, is an ideal electrode substrate. Its attractive features include access to a wide anodic potential range, low electrical resistance and residual currents and a reproducible surface structure. It is morphologically diverse, existing in a variety of forms suitable for electrochemical applications, e.g., carbon fibres, glassy carbon, graphite pastes and composites and carbon films. Carbon electrodes are especially effective at chemisorbing reagents that have extended  $\pi$  bond systems. Carbon paste and glassy carbon electrodes are used to monitor electrooxidation processes both in solution at rest and in the flowing electrolyte.<sup>10-17</sup>

#### 1.2.4.3.3 Glassy carbon electrode (GCE)

Glassy carbon is a solid isotropic material composed of thin convoluting microfibrils that interlock to form strong interfibrillar bonds. It is produced by thermal degradation approximately at a temperature of 1800<sup>0</sup> C of selected organic polymers.<sup>10</sup> It is suitable for use over the potential range from about +1.2 to -0.8 V vs. standard calomel electrode in acid medium. Of various electrode materials, glassy carbon electrode is particularly useful because of its high electrical conductivity, impermeability to gases, high chemical resistance, reasonable mechanical and dimensional stability and widest potential range of all carbonaceous electrodes.<sup>18</sup> The most striking feature of glassy carbon is its extremely low gas permeability compared with that of synthetic graphites, which arises from an extensive closed void network as opposed to the open spaces present in its artificial graphite counterparts, allowing only discontinuous gas permeation of the material. The peculiarities of its surface structure permit analysis in extreme environments, such as organic solvents. Although glassy carbon electrode serves as a very good electrode material, many attempts have been made to improve its electrochemical properties by

chemical modification. The chemical modifications of the electrode open wide opportunities for improving the selectivity and the sensitivity of the electroanalytical determination.<sup>10,19-21</sup>

#### 1.2.4.4 Reference electrodes

An ideal reference electrode has a potential that is known, constant and completely insensitive to the composition of the solution under study. It is also known as the unpolarized electrode. A good reference electrode must be stable with respect to time and temperature. Its potential must not change when the current necessary to make a measurement is passed through it. The potential offered by a standard hydrogen electrode is defined as the fundamental reference electrode. Due to the difficulty in setting up hydrogen electrode, secondary reference electrodes like calomel electrode and Ag/AgCl electrode are often used in place of the standard hydrogen electrode. Calomel reference electrodes consist of mercury in contact with a solution that is saturated with mercury(I) chloride and that also contains a known concentration of KCl. Pt wire connects the electrode to the rest of the circuit. Ag/AgCl electrode consists of an Ag wire that has been made an anode in a chloride containing solution. A thin porous film of AgCl forms on the Ag wire. The wire and its layer are immersed in a standard KCl solution.<sup>2,9</sup>

Calomel electrodes have high temperature coefficient. When the temperature is changed, the potential comes to a new value only slowly because of the time required for solubility equilibrium for the KCl and calomel to be re-established. Ag/AgCl electrodes can be used at temperatures greater than 60°C, whereas calomel electrodes cannot be. Hg(I) ions react with fewer sample components than do silver ions which can react with proteins. These reactions can lead to plugging off the junction between the electrode and analyte solution.<sup>22</sup>

#### 1.2.4.5 Auxiliary electrode

Auxiliary electrodes are often fabricated from electrochemically inert materials such as gold, platinum or carbon. Auxiliary electrode provides a surface for a redox reaction to balance the one occurring at the surface of the working electrode and does not need special care, such as polishing. To support the current generated at the working electrode, the surface area of the auxiliary electrode must be equal to, or larger than, that of the working electrode. During any electrochemical experiment, a redox reaction occurs at the surface of the auxiliary electrode to balance the redox reaction at the surface of the working electrode and the products of this reaction can diffuse to the working electrode and interfere with the redox reaction occurring at that site. However, in electroanalytical experiments such as cyclic voltammetry, the time scale of the experiment is too short for this diffusion to be able to cause significant interference, so there is no need to place the auxiliary electrode in a separate compartment. However, electrosynthetic experiments are typically much longer than electroanalytical experiments, so separation of the auxiliary electrode is required.<sup>22</sup>

#### 1.2.4.6 Various voltammetric techniques

The name electrochemical spectra are given to the results of voltammetric measurements. In electrochemical spectra, one varies the energy of the electronic states in the electrode and the electrons exit, or are received, when their energy or the energy of empty electronic states in the electrode overlaps with the energy of an empty or filled electronic state in an ion or molecule in the layer of the solution next to the electrode. Various voltammetric techniques include cyclic voltammetry, linear sweep voltammetry, step and pulse techniques and stripping voltammetry. Cyclic voltammetry has been applied to the investigation of simple electron transfer reactions; those with

two successive electron transfers and with multiple electron transfers. Derivative voltammogram increases the sharpness of detection of dissolved radicals and molecular fragments.<sup>2, 23</sup>

#### 1.2.4.6.1 Cyclic Voltammetry (CV)

Cyclic voltammetry (CV) is the experiment prelude to all experiments with which electrochemists begin their studies. It is a kind of road map or fingerprint for the experiment, indicating the potential region in which there is electrode activity. In CV the current response of a small stationary electrode in an unstirred solution is excited by a triangular potential wave form. The potential at which reversal of direction of scan takes place is called the switching potential. The range of switching potentials chosen for a given experiment is one in which a diffusion controlled oxidation or reduction of one or more analytes occurs. Important variables in a cyclic voltammogram are the cathodic peak potential  $E_{pc}$ , the anodic peak potential  $E_{pa}$ , the cathodic peak current  $i_{pc}$  and the anodic peak current  $i_{pa}$ . For a reversible electrode reaction, anodic and cathodic peak currents are approximately equal in absolute value but opposite in sign. For a reversible electrode reaction, difference in peak potentials,  $\Delta E_p$  is expected to be

$$\Delta E_p = |E_{pa} - E_{pc}| = 0.0529/n$$

where  $n$  is the number of electrons involved in the half reaction. Irreversibility because of slow electron transfer kinetics results in  $\Delta E_p$  exceeding the expected value.

The primary use of CV is as a tool for fundamental and diagnostic studies that provides qualitative information about electrochemical processes under various conditions. It has become an important tool for the study of

mechanisms and rates of oxidation/reduction processes, particularly, in organic and metallorganic systems. This method is normally the first technique selected for investigation of an electrochemically addressable system. Often CV's will reveal the presence of intermediates in oxidation/reduction reactions.<sup>22,24</sup> But CV also has several limitations. The electronic equipment used for producing the rapidly changing waveform and for recording the resulting time-current waves must be capable of responding fast in order to display the correct waveform. The magnitude of the waves produced depends partially on the concentration of redox species involved and partly on other factors such as scan rate. For accurate quantitative measurements, pulse techniques will normally give more reliable data.<sup>5</sup>

#### 1.2.4.6.2 Linear Sweep Voltammetry (LSV)

Linear sweep voltammetry is a general term applied to any voltammetric method in which the potential applied to the working electrode is varied linearly in time. The potential of the working electrode is ramped from an initial potential  $E_i$  to a final potential  $E_f$ . The value of the scan rate may be varied from as low as 10 mV/sec (typical for polarography experiments) to as high as 1,000,000 V/sec (attainable when ultramicroelectrodes are used as the working electrode). With a linear potential ramp, the faradaic current is found to increase at higher scan rates. This is due to the increased flux of electroactive material at the electrode at the higher scan rates. The amount of increase in the faradaic current is found to scale with the square root of the scan rate. This points to the fact that increasing the scan rate of a linear sweep voltammetric experiment could lead to increased analytical signal to noise. However, the capacitive contribution to the total measured current scales directly with the scan rate. As a result, the signal to noise of a linear sweep voltammetric experiment decreases with increasing scan rate.<sup>4,6,8</sup>

### 1.2.4.6.3 Step and pulse techniques

Many pulse techniques have been devised based on a succession of potential steps of varying height and in forward or reverse directions. The response in a potential step is a pulse of current which dies away with time as the electroactive species near the electrode surface is consumed. Superimposed on this faradaic response is a capacitive contribution due to double layer charging which dies away more quickly, often within 50  $\mu\text{s}$ . In step and pulse techniques the current is usually sampled after the capacitive current has died away. Pulse widths are adjusted to satisfy this condition and the additional condition that time has not been allowed for natural convection effects to influence the response. The first use of potential pulse techniques was at the dropping mercury electrode, synchronising the pulse period with drop time. Since then many applications at solid electrodes and at static mercury drop electrodes have arisen which do not suffer from the difficulties associated with drop growth. Detection limits of these techniques are of the order of  $10^{-7}$  M.<sup>6,8,25</sup>

#### 1.2.4.6.3.1 Normal Pulse Voltammetry (NPV)

Short potential pulses of increasing height are superimposed on a constant base potential in Normal Pulse Voltammetry (NPV). This base potential is chosen where no faradaic reaction occurs. Measurement of current at the end of the pulse and plotting the succession of points against the potential of the applied pulses gives a voltammetric profile of the same form as a steady state voltammogram. If irreversible adsorption of the product of the electrode reaction occurs, then this will be much reduced through the use of pulses. Pulse leads to higher mass transport. The time delay between pulses must be long enough to restore all concentration gradients to their original state before the next potential pulse is applied.<sup>6,8,26</sup>

#### 1.2.4.6.3.2 Differential Pulse Voltammetry (DPV)

Differential Pulse Voltammetry (DPV) measures the differences between two currents, just before the end of the pulse and just before pulse application. The base potential is incremented in a staircase form. The difference between the two sampled currents is plotted against the staircase potential and leads to a peak shaped waveform.

DPV is better than NPV because DPV better eliminates the contribution of non faradaic, mainly capacitive processes to the current signal. In NPV the charging current becomes larger as the pulse becomes larger in amplitude, except near the beginning of the scan, and secondly residual capacitive contributions will tend to be effectively subtracted out in DPV. The use of a large pulse amplitude allows one to obtain large signals from extremely dilute solutions, with some distortion in the curve shape, because the pulse amplitude is an appreciable portion of the total voltammetric wave. For resolving the signals due to two species with close half wave potentials, the peak response of DPV is more useful than that of NPV. However as the pulse amplitude increases so does the peak width, which means that, in practice  $\Delta E$  values of more than 100 mV are not viable.<sup>6,8</sup>

#### 1.2.4.6.3.3 Square Wave Voltammetry (SWV)

The square wave voltammetric waveform consists of a square wave superimposed on a staircase. The currents at the end of the forward and reverse pulses are both registered as a function of staircase potential. The difference between them, the net current is larger than either of its two component parts in the region of the peak which is centered on the half wave potential. Capacitive contributions can be effectively discriminated against, before they die away, since over a small potential range between forward and reverse

pulses, the capacity is constant and is thus annulled by subtraction. The pulses can be shorter than in DPV or NPV, i.e the square wave frequency can be higher. The advantages of SWV include increasing the speed of the experiment and lower consumption of electroactive species relative to DPV and reduced problems of blocking the electrode surface.<sup>6</sup>

#### 1.2.4.6.4 Stripping methods

Stripping methods encompass a variety of electrochemical procedures having a common, characteristic initial step. In all of these procedures, the analyte is first deposited on a working electrode, usually from a stirred solution. After an accurately measured period, the electrolysis is discontinued, the stirring is stopped and the deposited analyte is determined by one of the voltammetric procedures. During this second step in the analysis, the analyte is redissolved or stripped from the working electrode. In anodic stripping methods, the working electrode behaves as a cathode during the deposition step and as an anode during the stripping step, with the analyte being oxidized back to its original form. In a cathodic stripping method, the working electrode behaves as an anode during the deposition step and as a cathode during stripping. The deposition step amounts to an electrochemical preconcentration of the analyte. As a result of the preconcentration step, stripping methods yield the lowest detection limits of all voltammetric procedures. Only a fraction of the analyte is usually deposited during the electrodeposition step. Hence quantitative results depend not only on control of electrode potential, but also on factors like electrode size, time of deposition and stirring rate. Working electrodes for stripping methods have been formed from a variety of materials, including mercury, gold, silver, platinum and carbon in various forms. Adsorptive stripping methods are quite similar to the anodic and cathodic stripping methods. The working electrode is immersed in a stirred

solution of the analyte for several minutes. Deposition of the analyte then occurs by physical adsorption on the electrode surface rather than by electrolytic deposition. After sufficient analyte has been accumulated, the stirring is discontinued and the deposited material is determined by voltammetric measurements.<sup>22</sup>

### 1.3 Sensors

Chemical sensing is part of an information acquisition process in which some insight is obtained about the chemical composition of the system in real time. In this process an amplified electric signal results from the presence of some chemical species. Generally, it consists of two distinct steps: recognition and amplification. The coupling of the chemically selective layer to the physical part of the sensor which is called the transducer is very important. Chemical sensors are categorized into the following groups according to the transducer type:

- a) **Optical sensors:** In optical sensors, there is a spectroscopic measurement associated with the chemical reaction. Absorbance, reflectance and luminescence measurements are used in the different types of optical sensors.
- b) **Mass sensitive sensors:** These make use of the piezoelectric effect and are particularly useful as gas sensors. They rely on a change in mass on the surface of an oscillating crystal which shifts the frequency of oscillation. The extend of the frequency shift is a measure of the amount of material adsorbed on the surface.
- c) **Heat sensitive sensors:** They are often called calorimetric sensors in which the heat of a chemical reaction involving the analyte is monitored with a transducer such as a thermistor or a platinum thermometer. Flammable gas sensors make use of this principle.

- d) **Electrochemical sensors:** Electrochemical sensors are the largest and oldest group of chemical sensors. They are divided by their mode of measurement into potentiometric, voltammetric/amperometric and conductimetric.<sup>27,28</sup>

## 1.4 Modified electrodes

Electrodes encounter specific phenomena that reduce their applicability to analytical and synthetic schemes. Chief among these are fouling of the electrode by unwanted precipitation or adsorption processes and the slow electrochemical reaction rates of some species that require application of an overpotential to cause the desired reaction to occur. These phenomena often can be controlled by manipulating the chemical nature of the electrode surface. The concept of chemically modified electrodes was in part borne out of the frustrated electrochemist's desire to seize direct control over the chemical nature of the electrode surface. If the proper reagents are chosen, desirable properties such as reagent based control of the rates and selectivities of electrochemical reactions, freedom from adsorptive and coating effects and special optical or excited state features might be obtained.<sup>10</sup>

Chemically modified electrodes have found numerous important applications in solar energy conversion and storage, selective electro-organic synthesis, molecular electronics, electrochromic display devices, corrosion protection and electroanalysis. For electroanalytical purposes, electrocatalysis at chemically modified electrodes is used to amplify the detection signal. It consists in acceleration of heterogeneous electron transfer of the target analyte, which is slow at the same potential at a bare electrode, induced by an immobilized charge mediator, i.e. catalyst. Electrocatalysis is accomplished by charge mediation but not all mediation results in electrocatalysis. The formal

potential difference of the analyte and mediator redox couples should be thermodynamically favourable. Slow electrode reactions of many important analytes require a potential greatly exceeding their formal redox potentials in order that these reactions proceed at desirably high rates. The acceleration of such kinetically hindered electrode reactions by electrode confined charge mediators permits the quantification of these analytes at less extreme potentials, because catalyzed electrode reactions usually occur near the formal potential of the mediator. By applying less extreme potentials, both detectability and selectivity can be improved significantly as compared with those obtained at non modified electrodes. Also, the electrode fouling is decreased which may occur in case of direct electrochemical conversion of the analyte at more extreme potentials at a bare electrode. Variations of the formal redox potential of the immobilized catalyst can be used effectively to discriminate between analytes. Since the rate of electrocatalysis depends primarily on the difference of the formal redox potential of the catalyst and the analyte, selectivity can be tuned by selecting the proper catalyst. Several different chemically modified electrodes are fabricated for electroanalysis, including mediators immobilized in a monolayer film, multilayer films or metal or semiconducting microparticles dispersed in the host matrix ionomer or conducting polymer films. Catalyzed redox reactions of analyte result in catalytic currents, indicating a substantial chemical amplification of the detection signal.<sup>29</sup>

Surface modification involves more than just creating a physical barrier – it either changes the surface layers of the electrode itself or creates a layer with some form of chemical as well as physical selectivity. Thus, some electrode processes are enhanced while others are inhibited. The electroactive modifier layer acts as a mediator between the solution and the electrode

substrate in electron transfer. Much research has been conducted into the chemical modification of electrodes and this subject has been reviewed extensively.<sup>10</sup>

A chemically modified electrode is thus an electrode made up of a conducting or semiconducting material that is coated with a selected monomolecular, multimolecular, ionic or polymeric film of a chemical modifier and that by means of faradaic reactions or interfacial potential differences exhibits chemical, electrochemical or optical properties of the film.<sup>4</sup>

Modified electrodes can be prepared in the following ways:

- a) **Chemical modification using silane:** The electrode surface is activated by chemical reaction, such as with silane, which is then used to react with another chemical species that becomes immobilized on the surface.
- b) **Adsorption:** This is used for coating electrode surfaces with solutions of the modifier either by dipping or by the application of a drop of solution followed by evaporating the solvent. Self assembled monolayers on the electrode surface can be prepared by dipping the electrode in the desired solution.
- c) **Electrodeposition and electropolymerisation:** If adsorption is carried out under the influence of an applied potential, then thicker modifier layers usually result, but there is probably a greater guarantee of uniformity. Electropolymerisation of monomers is also possible. Such procedures are used for the formation of conducting polymers.

- d) Plasma: The electrode surface is cleaned by a plasma leaving the surface with dangling bonds and being highly active. Adsorption of any species, such as amines or ethenes, in the vicinity is very fast.<sup>6</sup>

Manipulation of the molecular composition of the electrode aims at improving sensitivity, selectivity and stability allowing for tailoring its response in order to meet analytical needs. Various types of modifiers used in the present work are discussed below.

### 1.4.1 Metalloporphyrin

Porphyrins are based on 16 atom rings containing four nitrogen atoms. They are of perfect size to bind nearly all metal ions.<sup>30</sup> Majority of elements in the periodic table form equatorial complexes with porphyrins and many of these metalloporphyrin complexes are capable of binding additional axial ligands. Axial coordination is a process that can profoundly alter the spectroscopic, electrochemical, structural and photophysical properties of metalloporphyrin and it is central to many aspects of biological and catalytic chemistry. Manganese porphyrins have been widely studied because of their relevance as model systems for the oxygen evolving complex in photosynthesis and other biological systems such as the cytochromes. Manganese porphyrins are known to exhibit +2 to +5 oxidation states. Although all these oxidation states are accessible, Mn<sup>III</sup> porphyrins are the most stable. Mn<sup>III</sup> ion cannot be removed easily from the porphyrin macrocycle, even using strong mineral acids, only partial demetallation is observed.<sup>31</sup> Metalloporphyrins and metallophthalocyanins are remarkable precursors in supramolecular chemistry and the rapid development of this chemistry led to assemblies possessing various architectures and properties (photo, electro and catalytic properties and others). Axial coordination of a metalloporphyrin gives only one or two binding sites with other molecules.

Additional binding centres can result in increasing the stability of supramolecular assemblies and can be created by incorporating coordinating substituents at the periphery of a porphyrinic cycle. Porphyrins possess the ability to bind a large variety of substrates depending on the porphyrin structure. Different supramolecular architectures based on porphyrin-substrate complexes are used for molecular recognition purposes, as receptors and sensors. Utilization of porphyrins in catalysis is also based on their ability to bind substrates.<sup>32</sup> Metalloporphyrin coated glassy carbon electrodes are used as electrocatalytic voltammetric sensors for numerous clinically important solutes.<sup>21</sup>

#### 1.4.2 Conducting polymers

It is generally recognized that the modern study of electrical conduction in conjugated polymers began in 1977 with the publication by a group at the University of Pennsylvania<sup>33</sup> describing the doping of polyacetylene. Although there was some work before<sup>34</sup> i.e. dating back to World War II and even reports of electrochemical synthesis in the nineteenth century,<sup>35</sup> the Nobel Committee recognized the seminal contribution of Heeger,<sup>36</sup> MacDiarmid<sup>37</sup> and Shirakawa<sup>38</sup> by awarding them the Nobel Prize for Chemistry in the year 2000.<sup>39</sup>

Naturally, interest soon turned to other conjugated polymers such as poly(*p*-phenylene), polypyrrole, polythiophene and polyaniline, and their derivatives, which showed similar behaviour but in many cases were stable and processable. Conjugated conducting polymers can be generally synthesized by chemical polymerization and electrochemical polymerization. At the IBM Lab in San Jose, Diaz used oxidative electrochemical polymerization to prepare polypyrrole<sup>40</sup> and polyaniline<sup>41</sup> for the first time. Electrochemical synthesis forms

the polymer in its doped state, with the counter-ion (usually an anion) incorporated from the electrolyte.<sup>39</sup> An important feature of the electropolymerization technique is the direct formation of conducting polymer films that are highly conductive, simple and suitable for use especially in electronic devices. The five classes of polymers have been mentioned as giving rise to electronic properties. By substitutions of side groups in its structure, each polymer may give rise to many new compounds so that the five electronically conducting groups could well eventually yield dozens of new electrode materials, each with its own surface structure and electrocatalytic properties.<sup>42</sup>

The electrochemical oxidation of aromatic heterocyclic, benzenoid or non benzenoid molecules frequently leads to the formation of an electrically conducting organic polymer film at the electrode surface. These films typically have good adhesion and electrical contact to the electrode surface. Thin films, when supported by an electrode surface, can be electrochemically cycled between the oxidized, conducting state and the neutral insulating state. Conducting polymer film coated electrodes have been widely utilized for analytical determination, biological applications, energy storage and conversion and in electronic devices for the reason that conducting polymer films have the advantages of inherent stability, flexible synthetic routes and dense electroactive sites.<sup>40, 43-46</sup>

Among these conjugated polymers, a group of them representing dyes such as phenazines, phenothiazines, phenoxazines, etc., find wide use in bioelectrochemistry as redox indicators and mediators. Dye molecules have been widely used as mediators to study the electrochemical response of active compounds. The electropolymerization of azine group compounds are usually performed by anodic oxidation in acidic medium. Polymerization of dyes can

form a cross linked oligomer which leads to the enhancement of its adsorptive ability.<sup>47-50</sup>

Modification of electrodes by dyes can be achieved by one of the following three methods of attachment:<sup>51</sup>

- a) Covalent linkage to chemically modified surfaces<sup>52-56</sup>
- b) Incorporation in polymeric films or macromolecular deposits<sup>57,58</sup>
- c) Deposition on electrode by constant or cycled potential oxidation of a dye containing solution<sup>59-69</sup>

The first dye modified electrode produced by the deposition on electrode by cycled potential oxidation was reported by Alberty et al. Constant potential oxidation of an aqueous solution of thionine produced a thin coating that adhered to the electrode.<sup>51,60</sup>

### **1.5 A brief overview of the reported works on metalloporphyrin and dye modified electrodes for the voltammetric/ amperometric determination of pharmaceutical compounds**

Electrodes coated with films of electroactive polymers including electropolymerized porphyrin film, have received wide attention.<sup>70</sup> The metalloporphyrin modified electrodes are shown to decrease by several hundred millivolts, the potential required for the oxidation of ascorbic acid, penicillamine, acetaminophen, dihydronicotinamide adenine dinucleotide, hydralaxine, epinephrine, cysteine and oxalic acid. The faster rates of electron transfer result in a well defined voltammetric response and increased sensitivity. The differential pulse peaks for caffeic acid, ascorbic acid, acetaminophen and dopamine are enhanced by 18, 10.5, 9.4 and 8.4 times respectively. When used for amperometric monitoring of flowing streams, the

coated electrode permitted detection at lower potentials than at the naked surface and greatly facilitated assays of urine samples.<sup>71</sup>

S. S. Huang et al reported a poly[tetra(p-aminophenyl)porphyrin nickel] modified glassy carbon electrode for the voltammetric determination of acetaminophen. A pair of redox peaks at around 430 mV and 300 mV appeared for acetaminophen. The anodic peak current was linear to the concentration of acetaminophen in the range of  $1.0 \times 10^{-6}$  M -  $2.0 \times 10^{-4}$  M. The method was applied for the determination of acetaminophen in tablets.<sup>72</sup>

The catalytic properties of the complexes of Fe(III), Mn(III), Ni(II) and Co(II) of meso-tetrakis(o-nitrophenyl)tetrabenzoporphyrin towards the electrochemical oxidation of ascorbic acid were examined. The catalytic activity increased in the order TBPCo(II), TBPMn(III), TBPFe(III), TBPNi(II).<sup>73</sup>

Mn(III) complex of 5,10,15,20-tetrakis[2-(2,3,4,6-tetraacetyl- $\beta$ -D-glucopyranosyl)-1-O-phenyl]porphyrin (MnT(oglu)PPCl) modified carbon paste electrode showed excellent selectivity towards metronidazole. The calibration graph obtained was linear over the range of  $2.9 \times 10^{-3}$  M -  $5.8 \times 10^{-8}$  M, with a detection limit of  $5.8 \times 10^{-8}$  M for metronidazole. Cyclic voltammetric measurements indicated that MnT(oglu)PPCl included in graphite-epoxy resin matrices could efficiently mediate electron transfer from the base electrode to metronidazole causing a decrease of reduction potential for metronidazole detection. The sensor could be regenerated by simply polishing with an alumina paper, with an excellent reproducibility (RSD=1.6%).<sup>74</sup>

The voltammetric behavior of norepinephrine in the presence of excess ascorbic acid was investigated at the meso-tetrakis(2-aminophenyl)porphyrin modified electrode by cyclic and square wave voltammetry in phosphate buffer

solution. The modified electrode gave higher selectivity and highly effective electroactivity to norepinephrine oxidation in voltammetric measurements of norepinephrine in the presence of ascorbic acid and epinephrine. In phosphate buffer solution of pH 7.4, the peak current increased linearly with the concentration of norepinephrine in two concentration ranges of  $1.0 \times 10^{-6}$  mol/dm<sup>3</sup> to  $7.0 \times 10^{-6}$  mol/dm<sup>3</sup>, the other at  $7.0 \times 10^{-6}$  mol/dm<sup>3</sup> to  $5.0 \times 10^{-5}$  mol/dm<sup>3</sup>.<sup>75</sup>

5-(4-hydroxyethoxyphenyl)-10,15,20-*tris*-phenylporphyrin was synthesized and the voltammetric behavior of gold electrodes modified with neutral free-base and positively charged cobaltous center porphyrin films through exposed hydroxyl and pre-assembled carboxyl terminal via coupled reaction were investigated using Fe(CN)<sub>6</sub><sup>3-/4-</sup>, ascorbic acid and dopamine as probe species. The voltammetric sensing of ascorbic acid at the physiological level in the presence of dopamine can be achieved on functionalized self-assembled monolayer of short chain cobaltous porphyrin. The selectivity of response can be improved by introducing structural defects and positively charged center (Co<sup>2+</sup>) in monolayer modified electrode. The results showed that the current of anodic peak and its concentration had a linear relationship in a wide range of concentration from  $4 \times 10^{-7}$  M to  $2 \times 10^{-2}$  M. The detection limit obtained by differential pulse voltammetry was  $6.9 \times 10^{-8}$  M.<sup>76</sup>

The amperometric determination of glucose was successfully carried out at cobalt(II)phthalocyanine-cobalt(II)tetra(5-phenoxy-10,15,20-triphenylporphyrin) (CoPc-(CoTPP)<sub>4</sub>) pentamer modified glassy carbon electrode. Glassy carbon electrode was modified with the pentamer and then followed by immobilization of glucose oxidase through cross linking with glutaraldehyde in the presence of bovine serum albumin and nafion cation exchange polymer. The biosensor exhibited good amperometric response characteristics to

glucose at a low overpotential of 400 mV with amperometric response time of 5 s and detection limit of  $1.0 \times 10^{-5}$  M.<sup>77</sup>

An amperometric dimetridazole sensor based on the supermolecular recognition by glycosylated metalloporphyrin, Mn(III) complex of 5,10,15,20-tetrakis [2-(2,3,4,6-tetraacetyl- $\beta$ -d-glucopyranosyl)-1-*O*-phenyl] porphyrin (MnT(*o*-glu)PPCl) which was immobilized on a glassy carbon electrode by chitosan is reported. The MnT(*o*-glu)PPCl-modified electrode showed excellent selectivity toward dimetridazole with respect to a number of interferents and exhibited stable response. Linear range of  $1.5 \times 10^{-3}$  M to  $2.7 \times 10^{-9}$  M is reported, with a detection limit of  $2.7 \times 10^{-9}$  M for dimetridazole. Cyclic voltammetric measurements indicated that MnT(*o*-glu)PPCl entrapped in chitosan matrices could decrease the reduction potential for dimetridazole detection. The sensor could be regenerated by washing in an alcohol solution, with an excellent reproducibility (R.S.D=2.6%). The prepared sensor is applied for the determination of dimetridazole in pharmaceutical preparations.<sup>78</sup>

Simultaneous electrochemical determination of uric acid and ascorbic acid on cobalt (II) tetrakisphenylporphyrin modified glassy carbon electrode was achieved by Li and co-workers. The anodic peaks of ascorbic acid and uric acid could be well separated and the difference in value is about 0.27 V. The linear range for uric acid and ascorbic acid were  $2.0 \times 10^{-6}$  M –  $1.0 \times 10^{-4}$  M and  $9.0 \times 10^{-6}$  M –  $2.0 \times 10^{-3}$  M with detection limits of  $5.0 \times 10^{-7}$  M and  $5.0 \times 10^{-6}$  M respectively. Owing to the strongly hydrophobic property of porphyrin, the modified electrode exhibited good stability and long life time. The sensor was utilized for the analysis of uric acid and ascorbic acid in human urine.<sup>79</sup>

An amperometric artemisinin sensor based on the supramolecular recognition of glycosylated metalloporphyrin, which is included in the Au-nanoparticles-chitosan film coated on the glassy carbon electrode is reported. Fe(III) complex of 5,10,15,20-tetrakis[2-(2,3,4,6-tetraacetyl- $\beta$ -d-glucopyranosyl)-1-O-phenyl]porphyrin [FeT(*o*-glu)PPCl] is employed as an artemisinin sensitive and selective amperometric sensor. [FeT(*o*-glu)PPCl]/Au nanoparticles modified electrodes showed excellent selectivity and sensitivity towards artemisinin with respect to a number of interferents and exhibited stable current response, which is attributed to the coordination of artemisinin with the [FeT(*o*-glu)PPCl] in the electrodes. The calibration graph is reported to be linear over the range of  $1.8 \times 10^{-7}$  M –  $1.7 \times 10^{-9}$  M, with a detection limit of  $1.7 \times 10^{-9}$  M for artemisinin. The prepared sensor is applied for the determination of artemisinin in plant samples.<sup>80</sup>

The use of iron tetrapyrrolineporphyrin (FeTPyPz) as a highly selective catalyst in the construction of an electrochemical sensor for estradiol valerate is reported. The sensor was prepared by modifying carbon paste with FeTPyPz. The best results were obtained in a mixture of acetonitrile and 0.1 M phosphate buffer solution of pH 6 in a volume ratio of 47:53. A linear response range was observed between 45 and 450  $\mu$ M and quantification and detection limits of 45 and 13  $\mu$ M respectively. The reproducibility for the sensor construction was better than 4% and the operational stability over 50 measurements was 1.8%. The sensor was successfully applied to determine estradiol valerate in a commercial formulation.<sup>81</sup>

A sensitive sensor for the determination of l-histidine using gold electrode modified with Fe(III) porphyrin bearing three 2,6-di-tert-butyl phenol and one palmitoyl chain was developed by K.K Atkowska et al. Direct chemisorptions method and embedment into dodecanethiol monolayer were

employed for the electrode modification. Determination of 1-histidine using square wave voltammetry at both types of electrodes was carried out. Embedment technique was found to be more precise in comparison to that obtained by the direct chemisorptions. Gold electrodes modified with Fe(III) porphyrin was applied for the electrochemical determination of 1-histidine in the artificial matrix mimicking human serum.<sup>82</sup>

Cu (II) complex of 5,10,15,20-tetrakis(3-methoxy-4-hydroxyphenyl) porphyrin [TMHPPCu(II)] modified carbon paste sensor for sulfamethoxazole is reported. Compared with bare carbon paste electrode, the TMHPPCu(II) modified carbon paste electrode exhibited excellent current enhancement effect on the electrochemical oxidation of sulfamethoxazole. A well-defined oxidation peak of sulfamethoxazole appeared at -140 mV in 0.1 M phosphate buffer solution of pH 6. All the experimental parameters were optimized and it was found that under optimum conditions the oxidation peak current was linear to the concentration of sulfamethoxazole in the range of  $1.0 \times 10^{-2}$  M -  $1.0 \times 10^{-8}$  M with a detection limit of  $1.5 \times 10^{-9}$  M. The developed sensor is reported to be successfully applied for the determination of sulfamethoxazole in pharmaceutical formulations and urine sample.<sup>83</sup>

Zn(II) complex of 5,10,15,20-tetrakis(3-methoxy-4-hydroxyphenyl) porphyrin (TMHPP) incorporated carbon paste sensor has been developed for the determination of metronidazole benzoate. Metronidazole benzoate gave a well defined reduction peak at -0.713V in 0.1 M phosphate buffer solution of pH around 7. The reduction peak current of metronidazole benzoate was found to be enhanced at TMHPPZn(II) modified electrode than that at the bare carbon paste electrode. Also the reduction occurred at a comparatively lower potential at the TMHPPZn(II) modified electrode. Under optimum conditions the reduction peak current was proportional to metronidazole benzoate

concentration over the range  $1 \times 10^{-3}$  M to  $1 \times 10^{-5}$  M. The detection limit was found to be  $4.36 \times 10^{-6}$  M.<sup>84</sup>

A new thiol-derivatized metalloporphyrin, 5-{3-methoxyl-4-(4-mercaptobutoxy)}phenyl-10,15,20-triphenylporphyrinatocobalt(MBPPCo) was synthesized and the electrochemical behavior of unitary or binary self-assembled monolayers of MBPPCo and thiols with carboxylic terminal groups was investigated using  $\text{Fe}(\text{CN})_6^{3-/4-}$  and ascorbic acid as probe species. The binary modified electrode showed a small increase in peak current but a large decrease in overpotential. When either positively charged MBPPCo or negatively charged thiol self assembled monolayers solely were used for anionic electroactive species [ $\text{Fe}(\text{CN})_6^{3-/4-}$  or ascorbic acid], slow electron transfer kinetics was obtained.<sup>85</sup>

5-[4-(3-mercaptopropoxy)phenyl]-10,15,20-tris(2-chlorophenyl)porphyrin was utilized for fabricating a self-assembled monolayer on a gold electrode. Then cobalt(II) was inserted into the monolayer by refluxing the cobalt(II) solution in which the pre-assembled porphyrin-modified electrode was immersed. The monolayers were characterized by cyclic voltammetry. Oxidation and catalytic mechanisms of dopamine on the modified electrode were also investigated and elucidated respectively. Catalytic currents increased linearly with dopamine concentration in the range of  $1 \times 10^{-9}$  M to  $2 \times 10^{-3}$  M with the correlation coefficient of 0.9989.<sup>86</sup>

A novel glassy carbon electrode modified with malachite green is reported. The optimization of electropolymerisation conditions of malachite green was carried out. 10 minutes was appropriate for electropolymerization. As the time was prolonged further, the film became thicker and the mass transferring resistance increased. Malachite green could be electropolymerised

and exhibited well defined voltammetric peaks in a phosphate buffering solution. The pH of the phosphate buffering solution had only a small effect on the polymerization process. The modified electrode was used to determine dopamine and ascorbic acid. Optimization of the modified electrode for dopamine measurements is done. The anodic peaks for ascorbic acid and dopamine were separated by 200 mV.<sup>87</sup>

Chen et al reported a cresol red modified glassy carbon electrode prepared using an electrochemical method. Cyclic voltammograms of the modified electrode indicate the presence of a couple of well-defined redox peaks and the formal potential shifts in the negative direction with increasing solution pH. The modified electrode exhibits high electrocatalytic activity toward ascorbic acid oxidation, with an overpotential of 300 mV less than that of bare glassy carbon electrodes and drastic enhancement of the anodic currents. The calibration graph obtained by linear sweep voltammetry for ascorbic acid is linear in the range of 50 - 500 mM. The electrode also markedly enhances the current response of dopamine and can separate the electrochemical responses of ascorbic acid and dopamine. The separation between the anodic peak potentials of ascorbic acid and dopamine is 190 mV by cyclic voltammetry. The linear sweep voltammetric peak currents for dopamine in the presence of 2 mM ascorbic acid vary linearly with a concentration of between 10 and 100  $\mu\text{M}$ .<sup>88</sup>

Ming et al reported the voltammetric behavior of dopamine at poly(methyl blue) modified electrode. In pH 7.0 phosphate buffer solution, the linear range for the determination of dopamine was  $8.0 \times 10^{-7}$  M -  $5.0 \times 10^{-4}$  M. The detection limit was  $5.0 \times 10^{-8}$  M. The method was applied for the determination of dopamine in the pharmaceutical formulations with satisfactory results.<sup>89</sup>

Wan et al reported the electrochemical synthesis of poly(malachite green) on the glassy carbon electrode in potentiodynamic mode. The existence of quinoid structure was rationalized by optical and electrochemical techniques. The conductivity of poly(malachite green) was obtained from its electrochemical impedance spectroscopy in terms of capacitance of the film. As poly(malachite green) film was found to be electronically conductive and showed a high speed of charge transfer during redox reaction, it was used as a catalytic layer for the oxidation of ascorbic acid and dopamine. The excellent catalytic ability towards ascorbic acid and dopamine on poly(malachite green) film coated glassy carbon electrode is attributed to the quinoid structure inside the polymer and the large surface area of the polymer. The oxidation of ascorbic acid was separated 180 mV from that of dopamine and the catalytic currents were linear with their concentration in a wide concentration range. The content of ascorbic acid and dopamine in vitamin pills and dopamine injections were determined separately and simultaneously. The presence of epinephrine, norepinephrine and uric acid influenced the detection of ascorbic acid and dopamine, whereas no interferences were found when other vitamins like thiamine, riboflavin, pyridoxine, nicotinamide, nicotic acid, folic acid, retinol palmate and tocopherol acetate were present.<sup>90</sup>

Electrochemical catalytic oxidation of ascorbic acid on the poly (malachite green) film coated glassy carbon electrode is reported. The oxidation was affected significantly by experimental conditions like active sites in polymer films, reactive molecules in solution, parameters like accumulation time, scan rate etc. Thick poly(malachite green) films were not totally active towards oxidation of solution species owing to the slow chemical reaction or insufficient charge compensation between the reaction zone and electrode.<sup>91</sup>

The electrochemical behaviors of tinidazole were investigated by electrochemical methods at the poly(carmine) film modified glassy carbon electrode. A well defined reduction peak is observed at 0.606 V. Compared with that at a bare GCE, the reduction peak potential of tinidazole shifts negatively and the reduction peak current increases significantly at the modified electrode. The influences of some parameters on the reduction of tinidazole were examined and a simple and sensitive electroanalytical method was developed for the determination of tinidazole. The reduction peak current is proportional to the concentration of tinidazole from  $1 \times 10^{-7}$  M to  $5 \times 10^{-5}$  M. The detection limit is about  $5.0 \times 10^{-8}$  M for 90 s accumulation at a constant potential of 0 V. The method was applied to determine tinidazole in drugs.<sup>92</sup>

A poly(methyl red) film-modified glassy carbon electrode for determination of norfloxacin is reported. The electrochemical behavior of norfloxacin was investigated and a well defined oxidation peak with high sensitivity was observed at the film electrode. Poly(methyl red) greatly enhanced the oxidation peak current of norfloxacin owing to the extraordinary properties of poly(methyl red) film. Based on this, a sensitive and simple voltammetric method was developed for measurement of norfloxacin. A sensitive linear voltammetric response for norfloxacin was obtained in the concentration range of  $1 \times 10^{-6}$  –  $1 \times 10^{-4}$  M with a detection limit of  $1 \times 10^{-7}$  M using linear sweep voltammetry. The practical application of this new analytical method was demonstrated with norfloxacin pharmaceuticals.<sup>93</sup>

A poly(thionine) thin film modified electrode was successfully assembled on the surface of the glassy carbon electrode by means of electrochemical polymerization, which was carried out with cyclic voltammetric sweeping in the potential range 0 to +1.4 V in perchloric acid solution containing 0.1 mM thionine. The film modified electrode exhibited a couple of well defined redox

peaks and the redox peaks decreased correspondingly without a shift of the peak potential after the addition of heparin. Under the optimum conditions the decrease of the peak current was proportional to the concentration of heparin in the range 4.0 to 22.0  $\mu\text{g/ml}$  and the detection limit was 0.28  $\mu\text{g/ml}$ . The effects of potentially interfering species were investigated and the method was successfully applied for the determination of heparin in a pharmaceutical formulation.<sup>94</sup>

The electrochemical behavior of tryptophan was investigated by cyclic and linear sweep voltammetry at poly(methyl red) film-modified glassy carbon electrode. The oxidation peak current of tryptophan at the modified electrode increased significantly, and the oxidation process was irreversible and adsorption-controlled. An analytical method was developed for the determination of tryptophan in a phosphate buffer solution at pH 3.5. The anodic peak current varied linearly with tryptophan concentration in the range  $1.0 \times 10^{-7}$  M to  $1.0 \times 10^{-4}$  M with a limit of detection of  $4.0 \times 10^{-8}$  M.<sup>95</sup>

A novel poly(p-xylenolsulfonephthalein) modified glassy carbon electrode is reported for the simultaneous determination of ascorbic acid, epinephrine and uric acid. Cyclic voltammetric, chronoamperometric and differential pulse voltammetric methods were used to investigate the modified electrode for the electrocatalytic oxidation of ascorbic acid, epinephrine and uric acid in aqueous solutions. The separation of the oxidation peak potentials for ascorbic acid – epinephrine and epinephrine – uric acid was about 200 mV and 130 mV, respectively. The detection limits were 4, 0.1, and 0.08  $\mu\text{mol/l}$  for ascorbic acid, epinephrine and uric acid respectively. The diffusion coefficient and the catalytic rate constant for the oxidation of epinephrine at the modified electrode were calculated. The method was applied for the determination of epinephrine in pharmaceutical and urine samples, ascorbic

acid in commercially available vitamin C tablet and uric acid in urine samples.<sup>96</sup>

Modified glassy carbon electrodes have been made by deposition of functionalised multiwalled carbon nanotubes (MWCNTs) followed by formation of poly(Nile blue) (PNB) films by electropolymerisation, using potential cycling in 0.1 M phosphate buffer solution at pH 6. The electrochemical oxidation of carbidopa and benserazide on these MWCNTs/PNB modified electrodes were investigated using cyclic and differential pulse voltammetry in 0.1 M phosphate buffer solution at different values of pH between 5.0 and 8.0. Both carbidopa and benserazide gave one diffusion-controlled irreversible oxidation peak in cyclic voltammetry. Analytical characterisation of carbidopa and benserazide were carried out in 0.1 M PBS, pH 5.0. Peak currents in differential pulse voltammetry were linear over the concentration range of  $1 \times 10^{-5}$  M to  $1 \times 10^{-4}$  M for carbidopa and  $4 \times 10^{-6}$  M to  $4 \times 10^{-5}$  M for benserazide. Higher sensitivities and lower detection limits, of 1.17  $\mu$ M for carbidopa and 0.50  $\mu$ M for benserazide is reported.<sup>97</sup>

Fabrication and electrochemical characteristics of a toluidine blue modified gold electrode were investigated. The electrode was applied for the determination of ascorbic acid. In phosphate buffer solution of pH 6.5, a sensitive oxidation peak for ascorbic acid was observed. The current is proportional to the concentration of ascorbic acid in the range of  $3.9 \times 10^{-5}$  M to  $1.0 \times 10^{-2}$  M with a detection limit of  $1.3 \times 10^{-5}$  M. The modified electrode has a good repeatability. It has been applied for the quantitative determination of ascorbic acid in tablets.<sup>98</sup>

Li et al reported electropolymerized brilliant cresyl blue on the surface of a carbon ionic liquid electrode by cyclic voltammetric sweep in the potential range from  $-0.5$  V to  $1.0$  V. The stable polymer film of brilliant cresyl blue obtained on the carbon ionic liquid electrode exhibited a pair of redox peaks. The characteristics of poly (brilliant cresyl blue) film were studied by different methods such as scanning electron microscopy, electrochemical impedance spectroscopy and cyclic voltammetry. This modified electrode showed excellent electrocatalytic response to ascorbic acid with the increase of the electrochemical responses. Under the optimal conditions a good linear voltammetric response could be obtained over the range of  $2.0 \times 10^{-5}$  M -  $3.0 \times 10^{-3}$  M and the detection limit was obtained as  $6.5 \mu\text{M}$ .<sup>99</sup>

$\text{TiO}_2$ -graphene/poly(methyl red) composite film modified glassy carbon electrode (PMR/ $\text{TiO}_2$ -GR/GCE) was first employed for the sensitive determination of acetaminophen. The electrochemical behavior of acetaminophen was investigated by cyclic voltammetry and differential pulse voltammetry. The studies revealed that the oxidation of acetaminophen was facilitated at PMR/ $\text{TiO}_2$ -GR/GCE in  $0.1$  M phosphate buffer. The peak current for acetaminophen was found to vary linearly with its concentration in the range of  $2.5 \times 10^{-7}$  M –  $5 \times 10^{-5}$  M with detection limit of  $2.5 \times 10^{-8}$  M. The proposed method was employed for the determination of acetaminophen in commercial pharmaceutical samples.<sup>100</sup>

A polymerized film of eriochrome black T (EBT) was prepared on the surface of a glassy carbon electrode in alkaline solution by cyclic voltammetry. The poly(EBT) film-coated GC electrode exhibited excellent electrocatalytic activity towards the oxidations of dopamine (DA), ascorbic acid (AA) and uric acid (UA) in  $0.05$  mM phosphate buffer solution (pH 4.0) and lowered the

overpotential for oxidation of DA. The polymer film modified GC electrode enhanced the redox currents of DA, AA and UA and could sensitively and separately determine DA at its low concentration in the presence of 4000 and 700 times higher concentrations of AA and UA, respectively. The separations of anodic peak potentials of DA-AA and UA-DA reached 210 mV and 170 mV, respectively, by cyclic voltammetry.<sup>101</sup>

Modification of carbon paste electrode using Eriochrome Black T is reported. The electrochemical study showed that catalytic oxidation of dopamine (DA) was more sensitive at EBTMCPE in 1 M KCl solution as supporting electrolyte. The effect of concentration and scan rate were studied. The electrode process was found to be diffusion-controlled. The EBTMCPE showed selective enhancement of oxidation peak current for DA in the presence of ascorbic acid (AA). In the presence of AA, DA-AA shows peak potential separation of 163 mV. The concentration effect of both AA and DA were studied.<sup>102</sup>

A simple commercial graphite pencil electrode was used to investigate the electrochemical oxidation of dopamine. The electropolymerised film of eriochrome black T was prepared on the surface of graphite pencil electrode by using cyclic voltammetry technique. The prepared electrode exhibited an excellent electrocatalytical activity towards the determination of dopamine. Simultaneous detection of dopamine and uric acid was investigated by using both cyclic voltammetric and differential pulse voltammetry technique. The modified electrode was also used for the detection of dopamine in injection.<sup>103</sup>

An electropolymerized film of eriochrome black T (EBT) has been prepared at a glassy carbon electrode by cyclic voltammetry. The poly(EBT) membrane at GCE exhibits an excellent electrocatalytic activity towards the

oxidation of epinephrine (EP), ascorbic acid (AA) and uric acid (UA) in acidic solution and reduced the overpotential for the oxidation of EP. The poly(EBT)-coated electrode could separately detect EP, AA and UA in their mixture with the potential differences of 180 mV and 160 mV for EP-AA and UA-EP, respectively, which are large enough to allow for determination of EP in the presence of AA and UA. Using differential pulse voltammetry, the peak current of EP recorded in pH 3.5 solution was linearly dependent on EP's concentration in the range of 2.5  $\mu\text{M}$  - 50  $\mu\text{M}$ . Due to its good selectivity and stability, the polymer-coated GCE was successfully applied for the determination of EP in real samples.<sup>104</sup>

## 1.6 Scope of the present investigation

Pharmaceutical analysis, even during this century, is not only an important field of activity in the interest of suffering mankind through increasing the safety of drug therapy, but it is also at the same time a source of inexhaustible intellectual pleasures. The scope of pharmaceutical analysis includes the analytical investigation of bulk-drug materials, the intermediates in their synthesis, products of drug research, drug formulations, impurities and degradation products of drugs, biological samples containing the drugs and their metabolites with the aim of obtaining data that can contribute to the maximal efficacy and maximal safety of drug therapy and the maximal economy of the production of drugs.

The efficacy, safety and economy of drug therapy are extremely important issues not only from the point of view of public health, but their financial, moreover political aspects are also immense. As a consequence of this, pharmaceutical and biomedical analysis is among the most important branches of applied analytical chemistry. To fulfill the rapidly increasing

demands as regards the number and the quality of analytical measurements, great efforts have been made and are being made to apply, moreover to further develop this field.

Due to the globalization of the drug market and the sharpening concurrence among the drug companies, pharmaceutical analysis has become one of the battlefields in the struggle. The importance of issues related to drug safety has greatly increased and this has led to the continual increase of demands as regards securing the quality of drugs, moreover often securing the safety of drug therapy.

Electrochemical techniques are powerful and versatile analytical techniques that offer high sensitivity, accuracy and precision as well as a large linear dynamic range, with relatively low-cost instrumentation. Electrochemical techniques are well suited for the determination of drugs in various samples, that is, as raw material, pharmaceutical dosage forms even those involving a complex matrix such as syrups, tablets, creams, suppositories or ointments or else in biological fluids. The principal advantage of the modern electrochemical methods is that the excipients do not interfere and generally the separation and extraction procedure is not necessary. Thus, sample preparation usually consists of dissolving out the active ingredient from the pharmaceutical dosage form with a suitable solvent and performing direct analysis on an aliquot portion of this solution. In addition to the analytical aspect, electrochemistry allows the establishment of the electrochemical behaviour of a given drug through mechanistic studies. This is of particular interest with respect to the pharmacological knowledge of the drug. Electrochemical techniques are most suitable to investigate the redox properties of a new drug; this can give insights into its metabolic fate. Electrochemical data are often correlated to the molecular structure and the pharmacological activity. Modern electrochemical

techniques can be used successfully for the determination of various pharmaceutical samples in biological media or in dosage forms.

Voltammetric methods are applicable for the determination of a wide variety of both organic and inorganic species. Voltammetry is frequently employed to complement and validate spectroscopic methods. Its features are compact equipment, relatively low investment and running costs, simple sample preparation, short analysis time, high accuracy and sensitivity. In addition, unlike the spectroscopic methods, voltammetry can distinguish between different oxidation states of metal ions as well as between free and bound metal ions. This is referred to as speciation analysis. Voltammetric results provide important information regarding the bioavailability and toxicity of heavy metals. Voltammetry also enables organic compounds to be determined with a high degree of sensitivity. This makes it possible to analyze many active pharmaceutical ingredients. Voltammetry is especially suitable for laboratories in which only a few parameters have to be monitored with a moderate sample throughput. It is frequently used for special applications which cannot be performed with other techniques or, if they can, require a lot of work. Although voltammetry represents a rather specialized area of instrumental analysis, voltammetric measurements and mechanistic probing of redox system of various electroactive samples of biological significance like drugs, metals, hormones and vitamins have been reported. The voltammetric and polarographic techniques are the more sensitive, reproducible and easily used electroanalytical methods can be an alternative to more frequently used separation and spectrometric methods. Furthermore, in some cases there is a relationship between voltammetry and pharmaceutical samples and the knowledge of the mechanism of their electrode reactions can give a useful clue in elucidation of the mechanism of their interaction with living cells. The

voltammetric and polarographic analysis of drugs in pharmaceutical preparations by far is the most common use of electrochemistry for analytical pharmaceutical problems. As a rule, many of the active compounds of the formulations can be readily oxidized or reduced.

Electrochemical reactions are greatly facilitated at the modified working electrodes. In continuation to spectrophotometric<sup>105-109</sup> and electrochemical<sup>19, 83,84,110-120</sup> drug analysis carried out in our lab, the present investigation involves modification of glassy carbon electrode using modifiers like metalloporphyrin and conducting polymers and their application as sensors for the determination of drugs such as trimethoprim, ambroxol, sulfamethoxazole domperidone and tinidazole. In order to understand how the electrode modifier helps in the facile electrochemical reaction, computational work was carried out on the interaction of the metalloporphyrin with the drug, trimethoprim.

.....❧.....

**MATERIALS AND METHODS**

- 2.1. *Reagents*
- 2.2. *Instruments used*
- 2.3. *Cleaning of glassy carbon electrode*
- 2.4. *Preparation of buffer solutions*

This chapter mentions the reagents and instruments used in the work. It also describes the preparation of various buffer solution and cleaning procedure of glassy carbon electrode.

**2.1 Reagents**

All reagents used for the investigations were of analytical reagent grade. Double distilled water was used for preparing all aqueous solutions. Nafion (5%) and Alumina were purchased from Sigma Aldrich Corporation, USA. Pyrrole and anisaldehyde were purchased from Sisco Research Laboratories Ltd, India and were freshly distilled prior to use. Ethanol was purchased from Changshu Yangyuan Chemicals, China. Manganese acetate, propionic acid, glacial acetic acid, citric acid monohydrate, malachite green, methyl red, eriochrome black T and all other common reagents were obtained from s.d fine chemicals Pvt. Ltd, Mumbai, India. Tri sodium citrate dihydrate, sodium acetate trihydrate, sodium dihydrogen orthophosphate and disodium hydrogen phosphate were purchased from Merck, Germany. Pure drugs such as Trimethoprim (TMP), Ambroxol

(AMX), Sulfamethoxazole (SMX), Domperidone (DOM) and Tinidazole (TNZ) were obtained as gift samples. Dosage forms containing the drugs were purchased from local medical shops.

## 2.2 Instruments used

All electrochemical experiments were performed on an Electrochemical analyzer (BAS Epsilon Bioanalytical system, U.S.A), interfaced to a PC. A three electrode system consisting of chemically modified glassy carbon electrode as the working electrode, Ag/AgCl electrode as the reference electrode and platinum wire as the auxiliary electrode was employed. The pH measurements were carried out in a Metrohm pH meter. Ultrasonic cleaning of the electrode was carried out in an ultrasonicator (Oscar Ultrasonics, Pvt. Ltd. Mumbai). The UV-Visible spectrum was recorded using Spectro UV-Visible Double beam UVD-3500 instrument. The FT-IR spectra of the powdered samples were recorded on JASCO 4100 FT IR spectrometer using KBr discs.  $^1\text{H}$  NMR spectra were recorded using JEOL GSX 400 NB FT NMR spectrometer. Elemental analysis was performed with Vario EL III CHNS analyzer. Scanning electron microscopic images were recorded using JOEL 6300 LV. AAS was recorded using thermo AA spectrometer.

## 2.3 Cleaning of glassy carbon electrode

Glassy carbon electrode was mechanically polished with alumina slurry until obtaining a mirror like surface. The electrode was then rinsed with double distilled water thoroughly and was ultrasonically cleaned in methanol. Finally it was sonicated in 1:1  $\text{HNO}_3$ , acetone, NaOH solution and double distilled water for 5 min respectively.

## **2.4 Preparation of buffer solutions**

### **2.4.1 Preparation of Phosphate Buffer Solution (PBS) of various pH**

PBS of different pH (2-10) were prepared by varying the amount of  $\text{NaH}_2\text{PO}_4$  and  $\text{Na}_2\text{HPO}_4$  in 100 ml distilled water.<sup>121</sup> Table 2.1 gives an illustration of the amount of the phosphate salts required to prepare PBS of different pH. The pH of all the solutions was checked using pH meter before use. As for the preparation of pH 2 and 3, the amount of  $\text{Na}_2\text{HPO}_4$  required is very less and difficult to weigh, these solutions were prepared by adjusting the pH of PBS pH 4 using orthophosphoric acid.

### **2.4.2 Preparation of Acetate Buffer Solution (ABS) of various pH**

ABS of different pH (2-10) were prepared using acetic acid and sodium acetate trihydrate by changing their amount in 100 ml distilled water.<sup>122</sup> Table 2.2 details the amount of  $\text{CH}_3\text{COOH}$  and  $\text{CH}_3\text{COONa}\cdot 3\text{H}_2\text{O}$  required to prepare ABS of various pH.

### **2.4.3 Preparation of Citrate Buffer Solution (CBS) of various pH**

CBS of different pH (2-10) were prepared by varying the amount of citric acid monohydrate and tri sodium citrate dihydrate in 100 ml distilled water.<sup>122</sup> The pH of the prepared solutions were checked using pH meter. Table 2.3 shows the amount of each reagent required to prepare CBS of different pH.

**Table 2.1. Preparation of PBS of different pH**

| <b>NaH<sub>2</sub>PO<sub>4</sub><br/>(in grams/100 ml)</b> | <b>Na<sub>2</sub>HPO<sub>4</sub><br/>(in grams/100 ml)</b> |
|--|--|
| 1.3799   | 0.0001   |
| 1.3790   | 0.0003   |
| 1.3780   | 0.0036   |
| 1.3615   | 0.0360   |
| 1.2143   | 0.3218   |
| 0.5836   | 1.5466   |
| 0.0940   | 2.497  |
| 0.010  | 2.6605   |
| 0.0010   | 2.6781   |

**Table 2.2. Preparation of ABS of different pH**

| <b>CH<sub>3</sub>COOH<br/>(in grams/100 ml)</b> | <b>CH<sub>3</sub>COONa.3H<sub>2</sub>O<br/>(in grams/100ml)</b> |
|---|---|
| 0.5994  | 0.0024  |
| 0.5900  | 0.0237  |
| 0.5098  | 0.2054  |
| 0.2161  | 0.8711  |
| 0.0319  | 1.2885  |
| 0.0336  | 1.3534  |
| 0.0034  | 1.3602  |
| 0.00038   | 1.3609  |
| 0   | 1.3609  |

Table 2.3. Preparation of CBS of different pH

| pH | Citric acid monohydrate<br>(in grams/100 ml) | Tri sodium citrate dihydrate<br>(in grams/100 ml) |
|----|--|---|
| 2  | 1.8786                                       | 0.0652  |
| 3  | 1.6426                                       | 0.4265  |
| 4  | 1.1993                                       | 1.1050  |
| 5  | 0.7034                                       | 1.8641  |
| 6  | 0.2423                                       | 2.5697  |
| 7  | 0.0343                                       | 2.8882  |
| 8  | 0.0036                                       | 2.9352  |
| 9  | 0.0004                                       | 2.9401  |
| 10 | 0  | 2.9406  |

.....

## METALLOPORPHYRIN MODIFIED ELECTRODE FOR THE VOLTAMMETRIC DETERMINATION OF TRIMETHOPRIM

|                 |                                    |
|-----------------|------------------------------------|
| <b>Contents</b> | 3.1. <i>Introduction</i>           |
|                 | 3.2. <i>Experimental</i>           |
|                 | 3.3. <i>Results and Discussion</i> |
|                 | 3.4. <i>Conclusions</i>            |

This chapter describes the preparation of manganese porphyrin (TMOPPMn(III)Cl), its characterization and its application in the voltammetric determination of trimethoprim (TMP). The voltammograms showed enhanced oxidation response at the TMOPPMn(III)Cl/GCE with respect to the bare GCE for TMP attributable to the electrocatalytic activity of TMOPPMn(III)Cl. Electrochemical parameters of the oxidation of TMP on the modified electrode were analysed. It is found that the oxidation peak current is proportional to the concentration of TMP over the range  $6 \times 10^{-8}$  M -  $1 \times 10^{-6}$  M with a very low detection limit of  $3 \times 10^{-9}$  M. Applicability to assay the drug in urine has also been studied.

### 3.1 Introduction

Trimethoprim (TMP), chemically 5-(3,4,5-trimethoxybenzyl)pyrimidine-2,4-diamine, the structure of which is shown in Figure 3.1, belongs to the class of chemotherapeutic agents known as dihydrofolate reductase inhibitors. It is used in prophylaxis treatment and urinary tract infections. TMP is a synthetic antibiotic that interferes with the production of tetrahydrofolic acid (a necessary chemical for bacteria and human cells to produce proteins), by

inhibiting the enzyme responsible for making tetrahydrofolic acid from dihydrofolic acid. Tetrahydrofolic acid is an essential precursor in the de novo synthesis of the intermediate thymidine monophosphate which is a precursor for DNA metabolite thymidine triphosphate. Bacteria cannot take up folic acid from the environment and are dependent on their own de novo synthesis. TMP inhibits the bacterial enzyme more than the corresponding human enzyme. TMP was commonly used in combination with sulfamethoxazole. The use of this combination, known as 'co-trimoxazole' was restricted in 1995. Still it is prescribed for some infections viz., prophylaxis in HIV-affected patients at risk of pneumocystic jirovecii pneumonia, Whipples disease and for those with some hematological malignancies. Use of TMP is contraindicated during pregnancy, especially in the first trimester, and for sufferers of certain blood disorders. It can also reduce the clearance of creatinine at renal tubules. Additionally, it can also lead to dangerously low levels of thrombocytes (cells that help blood clot) by lowering folic acid levels and associated bone marrow blood cell formation.<sup>123</sup> Thus the determination of TMP is of great importance and few methods exist for its determination. They include spectrophotometry,<sup>124</sup> molecular imprinting chemiluminiscence,<sup>125</sup> polarography,<sup>126</sup> adsorptive stripping voltammetry<sup>127</sup> and HPLC.<sup>128</sup> But most of these methods lack selectivity and sensitivity for the determination of TMP. Hence it is of immense importance to develop a technique for the determination of TMP with a high degree of selectivity and sensitivity and a low detection limit.

## 3.2 Experimental

### 3.2.1 Synthesis of 5,10,15,20-tetrakis(4-methoxyphenyl)porphyrin (TMOPP)

TMOPP was synthesized according to the Adler method.<sup>129</sup> 15 mmol of freshly distilled pyrrole (1.04 ml) and anisaldehyde (1.82 ml) were added to 80

ml of refluxing reagent grade propionic acid. After refluxing for 30 min, the solution was ice-cooled, filtered and the filter cake was washed thoroughly with methanol. After a hot water wash, the resulting purple crystals were air dried. The product was purified by column chromatography.

Elemental analysis of TMOPP

Calcd (%): C, 78.00; H, 5.10; N, 7.60

Found (%): C, 77.99; H, 5.00; N, 7.51

IR (KBr),  $\gamma$  ( $\text{cm}^{-1}$ ): 3363 (NH); 3000 (CH)

UV-Visible spectrum in  $\text{CH}_2\text{Cl}_2$ ,  $\lambda$  (nm): 364, 417, 516, 557, 651

$^1\text{H}$  NMR (500 MHz,  $\text{CDCl}_3$ ),  $\delta$  (ppm): 8.8 (s, 8H, pyrrolic  $\beta$  H), 3.39 (s, 12 H,  $\text{OCH}_3$ ), -3.5 (s, 2 H, NH), 8.2-7.3 (m, 16 H, aromatic)

### **3.2.2 Synthesis of [5,10,15,20-tetrakis(4-methoxyphenyl)porphyrinato] manganese(III)chloride (TMOPPMn(III)Cl)**

TMOPPMn(III)Cl was prepared according to the literature procedure.<sup>130</sup> The ligand TMOPP (0.5 g) and  $(\text{CH}_3\text{COO})_2\text{Mn}\cdot 4\text{H}_2\text{O}$  (0.5 g) were refluxed in 125 ml glacial acetic acid for 72 hours. The solvent was then stripped off and the residue was then extracted into 62.5 ml methanol. The filtered methanol solution was treated with 62.5 ml concentrated HCl and with 62.5 ml of distilled water. A green precipitate was formed immediately, which was isolated by filtration, washed with distilled water and air dried. The crude product was dissolved in 100 ml of benzene and filtered and 400 ml of petroleum ether were added. The cooled solution yielded lustrous green crystals and pure product was isolated by filtration. The molecular structure of TMOPPMn(III)Cl is displayed in Figure 3.2.

Elemental analysis of TMOPPMn(III)Cl

Calcd (%): C, 70.00; H, 5.00; N, 7.10; Mn, 6.74

Found (%): C, 69.03; H, 4.88; N, 6.44; Mn, 6.42

UV-Visible spectrum in CH<sub>2</sub>Cl<sub>2</sub>, λ (nm): 236, 388, 405, 481, 582, 621

IR (KBr), γ (cm<sup>-1</sup>): 3000 (CH); 455 (Mn-N).

<sup>1</sup>H NMR (500 MHz, CDCl<sub>3</sub>), δ (ppm): 8.9 (s, 8 H, pyrrolic β H), 4.0 (s, 12 H, OCH<sub>3</sub>), 8.2-7.3 (m, 16 H, aromatic)

### 3.2.3 Preparation of TMOPPMn(III)Cl modified glassy carbon electrode

2 mg of TMOPPMn(III)Cl was dissolved in a mixture of 300 μl nafion and 200 μl ethanol. The solution was then agitated ultrasonically for about half an hour to get a stable and homogeneous solution. The bare glassy carbon electrode (GCE) was cleaned as explained in section 2.3. The electrode was then allowed to dry. TMOPPMn(III)Cl /GCE was prepared by dropping 3μl of TMOPPMn(III)Cl solution onto the clean GCE surface and evaporating the solvent at room temperature.

### 3.2.4 Preparation of analyte sample

Stock solution of TMP ( $1 \times 10^{-2}$  M) was prepared in methanol. Standard solutions of the analyte ( $1 \times 10^{-3}$  M –  $1 \times 10^{-8}$  M) were prepared by serial dilution of the stock solution using PBS.

### 3.2.5 Analysis of sample

Sample solution was taken in the electrochemical cell. Differential pulse voltammograms from 0 V to 1.30 V at  $20 \text{ mVs}^{-1}$  were recorded and finally the peak current at about 1.080 V was measured for TMP. Prior to and after each

measurement, the TMOPPMn(III)Cl/GCE was activated by successive cyclic voltammetric sweeps between 0 V to 1.3 V at  $100 \text{ mVs}^{-1}$  in PBS until the voltammograms kept unchangeable.

### 3.3 Results and Discussion

#### 3.3.1 Surface studies of TMOPPMn(III)Cl/GCE

Surface morphological observations of TMOPPMn(III)Cl/GCE were carried out by scanning electron microscopy (SEM). Figures 3.3a and 3.3b depict the SEM images of the bare GCE and TMOPPMn(III)Cl/GCE respectively. The comparison points to the effective modification of the bare GCE. Cyclic voltammetry of 2 mM potassium ferricyanide solution was carried out at both bare GCE and TMOPPMn(III)Cl/GCE at different scan rates to calculate the effective surface area of them. The obtained current was plotted against the square root of scan rates in both the cases. The slopes of the straight lines were determined. By using the Randles-Sevcik equation for reversible reaction,

$$i_p = (2.687 \times 10^5) n^{3/2} \nu^{1/2} D^{1/2} A c$$

( $i_p$  refers to peak current,  $n$  is the number of electrons transferred,  $D$  is the diffusion coefficient,  $A$  is the surface area of the electrode,  $c$  is the concentration of potassium ferricyanide solution and  $\nu$  stands for scan rate), effective surface area of bare GCE and TMOPPMn(III)Cl/GCE were calculated. Taking  $n=1$  and  $D= 7.6 \times 10^{-6} \text{ cms}^{-1}$ , the effective surface area of bare GCE and TMOPPMn(III)Cl/GCE was calculated to be  $0.0669 \text{ cm}^2$  and  $0.2112 \text{ cm}^2$  respectively. The large surface area of the modified GCE compared to bare GCE is evident from the resultant values.

### 3.3.2 Investigation of the electrochemical activity of TMOPPMn(III)Cl/GCE

The above fabricated electrode was applied to study the electrocatalytic property of TMOPPMn(III)Cl. The studies showed that TMOPPMn(III)Cl/GCE couldn't sense the drugs sparfloxacin and sildenafil citrate voltammetrically. For the drugs like tinidazole and guaifenesin, TMOPPMn(III)Cl/GCE gave the voltammetric response at a higher potential with comparatively lower current than that obtained at bare GCE. But for trimethoprim and ambroxol, the oxidation occurred at a 100 mV lesser potential on TMOPPMn(III)Cl/GCE than on bare GCE, with considerable increase in peak current.

### 3.3.3 Electrochemical behaviour of TMP and the optimization of the developed method

#### 3.3.3.1 Comparison of the electrochemical behaviour of TMP at bare GCE and TMOPPMn(III)Cl/GCE

The electrochemical behaviour of TMP at a TMOPPMn(III)Cl/GCE has been investigated using Differential Pulse Voltammetry (DPV). Figure 3.4 shows the comparison of oxidation peak of  $1 \times 10^{-3}$  M TMP in PBS (pH 5) at a scan rate of  $20 \text{ mVs}^{-1}$  with pulse width 50 ms, pulse period 200 ms and pulse amplitude 50 mV at bare GCE and TMOPPMn(III)Cl/GCE. At the bare GCE, TMP yields an irreversible very low oxidation peak at 1.160 V (curve a). Under the same conditions, a well defined irreversible oxidation peak appears at 1.088 V for the TMOPPMn(III)Cl/GCE (curve b). Obviously, the anodic peak current of TMP at the TMOPPMn(III)Cl/GCE increases significantly and the peak potential shifts towards a more negative potential compared to that of a bare GCE. The increase in the peak current and the negative shift of oxidation potential may be attributed to the electrocatalytic activity of TMOPPMn(III)Cl. Further electrochemical studies of TMP on TMOPPMn(III)Cl/GCE were carried out.

### **3.3.3.2 Effect of various supporting electrolyte**

The electrochemical properties of  $10^{-3}$  M TMP in various medium such as PBS,  $H_2SO_4$ , HCl, KCl, tetra-n-butyl ammonium chloride,  $KNO_3$ , acetate buffer and NaOH of concentration 0.1 M were investigated by DPV. It was observed that the peak current is highest and the peak shape is well defined in PBS. Hence PBS was chosen as the experimental medium for the voltammetric studies of TMP.

### **3.3.3.3 Effect of pH of the medium**

The electrochemical studies of  $10^{-3}$  M TMP in PBS were carried out in the pH range of 3 to 10 using DPV, the graphical representation of which is shown in Figure 3.5. The best oxidation response was obtained in pH 5 as the peak current is the highest. Thus pH 5 was fixed as optimal pH.

### **3.3.3.4 Effect of the volume of TMOPPMn(III)Cl solution drop casted on GCE**

The amount of TMOPPMn(III)Cl solution on the GCE directly determines the thickness of the TMOPPMn(III)Cl film. It is found that the oxidation peak current of TMP increases, while gradually increasing the volume of TMOPPMn(III)Cl solution (2 mg in 300  $\mu$ l nafion and 200  $\mu$ l ethanol) from 1  $\mu$ l to 3  $\mu$ l. The observation is shown in Figure 3.6. The enhancement of current indicates that the number of catalytic sites increases with the increase of the amount of TMOPPMn(III)Cl. Further increasing the volume of TMOPPMn(III)Cl solution results in the decrease of the peak current. This is because nafion, used as one of the solvents, is a kind of insulator that blocks the electron transfer. Due to uncompensated resistive effects or lowering of the charge transfer rate, the peak current is conversely decreased. Hence, the volume of TMOPPMn(III)Cl solution was fixed to be 3  $\mu$ l.

### 3.3.3.5 Effect of accumulation of TMP

The accumulation step is usually a simple and effective way of enhancing the sensitivity. The influence of the accumulation time on the oxidation peak current of  $10^{-3}$  M TMP was tested using DPV. The results are plotted in Figure 3.7. The oxidation peak current increased gradually within the first 2 min indicating the enhancement of TMP concentration at the electrode surface. After that, as the accumulation time increases, the peak current tends to level off showing that the adsorptive equilibrium is reached. These results indicate that electrochemical oxidation of TMP on TMOPPMn(III)Cl/GCE is adsorption controlled.

### 3.3.3.6 Effect of scan rate and nature of electrochemical process

The influence of the scan rate on the oxidative peak current and potential of  $10^{-6}$  M TMP were investigated. Figure 3.8 describes the variation of anodic peak current with scan rate  $20 \text{ mVs}^{-1} - 80 \text{ mVs}^{-1}$  and Figure 3.9 shows the linear behaviour of anodic peak current with the scan rate in the range  $20 \text{ mVs}^{-1} - 60 \text{ mVs}^{-1}$ . This again points to the fact that the behaviour of TMP during the electrode reaction is controlled by adsorption rather than diffusion.

### 3.3.3.7 Investigation of the possible mechanistic pathway for the electrooxidation of TMP

Potential plotted against  $\ln$  scan rate gave a linear plot (Figure 3.10), slope of which is 0.0135. Based on the Laviron's equation,<sup>131</sup> the slope of this plot equals to  $RT/\alpha nF$ , where  $\alpha$  is assumed to be 0.5 for the totally irreversible electrode process. The calculation gave the number of electrons ( $n$ ) involved in the electrochemical reaction to be 3.8 (close to 4). Earlier report with respect to the electrochemical oxidation of TMP illustrates the identification of products using various techniques like measurement of melting point, TLC, IR

and mass spectroscopy, the results of which point to the formation of mononitroso and dinitroso derivatives.<sup>132</sup> TMP was electrooxidized in the pH range 3 – 10 to mononitroso derivative by 4e mechanism. The mononitroso derivative underwent electrooxidation to dinitroso derivative by 4e mechanism at pH less than 3. Based on the experimental observation of the involvement of 4e and on the previous report of identification of products of electrooxidation of TMP, a mechanism is proposed, which is illustrated in Scheme 3.1. The amino group at position 4 of the pyrimidine ring may be more easily oxidized than the one at position 2 which is a part of stable pyrimidine system. Again, a 4e oxidation of the mononitroso derivative can lead to the formation of dinitroso derivative.<sup>132</sup> But then, there should be two distinct peaks in the voltammogram corresponding to the formation of mono and dinitroso derivatives. In the present investigation, only a single oxidation peak for TMP is obtained in the pH range 3 – 10, which indicates the formation of mononitroso derivative by a 4e process, thus ruling out the possibility of 8e oxidation of TMP to dinitroso derivative. Thus a 4e oxidation for TMP is proposed.

### 3.3.3.8 Estimation of limit of detection of TMP

The effect of concentration of TMP in PBS (pH 5) on the modified GCE was studied using DPV. Figure 3.11 shows Differential pulse voltammograms of TMP on TMOPPMn(III)Cl/GCE at various concentrations ( $10^{-3}$  M –  $10^{-8}$  M). The results show that the oxidative peak current has a linear relationship with the concentration in the range  $6 \times 10^{-8}$  –  $1 \times 10^{-6}$  M which is shown in Figure 3.12. The linear regression equation is

$$i_p = 0.1634c + 2.1102 \quad (r = 0.9855, c \text{ in M, } i_p \text{ in } \mu\text{A})$$

The lower detection limit of TMP is  $3 \times 10^{-9}$  M ( $8.72 \times 10^{-10}$  gml<sup>-1</sup>).

### 3.3.3.9 Reproducibility and stability of TMOPPMn(III)Cl/GCE

The reproducibility of the electrode was examined by repetitive voltammetric determination of  $1 \times 10^{-3}$  M TMP using the same TMOPPMn(III)Cl/GCE. Comparable results were obtained with relative standard deviation (RSD) of 3.2% for  $n=9$  suggesting that the TMOPPMn(III)Cl/GCE has good reproducibility. After each determination, the modified electrode was run in PBS (pH=5). Moreover, TMOPPMn(III)Cl/GCE exhibited stable behaviour for 20 days.

### 3.3.4 Influence of foreign species on the oxidation of TMP

In order to examine the effect of foreign bodies on the anodic current of TMP, 100-fold concentration of KCl, NaCl, citric acid, dextrose, lactose, urea,  $K_2SO_4$ , glycine and ascorbic acid were added to  $10^{-3}$  M TMP. It is found that upto 100-fold concentration of KCl, NaCl, citric acid, dextrose, lactose, urea, and  $K_2SO_4$  have no influence on the signals of  $1 \times 10^{-3}$  M TMP, with deviation below 5%. However, glycine, sulfamethoxazole and ascorbic acid do interfere. Table 3.1 lists the influence of other substances on the oxidation signal of TMP. Since sulfamethoxazole is often used as part of a synergistic combination with TMP in tablets, the influence of sulfamethoxazole on the oxidation peak current of TMP was studied. It was found that same concentration of sulfamethoxazole did not interfere in the determination of TMP.

### 3.3.5 Application of the developed method in urine sample

An adequate amount of TMP corresponding to  $10^{-3}$  M was added to the urine sample. This solution was quantitatively diluted using PBS to obtain various concentrations ( $10^{-5}$  M –  $10^{-6}$  M). DPV at TMOPPMn(III)Cl/GCE were recorded and the unknown concentration was determined from the

calibration graph. The recovery obtained lie in the range of 96 – 100%. The results are tabulated in Table 3.2.

### **3.3.6 Comparison with the reported works**

The developed method was compared with the standard potentiometric titration method for the determination of TMP.<sup>133</sup> Stock solution of  $1 \times 10^{-3}$  M TMP was prepared in acetic acid. This was titrated with 0.1 M perchloric acid. Detection limit of  $2.90 \times 10^{-7}$   $\text{gmL}^{-1}$  was obtained for TMP with the standard method. A comparison of the present work with the already reported works is tabulated in Table 3.3.

## **3.4 Conclusions**

The voltammetric behaviour of TMP was investigated at a TMOPPMn(III)Cl/GCE by DPV. TMOPPMn(III)Cl film provides a good platform for the oxidation of TMP. The results showed that TMOPPMn(III)Cl could efficiently accelerate the electron transfer rate of TMP and hence can act as an electrocatalyst for the oxidation of TMP. The TMOPPMn(III)Cl/GCE is convenient to fabricate and is characterized by remarkable enhancement of the peak current and the reduction of anodic peak potential with the detection limit of  $3 \times 10^{-9}$  M. The proposed sensor was utilized for the analysis of TMP in urine and was found to perform successfully. The proposed method is an advanced substitute for the determination of TMP as certain predominant characteristics vested in this work put forth: low detection limit, simple process, accelerated speed of detection, cost effectiveness, good reproducibility, stability and excellent sensitivity for TMP.

**Table 3.1. Influence of  $1 \times 10^{-1}$  M of foreign species on the oxidation peak current of  $10^{-3}$  M TMP**

| Foreign species    | Signal change, % |
|--------------------|------------------|
| Potassium chloride | -2.50            |
| Sodium chloride    | -4.40            |
| Ascorbic acid      | 25.00            |
| Citric acid        | 1.30             |
| Dextrose           | 0.63             |
| Lactose            | -3.70            |
| Urea               | 3.04             |
| Sulfamethoxazole   | 9.15             |
| Glycine            | -8.24            |
| Potassium sulphate | 0.03             |

**Table 3.2. Determination of TMP in urine sample**

| Added amount of TMP (M) in urine sample | Found amount of TMP (M) in urine sample | Recovery % |
|---|---|------------|
| $2.00 \times 10^{-6}$                   | $1.94 \times 10^{-6}$                   | 96.8       |
| $4.00 \times 10^{-6}$                   | $3.90 \times 10^{-6}$                   | 97.5       |
| $8.00 \times 10^{-6}$                   | $7.98 \times 10^{-6}$                   | 99.8       |

**Table 3.3. Comparison of the developed method with other reported works for the determination of TMP**

| S.No. | Method   | Lower detection limit                                     |
|-------|--|---|
| 1     | Simultaneous ultraviolet spectrophotometric determination <sup>124</sup> | $8.96 \times 10^{-10}$ gml <sup>-1</sup>                  |
| 2     | Molecular imprinting chemiluminescence <sup>125</sup>                    | $2.00 \times 10^{-8}$ gml <sup>-1</sup>                   |
| 3     | Polarography <sup>126</sup>  | $5.00 \times 10^{-7}$ gml <sup>-1</sup>                   |
| 4     | Adsorptive stripping voltammetry <sup>127</sup>                          | $3.92 \times 10^{-9}$ gml <sup>-1</sup>                   |
| 5     | HPLC <sup>128</sup>  | $1.00 \times 10^{-8}$ gml <sup>-1</sup>                   |
| 6     | Potentiometric titration (Standard method) <sup>133</sup>                | $2.90 \times 10^{-7}$ gml <sup>-1</sup>                   |
| 7     | <b>Voltammetry using TMOPPMn(II)Cl/GCE (Present method)</b>              | <b><math>8.72 \times 10^{-10}</math> gml<sup>-1</sup></b> |

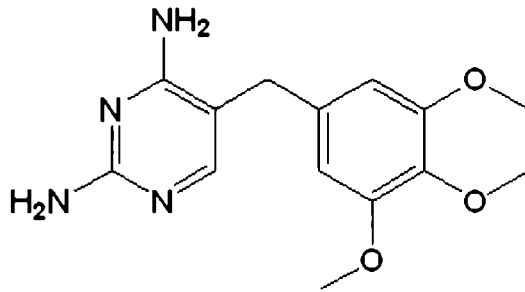


**Figure 3.1. Structure of TMP**

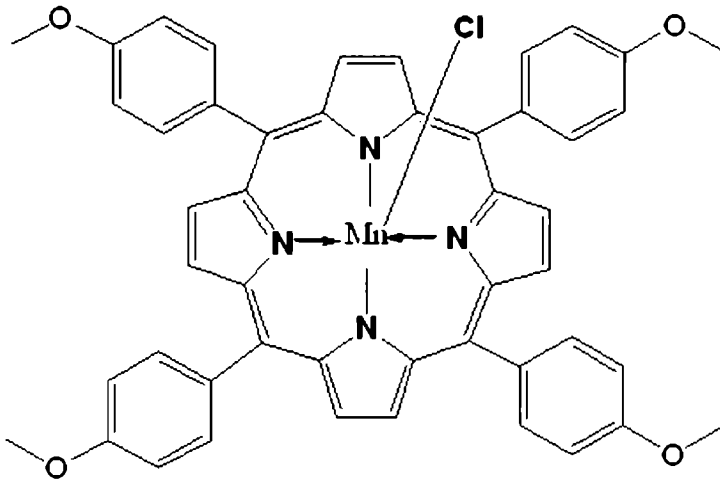


**Figure 3.2. Structure of TMOPPMn(III)Cl**

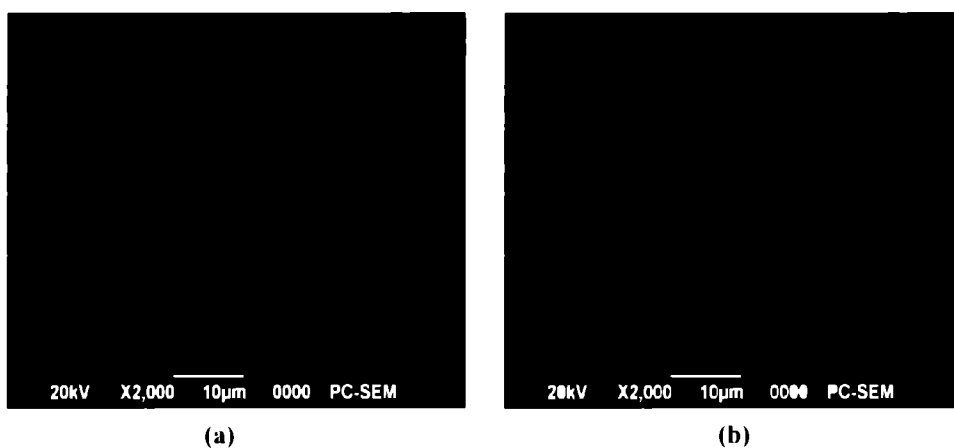


Figure 3.3. SEM images of a) bare GCE and b) TMOPPMn(III)Cl/GCE

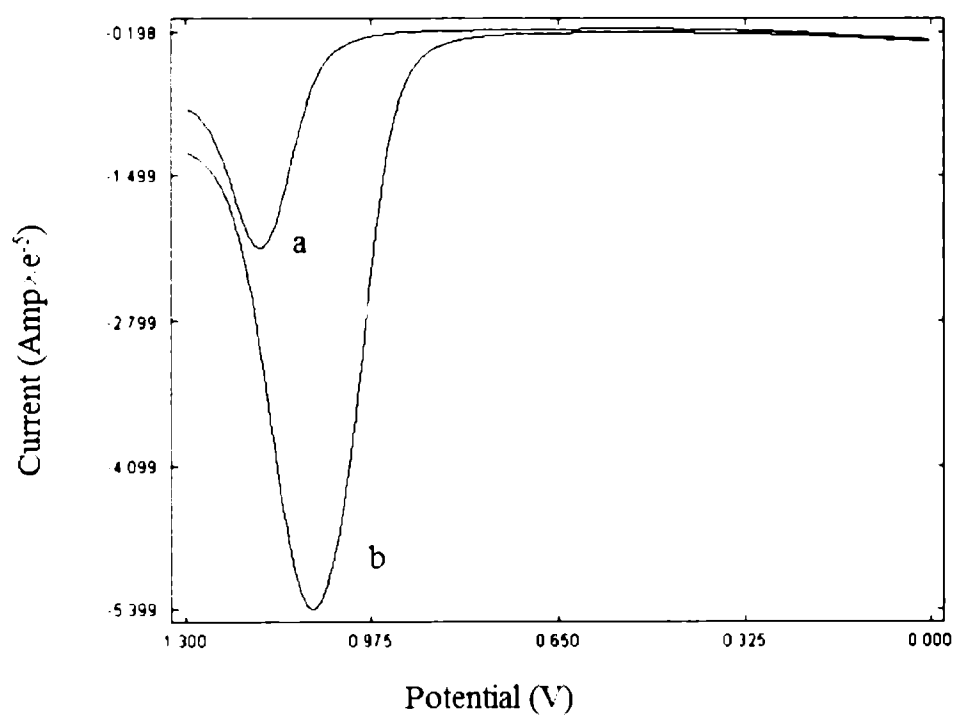
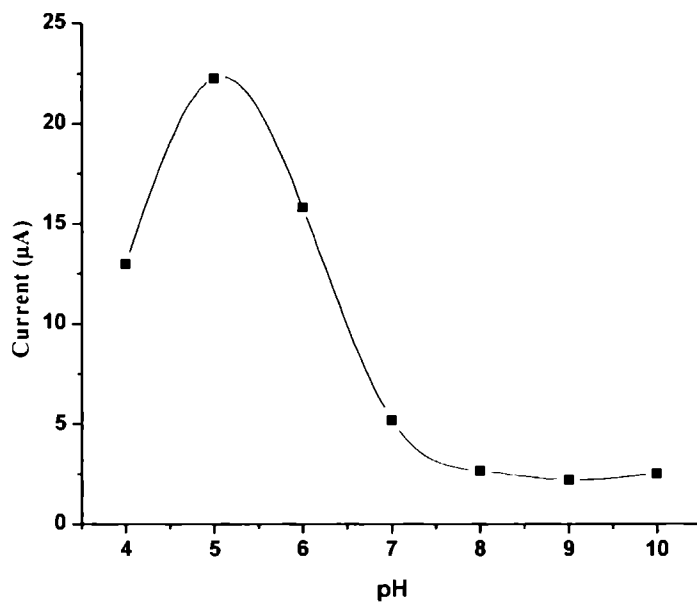
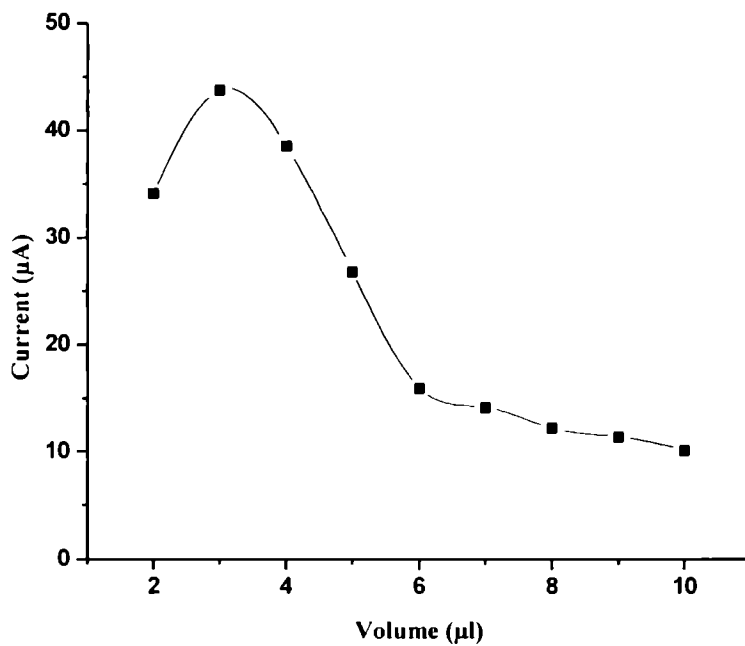


Figure 3.4. Differential pulse voltammogram of  $1 \times 10^{-3}$  TMP at (a) bare GCE (b) TMOPPMn(III)Cl/GCE



**Figure 3.5. Relationship between anodic peak current and pH of the medium**



**Figure 3.6. Relationship between anodic peak current and volume of the modifier**

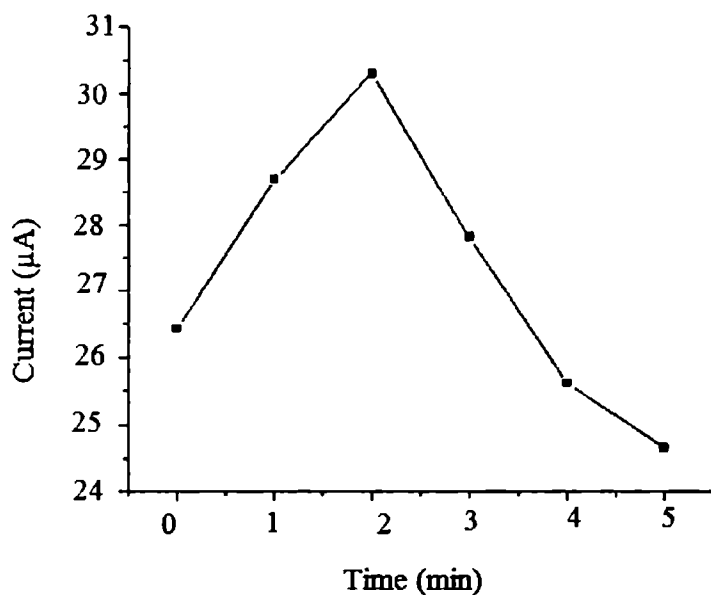


Figure 3.7. Effect of accumulation time of TMP on the anodic peak current

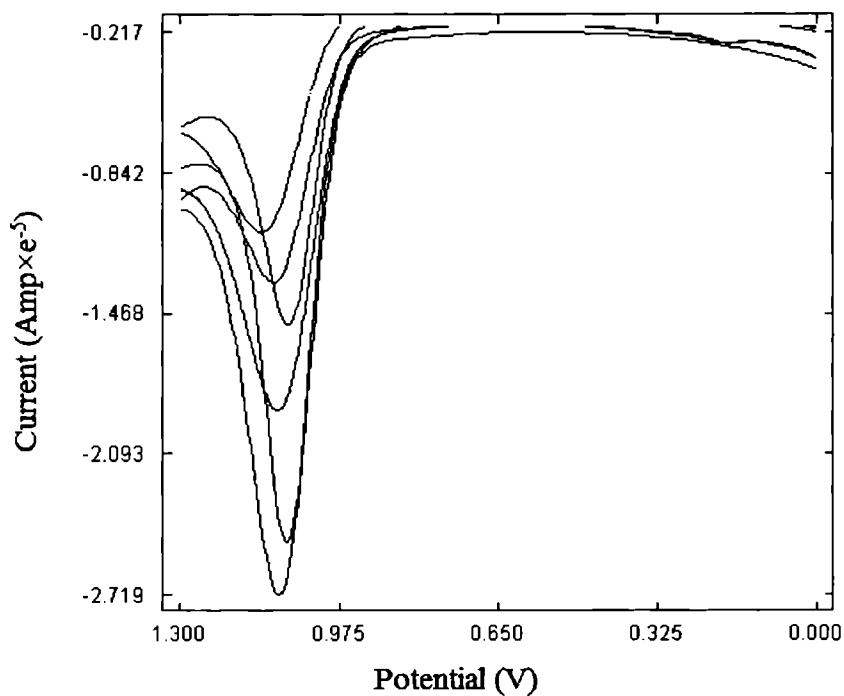
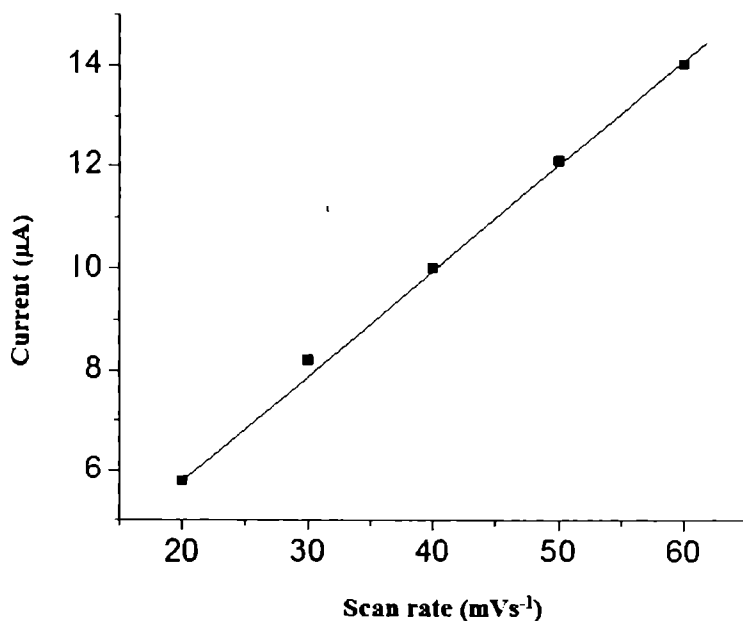
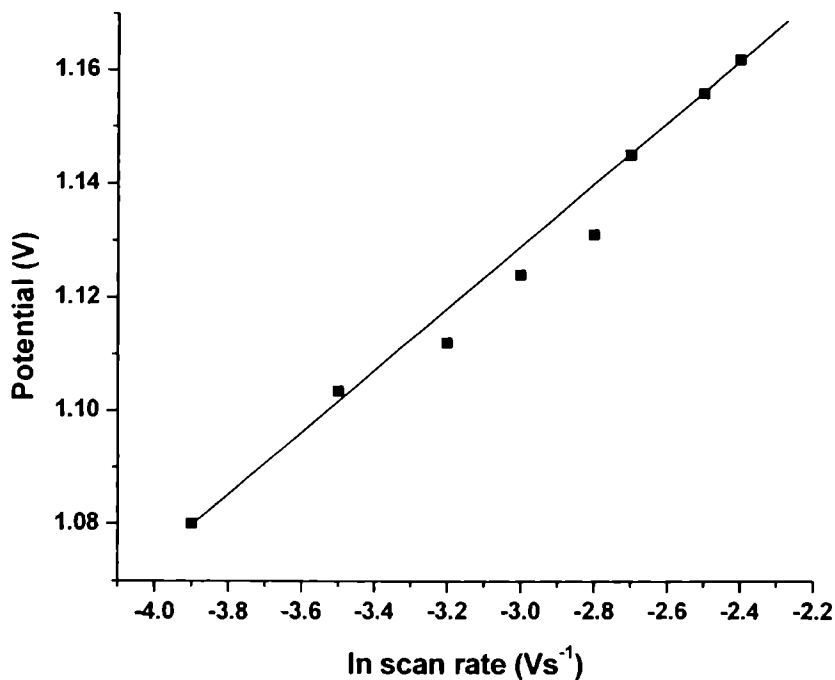


Figure 3.8. Differential pulse voltammograms of  $10^{-6}$  M TMP at scan rates 20, 30, 40, 50, 60, 70, 80  $\text{mVs}^{-1}$  (from top to bottom)



**Figure 3.9.** Variance of anodic peak current of TMP with scan rate in the range 20 – 60 mVs<sup>-1</sup>



**Figure 3.10.** Plot of ln scan rate versus anodic potential

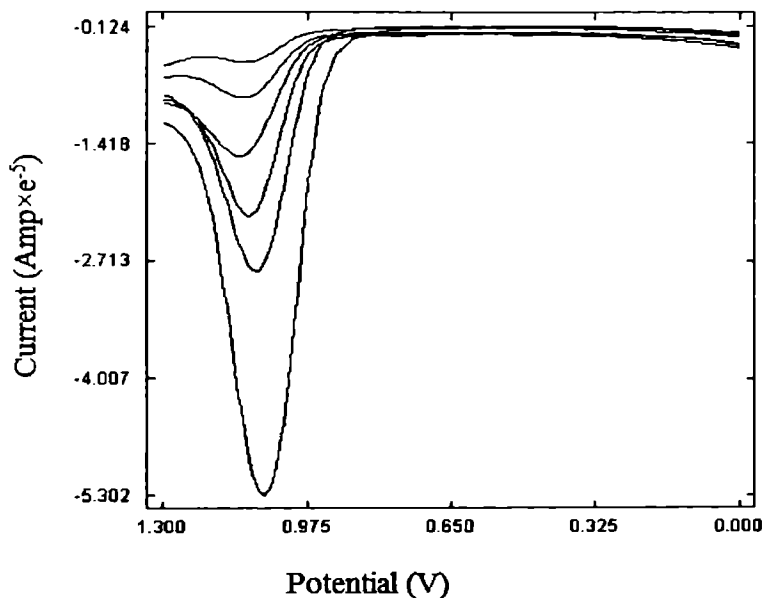


Figure 3.11. Differential pulse voltammograms of oxidation of TMP of concentrations  $10^{-3}$ ,  $10^{-4}$ ,  $10^{-5}$ ,  $10^{-6}$ ,  $10^{-7}$ ,  $10^{-8}$  M (from bottom to top)

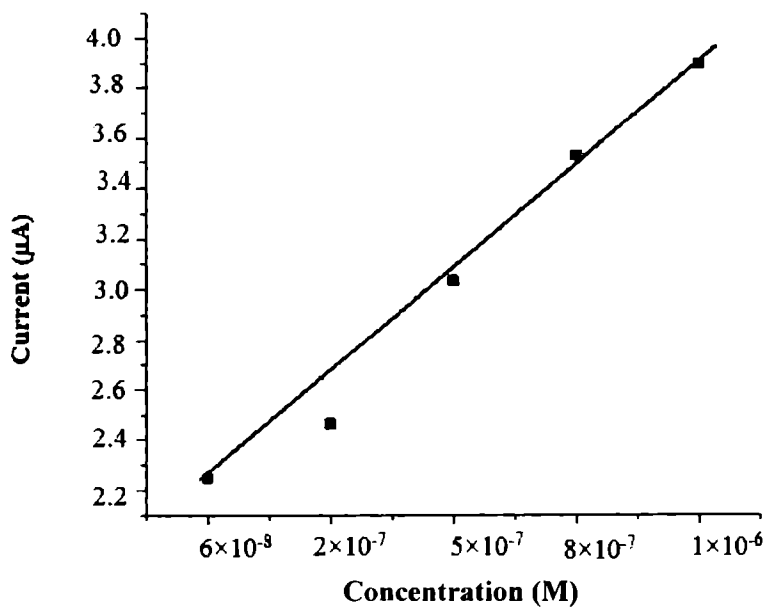
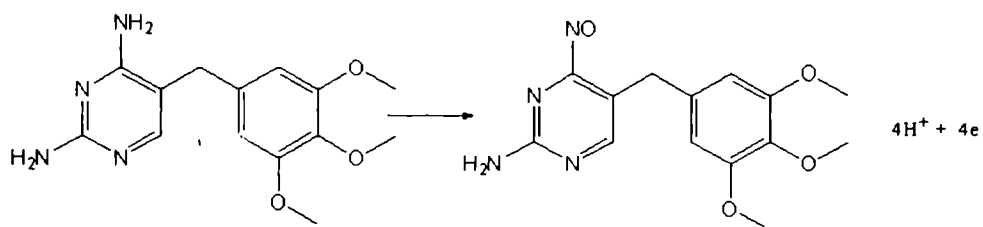


Figure 3.12. Dependence of peak current on the concentrations of TMP in the range  $6 \times 10^{-8}$  -  $1 \times 10^{-6}$  M



**Scheme 3.1. Mechanism of oxidation of TMP**

.....

## METALLOPORPHYRIN MODIFIED ELECTRODE FOR THE VOLTAMMETRIC DETERMINATION OF AMBROXOL

|                 |                                    |       |
|-----------------|------------------------------------|-------|
| <b>Contents</b> | 4.1. <i>Introduction</i>           | ..... |
|                 | 4.2. <i>Experimental</i>           | ..... |
|                 | 4.3. <i>Results and Discussion</i> | ..... |
|                 | 4.4. <i>Conclusions</i>            | ..... |

This chapter discusses TMOPPMn(III)Cl modified glassy carbon electrode (TMOPPMn(III)Cl/GCE) for the determination of ambroxol (AMX). The electrocatalytic nature of TMOPPMn(III)Cl/GCE for the determination of AMX is evident from the favorable reduction in oxidation overpotential of AMX. Various electrochemical parameters were optimized for the determination of AMX. The detection limit of AMX is found to be  $4.6 \times 10^{-9}$  M. The developed sensor was used for the determination of AMX in human urine and pharmaceutical product.

### 4.1 Introduction

Ambroxol (AMX), the structure of which is shown in Figure 4.1 is a mucolytic agent used in the treatment of respiratory disorders associated with viscid or excessive mucus. It is the active ingredient of Mucosolvan, Mucobrox, Lasolvan, Mucoangin, Surbronic and Lysopain. The substance is a mucoactive drug with several properties including secretolytic and secretomotoric actions that restore the physiological clearance mechanisms of the respiratory tract, which play an important role in the body's natural defence mechanisms. It stimulates the synthesis and release of surfactant by type

II pneumocytes. Surfactants act as an anti-glue factor by reducing the adhesion of mucus to the bronchial wall, in improving its transport and in providing protection against infection and irritating agents.

Preclinically, AMX, has been shown to increase respiratory tract secretion. It enhances pulmonary surfactant production and stimulates ciliary activity. It is an active metabolite of bromhexine and acts to reduce the viscosity and tenacious mucus secretions by fragmentation of long mucopolysacchride chains. These actions result in improved mucus flow and transport. AMX is indicated as "secretolytic therapy in bronchopulmonary diseases associated with abnormal mucus secretion and impaired mucus transport. It promotes mucus clearance, facilitates expectoration and eases productive cough, allowing patients to breathe freely and deeply". There are many different formulations developed since the first marketing authorisation in 1978. AMX is available as syrup, tablets, pastilles, dry powder sachets, inhalation solution, drops and ampules as well as effervescent tablets.

There are no absolute contraindications for AMX, but in patients with gastric ulceration relative caution should be observed. It is advisable to avoid its use during the first trimester of pregnancy.<sup>134</sup>

Several analytical methods have been reported for the determination of AMX in pharmaceutical formulations or biological samples that include HPLC,<sup>135-137</sup> gas chromatography,<sup>137</sup> UV-visible spectrophotometry,<sup>137-139</sup> capillary isotachopheresis,<sup>140</sup> sequential injection chromatography,<sup>141</sup> capillary electrophoresis,<sup>142</sup> LC-MS,<sup>143</sup> capillary gas liquid chromatography,<sup>144</sup> potentiometry,<sup>145</sup> voltammetry<sup>146-148</sup> and amperometry.<sup>149</sup> Some of these reported methods require time-consuming sample preparation or expensive instrumentation. In the effort to develop a voltammetric method for the

determination of AMX, with much lower detection limit than that of the reported works, the present study employed a glassy carbon electrode (GCE) which was modified with [5,10,15,20-tetrakis(4-methoxyphenyl)porphyrinato] manganese(III)chloride (TMOPPMn(III)Cl). As no work dealing with the electrooxidation of AMX on metalloporphyrin incorporated GCE has been reported, it was of interest to pursue the anodic behaviour of the AMX because of the presence of an electrooxidisable amino group in it.

## **4.2 Experimental**

### **4.2.1 Fabrication of TMOPPMn(III)Cl modified GCE (TMOPPMn(III)Cl/GCE)**

2 mg of TMOPPMn(III)Cl was dissolved in a mixture of 300  $\mu$ l nafion and 200  $\mu$ l ethanol. The solution was then agitated ultrasonically for about half an hour to get a stable and homogeneous solution. The GCE was cleaned as detailed in section 2.3. TMOPPMn(III)Cl/GCE was prepared by dropping 2 $\mu$ l of TMOPPMn(III)Cl solution onto the clean GCE surface and evaporating the solvent at room temperature.

### **4.2.2 Preparation of analyte sample**

Stock solution of AMX ( $1 \times 10^{-2}$  M) was prepared in methanol. Standard solutions of the analyte ( $1 \times 10^{-3}$  M –  $1 \times 10^{-8}$  M) were prepared by serial dilution of the stock solution using acetate buffer.

### **4.2.3 Electrochemical measurements of AMX**

AMX in acetate buffer solution was taken in the electrochemical cell and was analysed using various voltammetric techniques. Differential pulse voltammograms of AMX from 0 mV to 1500 mV were recorded and finally peak current at 884 mV was measured for AMX. Surface studies of TMOPPMn(III)Cl/GCE were done and is detailed in section 3.3.1.

### 4.3 Results and discussion

#### 4.3.1 Electrocatalytic oxidation of AMX on TMOPPMn(III)Cl/GCE and optimization of the developed method

##### 4.3.1.1 Comparison of the electrochemical behaviour of AMX at bare GCE and TMOPPMn(III)Cl/GCE

The electrochemical behaviour of AMX at a TMOPPMn(III)Cl/GCE has been investigated using Differential Pulse Voltammetry (DPV) and Linear Sweep Voltammetry (LSV). Figure 4.2 shows the differential pulse (DP) voltammograms of  $10^{-3}$  M AMX in acetate buffer of pH 2 at bare GCE (curve a) and TMOPPMn(III)Cl/GCE (curve b) respectively. All the DPV experiments of AMX were performed at pulse width 50 ms, pulse period 200 ms and pulse amplitude 50 mV. It is evident that the electrooxidation of AMX occurs at 1012 mV on bare GCE. However, the same process occurs at a potential of 884 mV on the modified GCE. A slight enhancement in current response (1.5 times) is observed with the modified GCE compared to bare GCE. The voltammetric behavior of a mixture of  $10^{-3}$  M of TMP and AMX was analysed on TMOPPMn(III)Cl/GCE. From Figure 4.3 it is clear that two distinct peaks corresponding to the oxidation of TMP (curve a) and AMX (curve b) are obtained.

##### 4.3.1.2 Influence of various supporting electrolyte

The electrochemical performance of  $10^{-3}$  M AMX was tested in various supporting electrolytes like acetate buffer, citrate buffer, phosphate buffer, lithium perchlorate, potassium nitrate, sulphuric acid and sodium hydroxide to investigate which of them yielded the best sensor response using DPV. On the basis of higher peak current and better peak shape, it is inferred that the oxidation response of AMX at the modified electrode is much better in acetate buffer than that in other medium. Thus acetate buffer was used as the experimental medium for the further studies of AMX.

#### **4.3.1.3 Effect of pH of the medium**

The voltammetric response of  $10^{-3}$  M AMX in acetate buffer of various pH (2-10) was investigated using DPV. It is to be mentioned that the modified electrode exhibited no electrochemical response in basic conditions. As pH increased from 2 to 7, anodic current decreased as shown in Figure 4.4. Maximum current was obtained at pH 2 and hence pH 2 was fixed as the optimal pH.

#### **4.3.1.4 Effect of volume of TMOPPMn(III)Cl solution dropped on GCE**

The amount of TMOPPMn(III)Cl solution on the GCE directly determines the thickness of the TMOPPMn(III)Cl film. As can be seen from Figure 4.5, it is found that the oxidation peak current of  $10^{-3}$  M AMX increases, while gradually increasing the volume of TMOPPMn(III)Cl solution from 1 to 2  $\mu$ l. The enhancement of current indicates that the number of catalytic sites increase with the increase of the amount of TMOPPMn(III)Cl. Further increasing the volume of TMOPPMn(III)Cl solution, results in the decrease of the peak current. This is because nafion used as one of the solvent is a kind of insulator that blocks the electron transfer. Due to uncompensated resistive effects or lowering of the charge transfer rate, the peak current is conversely decreased. Hence, the volume of TMOPPMn(III)Cl solution was fixed to be 2  $\mu$ l.

#### **4.3.1.5 Effect of preconcentration of AMX**

A study on the preconcentration of  $10^{-3}$  M AMX on TMOPPMn(III)Cl/GCE as shown in Figure 4.6 reveals that as accumulation time increases, anodic peak current decreases which indicates that AMX does not undergo an adsorptive preconcentration.

#### **4.3.1.6 Effect of scan rate on the oxidation of AMX**

To ascertain the nature of electrochemical process of AMX and to know the mechanism of electrooxidation of AMX on the modified electrode, the

effect of the potential sweep rate upon the voltammetric response of  $10^{-3}$  M AMX in acetate buffer of pH 2 was studied using linear sweep voltammetry. The scan rate was varied from  $10 \text{ mVs}^{-1}$  to  $100 \text{ mVs}^{-1}$ . The peak current increases with the scan rate and in addition exhibited a linear relation to square root of scan rate as described in Figure 4.7 with the linear regression equation  $i_p = 3.5456v^{1/2} + 2.9147$ , where  $v^{1/2}$  stands for square root of scan rate ( $r = 0.9954$ ). This confirms the electrooxidation of AMX to be diffusion controlled.

#### 4.3.1.7 Investigation of the possible mechanistic pathway for the electrooxidation of AMX

The plot of  $\ln$  scan rate versus anodic potential of AMX resulted in a linear graph as shown in Figure 4.8 with a slope of 0.0487. Based on the Laviron's equation,<sup>131</sup> the slope of this plot equals to  $RT/\alpha nF$ , where  $\alpha$  is assumed to be 0.5 for the totally irreversible electrode process. The calculation gave the number of electrons involved in the electrochemical reaction ( $n$ ) to be 1.1, which can be considered as one electron process. Based on literature reports,<sup>146,150,151</sup> and based on calculated value, the possible path taken by AMX for its electrooxidation is described in scheme 4.1.

#### 4.3.1.8 Quantification of AMX

In order to evaluate the efficiency of the catalytic reaction at the modified electrode, the effect of concentration of AMX upon its DP voltammetric response was examined. Figure 4.9 shows the DP voltammograms of electrooxidation of AMX of concentrations in the range  $10^{-3}$  M –  $10^{-8}$  M in acetate buffer of pH 2.

The anodic current showed linearity with increasing concentration of AMX in the range  $3 \times 10^{-8}$  M -  $3 \times 10^{-7}$  M and the linear regression equation is given as  $i_p = 0.9741c + 2.4168$ , where  $c$  stands for concentration ( $r = 0.9999$ ,  $n = 5$ ). From

the calibration curve, shown in Figure 4.10, detection limit of  $4.6 \times 10^{-9}$  M ( $1.9 \times 10^{-12}$  gml<sup>-1</sup>) could be achieved.

#### **4.3.1.9 Reproducibility and stability**

Relative standard deviation of 4.9% for the current response of  $10^{-3}$  M AMX (n=10) shows good reproducibility. The long term stability of TMOPPMn(III)Cl/GCE was evaluated by measuring the current responses at a fixed AMX concentration of  $10^{-3}$  M over a period of 3 weeks. The electrode was used daily and was stored in distilled water after use. The experimental results indicated that the current responses deviated only 5.8% revealing that the fabricated sensor possesses long term stability.

#### **4.3.2 Selectivity**

As shown in Table 4.1, the additions of upto  $10^{-1}$  M of citric acid, urea, NaCl, K<sub>2</sub>SO<sub>4</sub> and lactose do not interfere with the voltammetric response of  $10^{-3}$  M AMX. However glycine and ascorbic acid is found to interfere severely.

#### **4.3.3 Application potential of the sensor**

Experiments were performed analyzing commercial formulation containing AMX namely, Mucolite. After powdering five tablets, their average mass was determined. Required amount of it to prepare  $10^{-3}$  M was transferred to 25 ml standard flask and made up to the mark using methanol. The solution was filtered. Solutions of different concentrations were made by taking suitable aliquots of the clear filtrate and diluting them with acetate buffer. DP voltammograms of the oxidation of various concentrations of the tablet were recorded and the unknown concentrations were determined from the calibration graph. The recoveries are in the range of 97-99%. Coefficient

of variance (C.V) for six replicate determinations was found to be 3.06% and the results are tabulated in Table 4.2.

The urine sample was spiked with AMX by adding several aliquots of AMX in different proportion to get various concentration of AMX ( $10^{-4}$  M to  $10^{-6}$  M). The DP voltammograms were recorded applying the optimal conditions for their analytical determination. Recoveries lie in the range of 98-101%. The results of the voltammetric analysis of spiked samples of urine shows good recovery as can be seen from Table 4.3.

#### 4.3.4 Comparison with the reported works

The developed method was compared with the UV spectrophotometry, the standard method for the determination of AMX.<sup>152</sup> Stock solution  $1 \times 10^{-3}$  M AMX was prepared in 0.05 M  $H_2SO_4$ . Various concentration of AMX were prepared by diluting the stock solution with 0.05 M  $H_2SO_4$ . The UV measurements gave a lower detection limit of  $7.6 \times 10^{-9}$  gml<sup>-1</sup>. A comparison of the reported works with the present work is tabulated in Table 4.4.

#### 4.4 Conclusions

In summary, a simple voltammetric method has been developed for the determination of AMX using TMOPPMn(III)Cl/GCE, evaluated the electrochemical performance and achieved a sensitive determination of AMX in nanomolar concentrations. TMOPPMn(III)Cl/GCE exhibited a lowest detection limit of  $4.6 \times 10^{-9}$  M. The electrocatalytic nature of TMOPPMn(III)Cl/GCE for the determination of AMX is evident from the favorable reduction in oxidation overpotential of AMX. The significant advantages of this method are that it comprises low detection limit, sensitivity, cost effectiveness, stability and reproducibility. It is also shown that the developed sensor can be used for the determination of AMX in human urine and pharmaceutical product.

**Table 4.1. Influence of  $10^{-1}$  M of foreign species on the anodic peak current of  $10^{-3}$  M AMX**

| Foreign species    | Signal change (%) |
|--------------------|-------------------|
| Citric acid        | -3.00             |
| Urea               | -4.90             |
| Sodium chloride    | -4.60             |
| Potassium sulphate | -3.30             |
| Lactose            | 4.80              |
| Glycine            | 30.50             |
| Ascorbic acid      | -24.60            |

**Table 4.2. Determination of AMX in tablet**

| Tablet    | Declared amount (mg/tablet) | Found amount* (mg/tablet) | S.D  | C.V (%) |
|-----------|-----------------------------|---------------------------|------|---------|
| Ambrolite | 30                          | 29                        | 0.89 | 3.06    |

*Average of six replicates\**

**Table 4.3. Determination of AMX in urine sample**

| Added amount of AMX (M) in urine sample | Found amount of AMX (M) in urine sample | Recovery% |
|---|---|-----------|
| $3.00 \times 10^{-7}$                   | $2.96 \times 10^{-7}$                   | 98.6      |
| $7.00 \times 10^{-7}$                   | $7.06 \times 10^{-7}$                   | 100.9     |
| $9.00 \times 10^{-7}$                   | $8.91 \times 10^{-7}$                   | 99.1      |

**Table 4.4. Comparison of the developed method with other reported works for the determination of AMX**

| S.No: | Method   | Lower Detection limit                                    |
|-------|--|--|
| 1     | HPLC <sup>135</sup>  | $4.0 \times 10^{-9} \text{ gml}^{-1}$                    |
| 2     | HPLC <sup>136</sup>  | $7.4 \times 10^{-7} \text{ gml}^{-1}$                    |
| 3     | HPLC <sup>137</sup>  | $1.8 \times 10^{-7} \text{ gml}^{-1}$                    |
| 4     | GC <sup>137</sup>  | $2.1 \times 10^{-6} \text{ gml}^{-1}$                    |
| 5     | UV spectrometric method <sup>137</sup>                         | $8.0 \times 10^{-8} \text{ gml}^{-1}$                    |
| 6     | Derivative UV spectrophotometric method <sup>138</sup>         | $5.0 \times 10^{-6} \text{ gml}^{-1}$                    |
| 7     | Automatic extraction spectrophotometric method <sup>139</sup>  | $5.0 \times 10^{-7} \text{ gml}^{-1}$                    |
| 8     | Capillary isotachopheresis <sup>140</sup>                      | $4.0 \times 10^{-6} \text{ gml}^{-1}$                    |
| 9     | Sequential injection Chromatography <sup>141</sup>             | $5.0 \times 10^{-7} \text{ gml}^{-1}$                    |
| 10    | Capillary electrophoresis and fluorescence <sup>142</sup>      | $8.0 \times 10^{-9} \text{ gml}^{-1}$                    |
| 11    | LC – MS <sup>143</sup>   | $2.0 \times 10^{-10} \text{ gml}^{-1}$                   |
| 12    | Capillary gas liquid chromatography <sup>144</sup>             | $3.0 \times 10^{-9} \text{ gml}^{-1}$                    |
| 13    | Potentiometry <sup>145</sup>                                   | $9.8 \times 10^{-11} \text{ gml}^{-1}$                   |
| 14    | Voltammetry <sup>146</sup>                                     | $3.6 \times 10^{-7} \text{ gml}^{-1}$                    |
| 15    | Adsorptive stripping voltammetry <sup>147</sup>                | $2.0 \times 10^{-7} \text{ gml}^{-1}$                    |
| 16    | Voltammetry using MWCNT/GCE <sup>148</sup>                     | $2.5 \times 10^{-6} \text{ gml}^{-1}$                    |
| 17    | Amperometry <sup>149</sup>                                     | $2.9 \times 10^{-8} \text{ gml}^{-1}$                    |
| 18    | UV spectrophotometry <sup>152</sup><br>(standard method)       | $7.6 \times 10^{-9} \text{ gml}^{-1}$                    |
| 19    | <b>Voltammetry using TMOPPMn(III)Cl/GCE<br/>(present work)</b> | <b><math>1.9 \times 10^{-12} \text{ gml}^{-1}</math></b> |

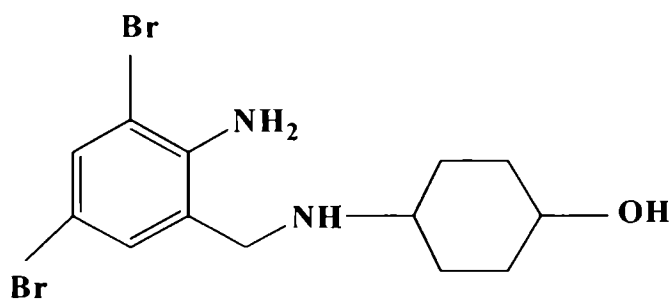


**Figure 4.1. Structure of AMX**

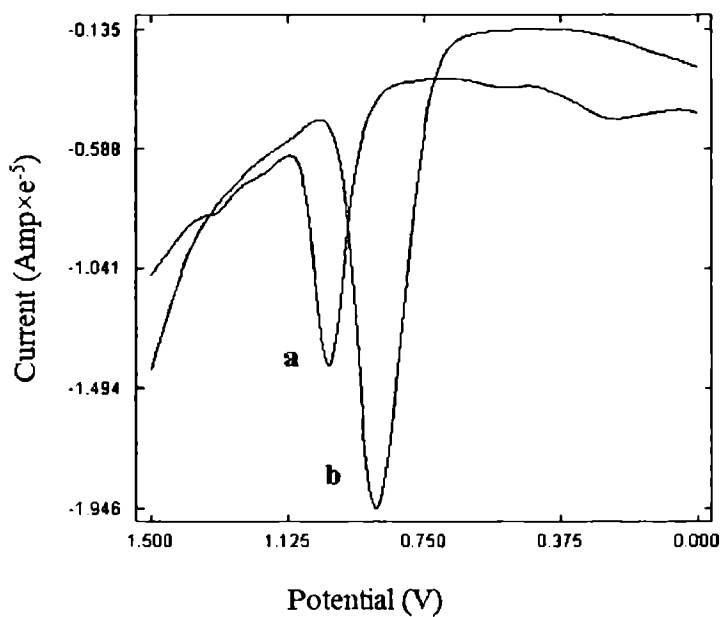


**Figure 4.2. Differential pulse voltammograms of the oxidation of  $10^{-3}$  M AMX at a) bare GCE b) TMOPPMn(III)Cl/GCE**

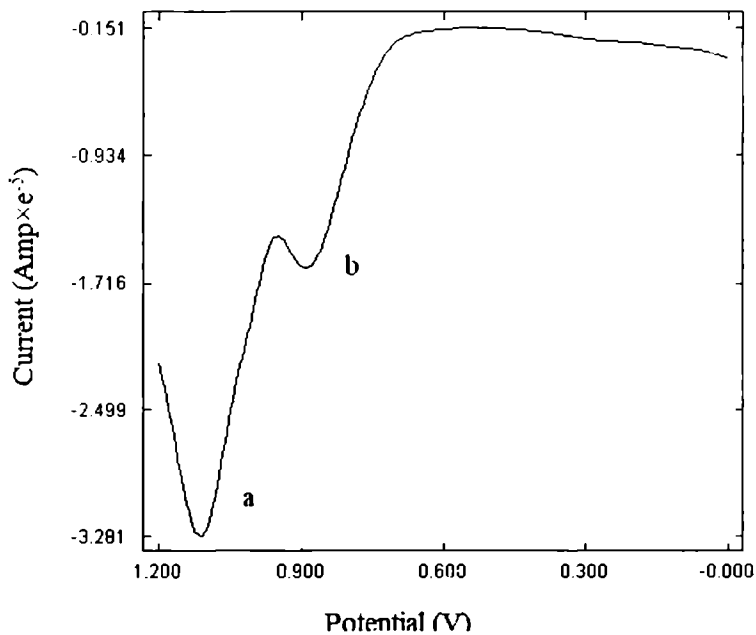


Figure 4.3. Differential pulse voltammograms of the oxidation of  $10^{-3}$  M of (a) TMP and (b) AMX at TMOPPMn(III)Cl/GCE

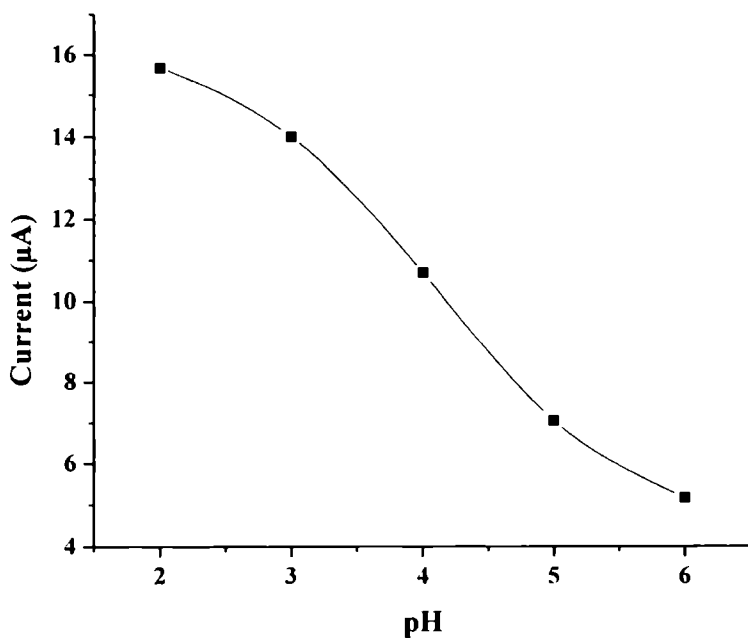
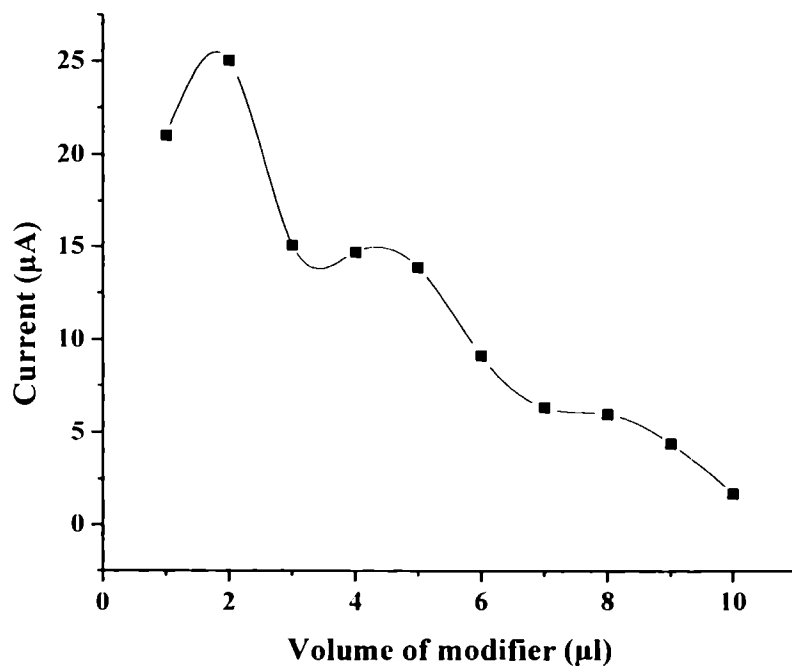
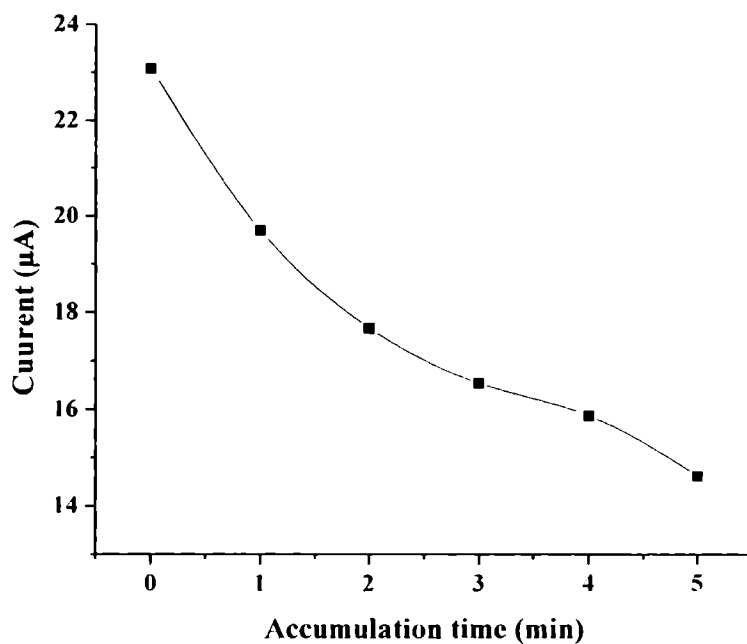


Figure 4.4. Variation of anodic peak current with pH of the medium



**Figure 4.5.** Relationship between anodic peak current and volume of the modifier



**Figure. 4.6.** Effect of accumulation time of AMX on the anodic peak current

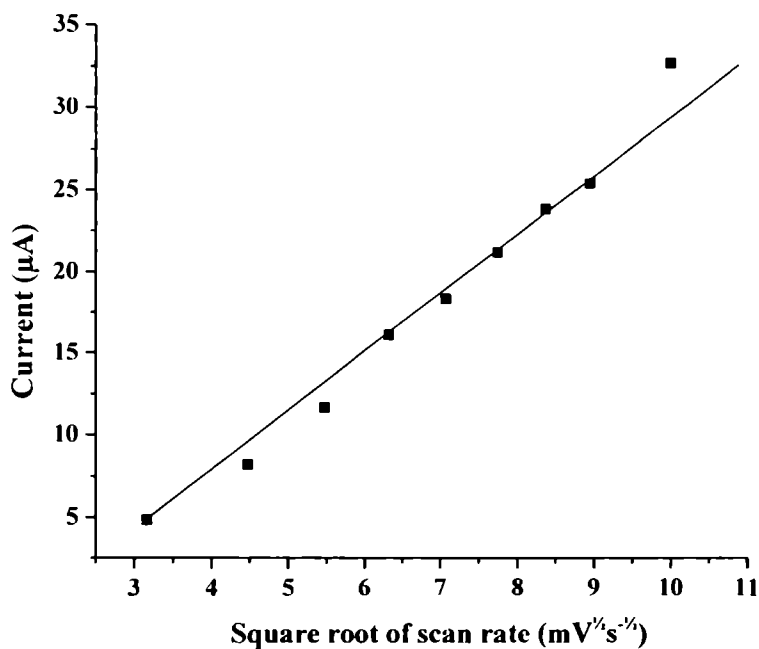


Figure 4.7. Plot of square root of scan rate versus anodic peak current of  $10^{-3}$  M AMX

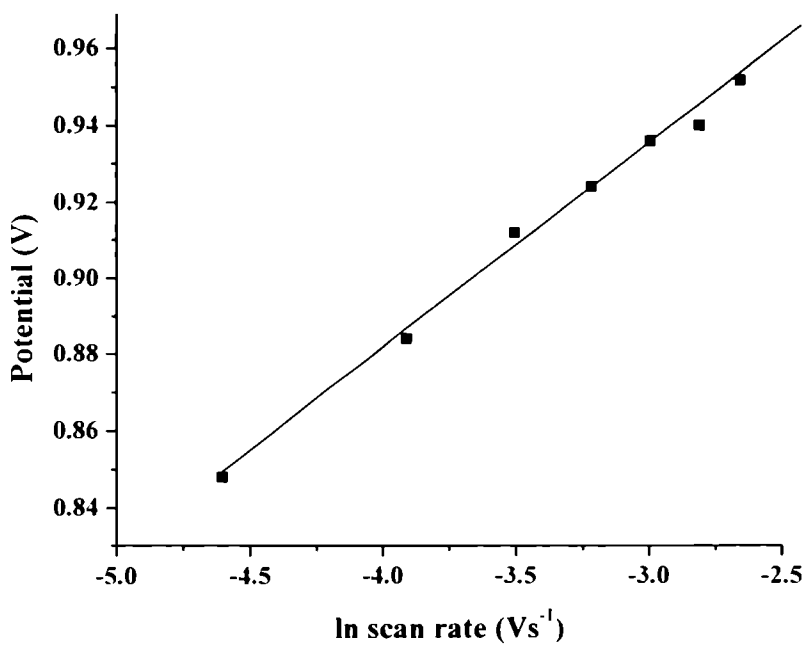
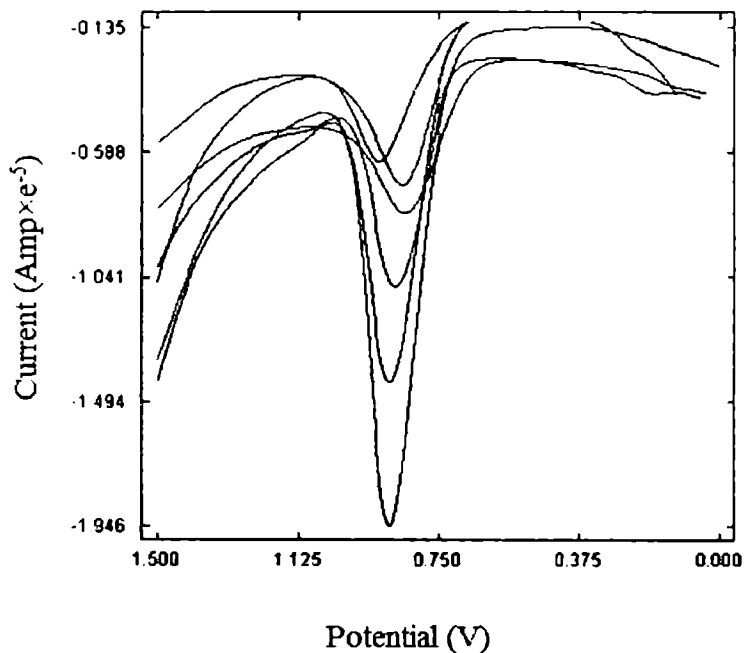
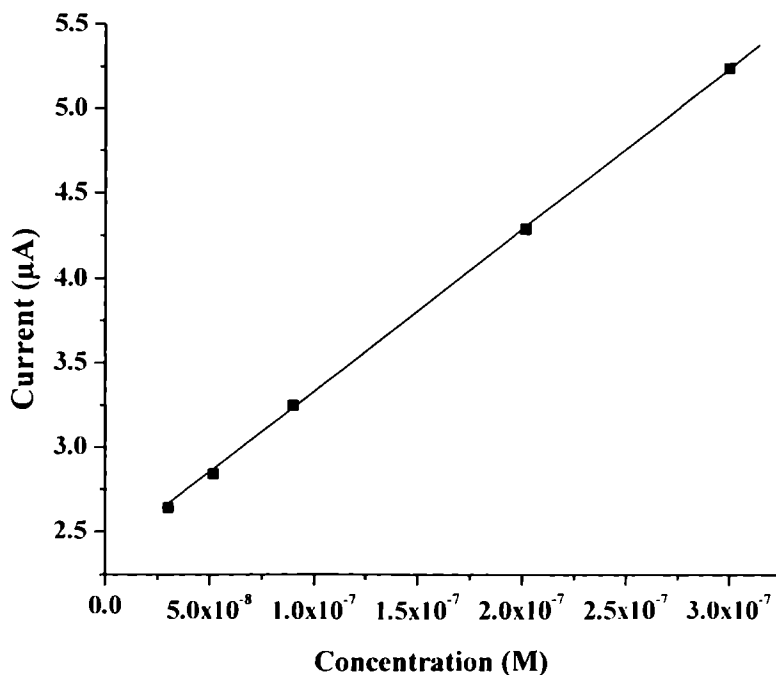


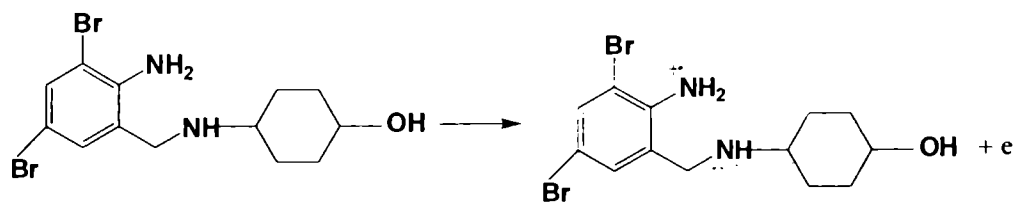
Figure.4.8. Variation of ln scan rate versus anodic potential



**Figure 4.9.** Differential pulse voltammograms of the oxidation of  $10^{-3}$ ,  $10^{-4}$ ,  $10^{-5}$ ,  $10^{-6}$ ,  $10^{-7}$ ,  $10^{-8}$  M AMX (in the order of bottom to top)



**Figure 4.10.** Nature of dependence of anodic peak current with concentration in the range  $3 \times 10^{-8}$  -  $3 \times 10^{-7}$  M



**Scheme 4.1. Suggested mechanism for the electrooxidation of AMX**

.....

## POLY(MALACHITE GREEN) MODIFIED GLASSY CARBON ELECTRODE FOR THE VOLTAMMETRIC DETERMINATION OF SULFAMETHOXAZOLE

|                 |                                    |
|-----------------|------------------------------------|
| <b>Contents</b> | 5.1. <i>Introduction</i>           |
|                 | 5.2. <i>Experimental</i>           |
|                 | 5.3. <i>Results and Discussion</i> |
|                 | 5.4. <i>Conclusions</i>            |

This chapter details the electrooxidation of sulfamethoxazole (SMX) at poly(malachite green) modified glassy carbon electrode (PMG/GCE). At the PMG/GCE, the anodic peak of SMX shifted by about 652 mV to lower potential than that at bare GCE. A concentration range of  $10^{-3}$  M -  $10^{-9}$  M of SMX was analysed and a linear response range was observed between  $3 \times 10^{-9}$  M -  $1 \times 10^{-7}$  M with a detection limit of  $1 \times 10^{-9}$  M. A detailed investigation regarding the electrochemical characteristics and selectivity was carried out. To evaluate the application potential of the developed sensor, it was successfully applied to determine SMX in commercial formulation and body fluid.

### 5.1 Introduction

Sulfamethoxazole (SMX) represented in Figure 5.1 is an antibacterial drug which has been used since 1960's in the treatment of various systemic infections in humans and other species. Its primary activity is against susceptible forms of streptococcus, staphylococcus aureus, escherichia coli, haemophilus influenzae and oral anaerobes. SMX is often used as a synergistic

combination with trimethoprim in the ratio 5:1. It has been mainly used in the treatment of acute urinary tract infections. It has also been used against gonorrhoea, meningitis and serious respiratory tract infections and prophylactically against susceptible meningococci. It can also be used to treat toxoplasmosis and it is the drug of choice for *Pneumocystis pneumonia*, which affects primarily patients with HIV. Despite its relatively unfavourable pattern of tissue distribution, it is the sulfonamide most commonly used around the world in combination with trimethoprim or pyrimethamine for the treatment of various systemic infections. Sulfonamides are structural analogs and competitive antagonists of para-aminobenzoic acid. They inhibit normal bacterial utilization of para-aminobenzoic acid for the synthesis of folic acid, an important metabolite in DNA synthesis. The effects seen are usually bacteriostatic in nature. Folic acid is not synthesized in humans, but is instead a dietary requirement. This allows for the selective toxicity to bacterial cells over human cells. Bacterial resistance to SMX is caused by mutations in the enzymes involved in folic acid synthesis that prevent the drug from binding to it. The main fraction of the drug is excreted in the urine.

The most common side effect of SMX is gastrointestinal upset that cause nausea, severe stomach or abdomen pains. Allergies to sulfa-based medications typically cause skin rashes, hives and breathing trouble. Headaches and muscle pains commonly occur when taking SMX. It is also a substance that induces Stevens–Johnson syndrome.<sup>153</sup>

Some of the methods reported for the determination of SMX include titrimetry,<sup>154</sup> HPLC,<sup>155-157</sup> reversed phase liquid chromatography,<sup>158</sup> spectrophotometry,<sup>159,160</sup> flow injection method,<sup>161-163</sup> capillary electrophoresis,<sup>164,165</sup> LC-MS<sup>166</sup> and voltammetry.<sup>19,84,167-172</sup> Most of the methods for the determination

of sulfa-drugs suffer from disadvantages like lack of sensitivity, involves heating or extraction, requires long time for the completion of reaction, narrow detection limit etc. Voltammetric methods are comparatively rapid, simple and less expensive. In the effort to develop a voltammetric method that would result in very low detection limit of SMX with high selectivity and sensitivity, poly(malachite green) modified glassy carbon electrode (PMG/GCE) was fabricated. The structure of malachite green is depicted in Figure 5.1.

## **5.2 Experimental**

### **5.2.1 Fabrication of poly(malachite green) modified glassy carbon electrode PMG/GCE**

Glassy carbon electrode was cleaned as explained in section 2.3. The cleaned GCE was electroactivated by cyclic sweepings from -600 mV to 1500 mV at  $50 \text{ mVs}^{-1}$  for 10 minutes in 0.5 M  $\text{H}_2\text{SO}_4$ . Electropolymerisation of malachite green was conducted on the resulting GCE by scanning from -1400 mV to 1000 mV at a sweep rate of  $100 \text{ mVs}^{-1}$  in  $10^{-4}$  M malachite green using 0.01 M phosphate buffer solution (pH 6.7) for 20 cycles.<sup>87,91</sup> Finally a colourful and transparent film was found to form on the electrode surface. The obtained PMG/GCE was washed with double distilled water. Figure 5.3 displays the cyclic voltammograms of the electropolymerisation. One obvious anodic peak and cathodic peak were noticed. The surface of the modified electrode was examined by SEM.

### **5.2.2 Preparation of analyte sample**

Stock solution of SMX ( $1 \times 10^{-2}$  M) was prepared in methanol. Standard solutions of the analyte ( $1 \times 10^{-3}$  M –  $1 \times 10^{-9}$  M) were prepared by serial dilution of the stock solution using citrate buffer.

### 5.2.3 Voltammetric measurements of SMX

The voltammetric behavior of SMX on PMG/GCE in citrate buffer was studied by sweeping the potential from 0 V to 1.2 V and peak current at 253 mV was recorded. This was followed by optimization of the electrochemical parameters.

## 5.3 Results and Discussion

### 5.3.1 Surface studies of PMG/GCE

The surfaces of bare GCE and PMG/GCE were characterised using SEM measurements. Figure 5.4a and 5.4b reveals the surfaces of bare GCE and PMG/GCE respectively which proves considerable modification of GCE with PMG. PMG forms a porous network, which is evident from Figure 5.4c. The porosity can lead to large surface area of PMG/GCE.

Cyclic voltammetry of  $2 \times 10^{-3}$  M potassium ferricyanide solution was carried out at both bare GCE and PMG/GCE at different scan rates. The obtained current was plotted against the square root of scan rates in both the cases. The slopes of the straight lines were determined and from the Randles-Sevcick equation for reversible reaction,

$$i_p = (2.687 \times 10^5) n^{3/2} \nu^{1/2} D^{1/2} A c$$

effective surface area of bare GCE and PMG/GCE were calculated, where  $i_p$  refers to peak current,  $n$  is the number of electrons transferred,  $D$  is the diffusion coefficient,  $A$  is the surface area of the electrode,  $c$  is the concentration of potassium ferricyanide solution and  $\nu$  stands for scan rate. Taking  $n=1$  and  $D=7.6 \times 10^{-6} \text{ cm}^2 \text{ s}^{-1}$ , the effective surface area of bare GCE was obtained as  $0.0669 \text{ cm}^2$  while that of PMG/GCE was calculated to be  $0.2934 \text{ cm}^2$ . The large surface area of PMG/GCE compared to bare GCE is evident

from the calculated values obtained, which is due to the porous nature of PMG revealed by the SEM images.

With the knowledge that PMG is conducting and has catalytic nature (owing to the large surface area and presence of functional groups),<sup>90,91</sup> PMG/GCE was used as the sensing matrix for the electrochemical determination of SMX.

### **5.3.2 Investigation of the electrochemical activity of PMG/GCE**

The voltammetric response of PMG/GCE towards various drugs was tested. It was found that ceftriaxone sodium and alendronate sodium couldn't be sensed by PMG/GCE, whereas acyclovir gave the response at a slightly higher potential than that at bare GCE with little improvement in current. But for SMX, the potential lowering was by 652 mV.

### **5.3.3 Electrochemical behavior of SMX and optimization of the developed method**

#### **5.3.3.1 Comparison of the electrochemical behavior of SMX at bare GCE and PMG/GCE**

The electrochemical oxidation of  $1 \times 10^{-3}$  M SMX was studied on bare GCE and PMG/GCE using square wave voltammetry (SWV) with square wave amplitude 25 mV and frequency 15 Hz. Figure 5.5 compares the oxidation responses of SMX at bare GCE and PMG/GCE. An anodic peak at 908 mV (curve a) and 252 mV (curve b) was obtained for SMX at bare GCE and PMG/GCE respectively.

Indeed PMG on GCE facilitates the oxidation of SMX to occur at a very low potential compared to that of bare GCE. Further, the oxidation of SMX was found to be an irreversible process evidenced by the absence of reduction

peak in the reverse scan. More electrochemical studies of SMX were carried out on PMG/GCE and optimal conditions were probed for.

### 5.3.3.2 Influence of various supporting electrolyte

The medium in which the electrochemical reaction takes place might have a pronounced effect on the response of the analyte and therefore the oxidation process of  $1 \times 10^{-3}$  M of SMX was monitored in various electrolytes like acetate buffer, citrate buffer, phosphate buffer, lithium perchlorate, potassium nitrate, sodium hydroxide, potassium chloride and sulphuric acid by SWV. On the basis of higher peak current and better peak shape, it is inferred that the oxidation response of SMX at the modified electrode is much better in citrate buffer than that in other medium. Thus citrate buffer was used as the experimental medium for the further studies of SMX.

### 5.3.3.3 Effect of pH of the medium

The electrochemical response of  $1 \times 10^{-3}$  M SMX in citrate buffer of various pH (3 to 10) were evaluated by SWV. The experimental results showed that pH has a significant influence on the anodic peak current of SMX at PMG/GCE. It is deduced that as pH increases, anodic current increases and maximum current is obtained at pH 6, as can be seen from Figure 5.6. Above pH 6, the peak current diminished and for pH 9 and above no peak was obtained. This suggests the involvement of  $H^+$  in the oxidation of SMX at PMG/GCE. It is already reported that PMG forms a highly permeable membrane, where the permeation of  $H^+$  is in high speed.<sup>90</sup> Further studies were carried out with SMX in citrate buffer of pH 6.

### 5.3.3.4 Effect of accumulation of SMX

The preconcentration of  $1 \times 10^{-6}$  M SMX at PMG/GCE and the application of subsequent SWV scan were performed. The accumulation was carried out for

different time span and after each accumulation step, anodic current of SMX was recorded using SWV and it was found that as accumulation time increases, current decreases. The results are shown in Figure 5.7. SMX does not undergo an adsorptive preconcentration at PMG/GCE.

### 5.3.3.5 Effect of scan rate

To ascertain the nature of the electrochemical process at PMG/GCE, the potential was scanned at increasing rates from 20 mVs<sup>-1</sup> to 80 mVs<sup>-1</sup> under the same experimental conditions for 10<sup>-3</sup> M SMX. A linear relationship was observed between the peak intensity  $i_p$  and the square root of the scan rate  $v^{1/2}$  (Figure 5.8) demonstrating that the phenomena is diffusion controlled rather than adsorption controlled. The regression equation for the linear graph is

$$i_p = 0.4625v^{1/2} + 2.0054 \quad (r = 0.9997, n = 5).$$

### 5.3.3.6 Probe for the possible mechanism of electrooxidation of SMX

Para amino substituted sulfonamides can be electrochemically oxidized at the -NH<sub>2</sub> group, but the reduction of -SO<sub>2</sub> group is very difficult to achieve. Earlier investigations<sup>173-175</sup> have addressed the electrochemical behaviour of sulfonamides and proposed an irreversible two electron pH dependent reaction path way for their oxidation in aqueous solutions.<sup>175</sup> In order to have an insight into the mechanism of the electrochemical oxidation of SMX at PMG/GCE, anodic potential E was plotted against ln scan rate as shown in Figure 5.9. The slope of the linear graph was determined. Based on the Laviron's equation,<sup>131</sup> the slope of this plot equals to RT/ $\alpha nF$ , where  $\alpha$  is assumed to be 0.5 for the totally irreversible electrode process. The calculation gave the number of electrons involved in the electrochemical reaction (n) to be 1.8 (close to 2). Thus SMX follows a two electron path

for its electrochemical oxidation at PMG/GCE. Based on this, a mechanism<sup>175</sup> can be proposed for the electrochemical oxidation of SMX, which is detailed in scheme 5.1. As can be seen in the mechanism, the protonated molecule of sulfamethoxazole loses two electrons and two protons to give iminobenzoquinone.

### 5.3.3.7 Estimation of lower detection limit of SMX

SWV of electrooxidation of  $3 \times 10^{-9}$  M -  $1 \times 10^{-3}$  M SMX were carried out. Under the optimal conditions, the oxidative peak current  $i_p$  of SMX has built up linearly with increasing concentration  $c$  in the range  $3 \times 10^{-9}$  M to  $1 \times 10^{-7}$  M (Fig 5.10) with the linear regression equation

$$i_p = 0.1056c + 1.3912 \quad (r = 0.9783)$$

Detection limit was estimated to be  $1 \times 10^{-9}$  M ( $2.28 \times 10^{-9}$  gml<sup>-1</sup>)

### 5.3.3.8 Reproducibility and stability of PMG/GCE

$1 \times 10^{-3}$  M SMX was determined repeatedly at the same surface of PMG/GCE for successive fifteen times and the average current was found to be 7.2234  $\mu$ A with a relative standard deviation (RSD) of 4.6%, which indicates good reproducibility.

### 5.3.4 Selectivity of PMG/GCE towards SMX

Electrochemical behaviour of SMX in presence of foreign species like glycine, urea, ascorbic acid, sodium chloride, potassium sulphate, lactose, dextrose and trimethoprim was investigated using SWV. As can be seen from Table 5.1 upto hundred fold concentration of the listed foreign species other than glycine did not interfere in the anodic response of  $1 \times 10^{-3}$  M SMX

(deviation below 5%). The results show the good selectivity of the modified electrode.

### **5.3.5 Application of the sensor in real samples**

In order to demonstrate the application potential of the developed sensor, preliminary experiments were performed analyzing commercial formulation containing SMX namely Bactrim. After powdering five tablets, their average mass was determined. Required amount of it to prepare  $10^{-3}$  M was transferred to 25 ml standard flask, dissolved and made up to the mark using methanol. The solution was filtered. Solutions of different concentrations were made by taking suitable aliquots of the clear filtrate and diluting them with citrate buffer. SW voltammograms of the oxidation of SMX in the tablet were recorded and the unknown concentrations were determined from the calibration graph. The recoveries are in the range of 95-97% and C.V for six replicate determinations was found to be 1.67 ( $\leq 3\%$ ) as shown in Table 5.2.

In order to test the accuracy of the proposed method, several aliquots of SMX were spiked into urine samples in different proportion to get various concentration of SMX ( $10^{-4}$  M to  $10^{-6}$  M). The SW voltammograms were recorded applying the optimal conditions for their analytical determination. Recoveries lie in the range of 96-103% as can be seen from Table 5.3.

### **5.3.6 Comparison with the reported works**

The present work was compared with the spectrophotometric method, the standard method for the determination of SMX.<sup>133</sup> A lower detection limit of about  $10^{-7}$  M is obtained using the standard method. Table 5.4 shows the

comparison of the present method with some of the reported works for the determination of SMX.

#### 5.4 Conclusions

An electronically conducting polymer PMG was synthesized electrochemically on the surface of the GCE. The surface of the PMG/GCE thus developed was characterized using SEM. PMG/GCE exhibited excellent catalytic activity towards the oxidation of SMX due to its large surface area and presence of functional groups. The oxidation overpotential of SMX could be lowered drastically at the PMG/GCE. Oxidation of SMX on PMG/GCE was found to be irreversible, diffusion controlled and occurs through 2 electron process. A very low detection limit of  $1 \times 10^{-9}$  M could be achieved for SMX. The modified electrode featured good reproducibility, selectivity and stability and allowed satisfactory determination of SMX in commercial sample and spiked urine samples.

**Table 5.1. Influence of  $10^{-1}$  M of foreign species on the anodic peak current of  $10^{-3}$  M SMX**

| S.No: | Foreign species    | Signal change % |
|-------|--------------------|-----------------|
| 1     | Glycine            | -6.20           |
| 2     | Urea               | -4.75           |
| 3     | Ascorbic acid      | -2.33           |
| 4     | Sodium chloride    | -4.92           |
| 5     | Potassium sulphate | -3.97           |
| 6     | Lactose            | 4.40            |
| 7     | Dextrose           | 4.82            |
| 8     | Trimethoprim       | 3.84            |

**Table 5.2. Determination of SMX in tablet**

| Tablet  | Declared amount<br>(mg/tablet) | Found amount*<br>(mg/tablet) | S.D  | C.V<br>(%) |
|---------|--------------------------------|------------------------------|------|------------|
| Bactrim | 400 mg                         | 367 mg                       | 6.12 | 1.67       |

*Average of six replicates\**

**Table 5.3. Determination of SMX in urine sample**

| Added amount of SMX<br>(M) in urine sample | Found amount of SMX<br>(M) in urine sample | Recovery% |
|--|--|-----------|
| $1.00 \times 10^{-7}$                      | $0.96 \times 10^{-7}$                      | 96.0      |
| $5.00 \times 10^{-7}$                      | $4.77 \times 10^{-7}$                      | 95.4      |
| $8.00 \times 10^{-7}$                      | $8.21 \times 10^{-7}$                      | 102.6     |

**Table 5.4. Comparison of the present work with some of the reported works**

| S.No: | Method  | Lower detection limit                   |
|-------|---|---|
| 1     | HPLC <sup>155</sup>   | $2.50 \times 10^{-8} \text{ gml}^{-1}$  |
| 2     | HPLC <sup>156</sup>   | $1.00 \times 10^{-7} \text{ gml}^{-1}$  |
| 3     | HPLC <sup>157</sup>   | $3.90 \times 10^{-7} \text{ gml}^{-1}$  |
| 4     | Reverse phase liquid chromatography <sup>158</sup>  | $3.56 \times 10^{-6} \text{ gml}^{-1}$  |
| 5     | Spectrophotometry <sup>159</sup>  | $4.00 \times 10^{-6} \text{ gml}^{-1}$  |
| 6     | Spectrophotometry <sup>160</sup>  | $3.35 \times 10^{-7} \text{ gml}^{-1}$  |
| 7     | Flow injection method <sup>161</sup>  | $9.50 \times 10^{-6} \text{ gml}^{-1}$  |
| 8     | Flow injection spectrophotometry <sup>162</sup>   | $5.00 \times 10^{-7} \text{ gml}^{-1}$  |
| 9     | Flow injection fluorimetry <sup>163</sup>   | $7.00 \times 10^{-9} \text{ gml}^{-1}$  |
| 10    | Capillary zone electrophoresis <sup>164</sup>   | $1.00 \times 10^{-5} \text{ gml}^{-1}$  |
| 11    | Capillary electrophoresis <sup>165</sup>  | $2.53 \times 10^{-8} \text{ gml}^{-1}$  |
| 12    | LC-Tandem MS <sup>166</sup>   | $4.30 \times 10^{-16} \text{ gml}^{-1}$ |
| 13    | Voltammetry using Boron Doped Diamond electrode <sup>167</sup>                                  | $3.65 \times 10^{-9} \text{ gml}^{-1}$  |
| 14    | Voltammetry using MWCNT/GCE <sup>19</sup>   | $2.53 \times 10^{-6} \text{ gml}^{-1}$  |
| 15    | Voltammetry using Boron Doped Diamond electrode <sup>168</sup>                                  | $2.91 \times 10^{-7} \text{ gml}^{-1}$  |
| 16    | Voltammetry using poly(3-methyl thiophene) modified GCE <sup>169</sup>                          | $1.01 \times 10^{-8} \text{ gml}^{-1}$  |
| 17    | Voltammetry using metalloporphyrin modified carbon paste electrode <sup>84</sup>                | $3.80 \times 10^{-10} \text{ gml}^{-1}$ |
| 18    | Voltammetry using MWCNT/GCE <sup>170</sup>  | $1.27 \times 10^{-7} \text{ gml}^{-1}$  |
| 19    | Voltammetry on electropolymerized molecularly imprinted overoxidised polypyrrole <sup>171</sup> | $9.09 \times 10^{-8} \text{ gml}^{-1}$  |
| 20    | Voltammetry using carbon nanotube paste electrode <sup>172</sup>                                | $1.00 \times 10^{-7} \text{ gml}^{-1}$  |
| 21    | UV spectrophotometry (standard method) <sup>133</sup>   | $2.53 \times 10^{-8} \text{ gml}^{-1}$  |
| 22    | Voltammetry using PMG/GCE (Present work)  | $2.28 \times 10^{-9} \text{ gml}^{-1}$  |

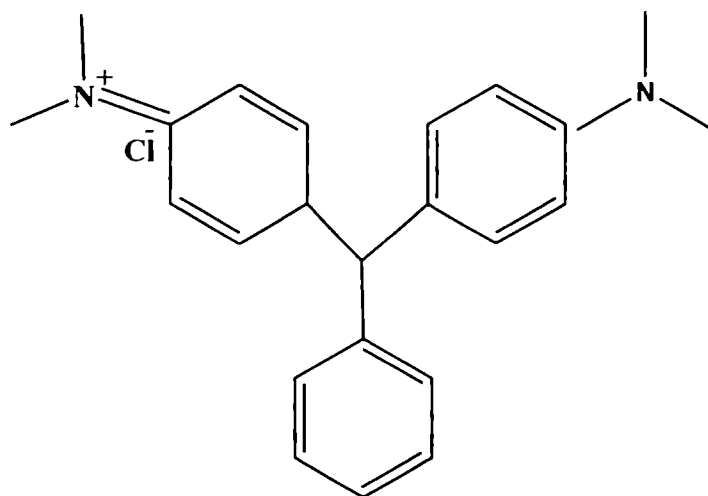


**Figure 5.1. Structure of malachite green**

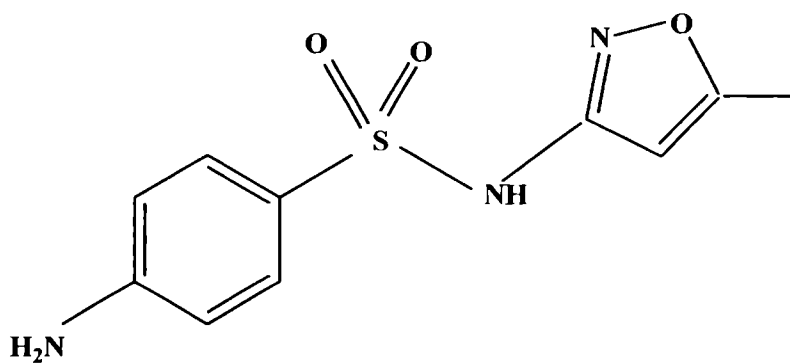


**Figure 5.2. Structure of SMX**

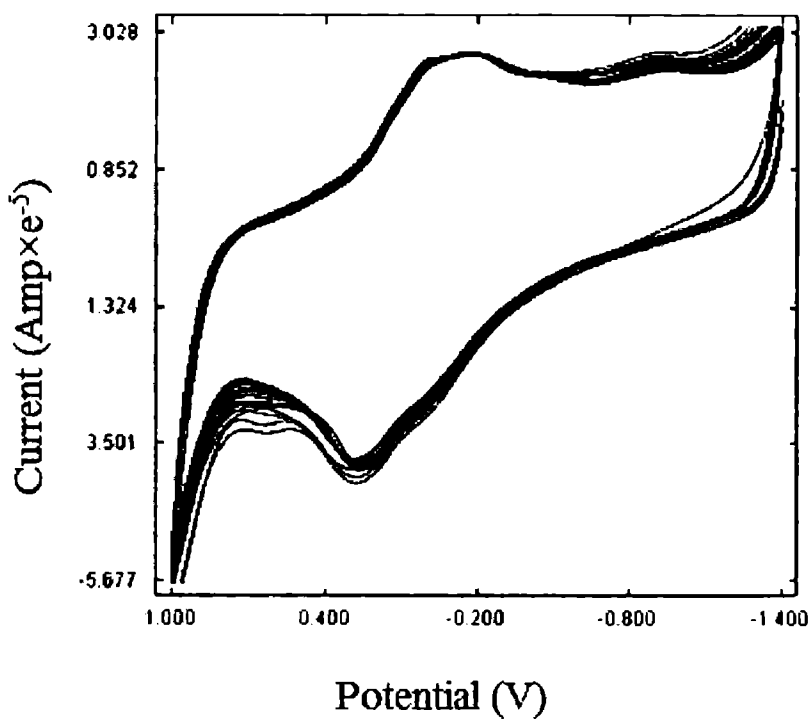
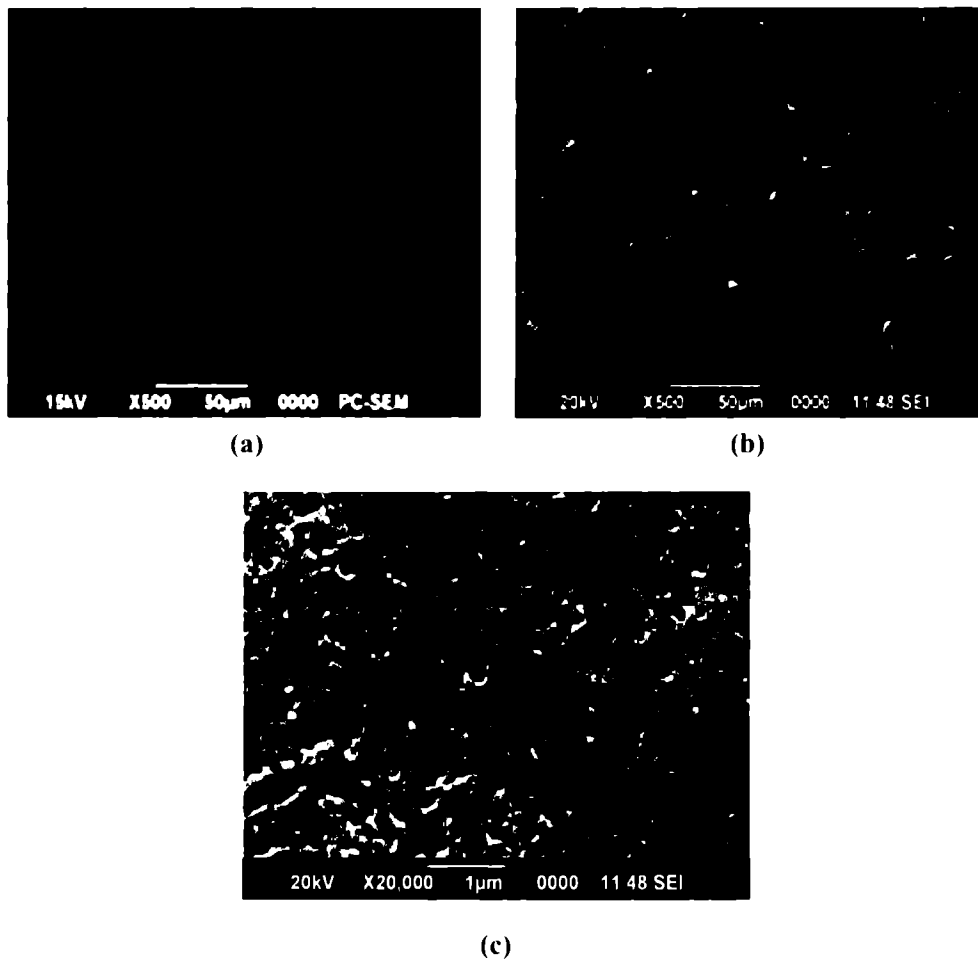


Figure 5.3. Cyclic voltammograms of polymerisation of malachite green on GCE at a scan rate of  $100 \text{ mVs}^{-1}$



**Figure 5.4.** SEM images of (a) bare GCE at 500× magnification (b) PMG/GCE at 500× magnification (c) PMG/GCE at 20000 × magnification

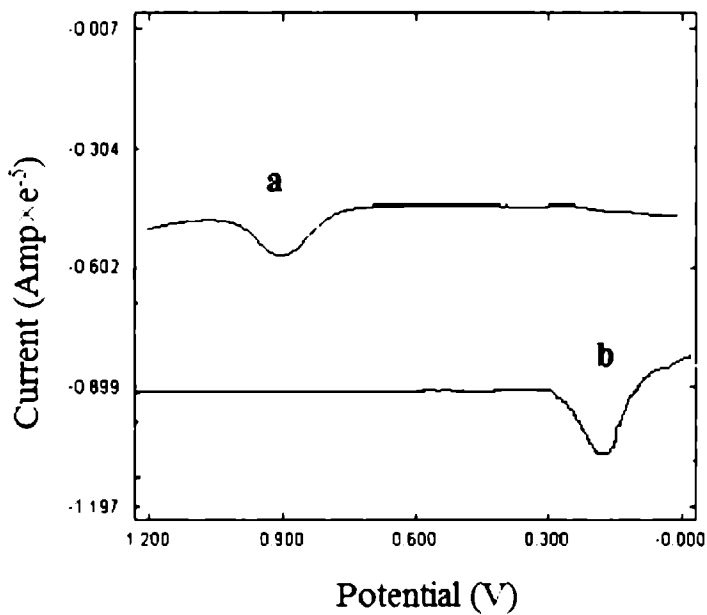


Figure 5.5. Square wave voltammograms of electrochemical oxidation of  $1 \times 10^{-3}$  M SMX on (a) bare GCE and (b) PMG/GCE

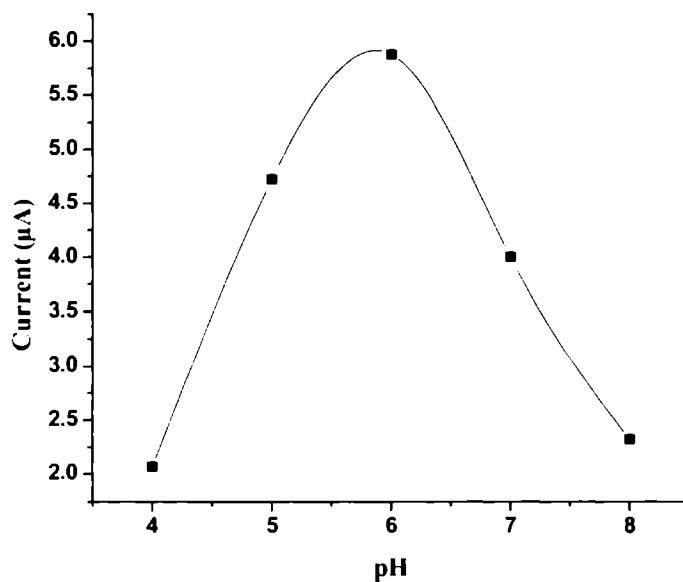
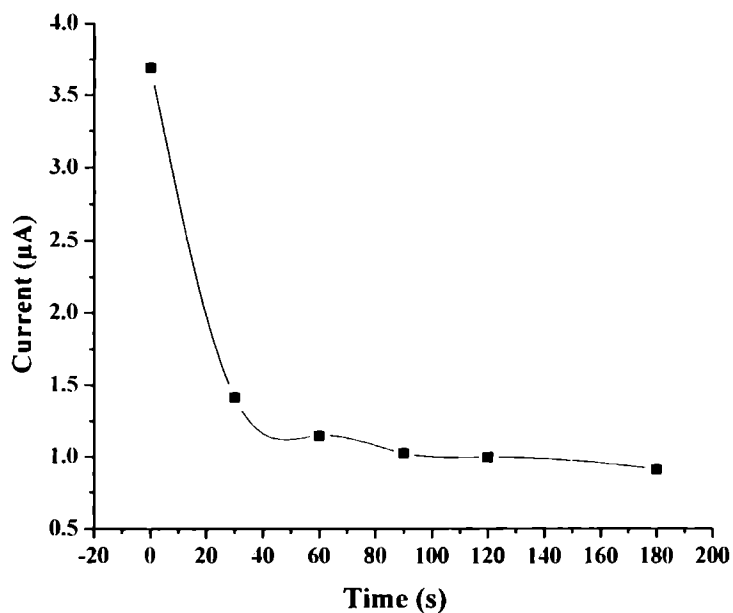
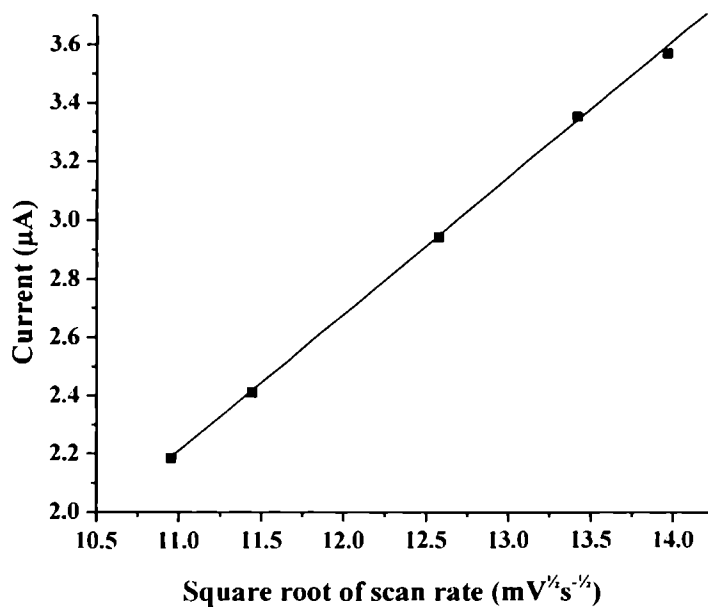


Figure 5.6. Variation of anodic peak current with pH



**Figure. 5.7. Effect of accumulation time of SMX on the anodic peak current**



**Figure 5.8. Variation of the anodic peak current of SMX as a function of square root of scan rate**

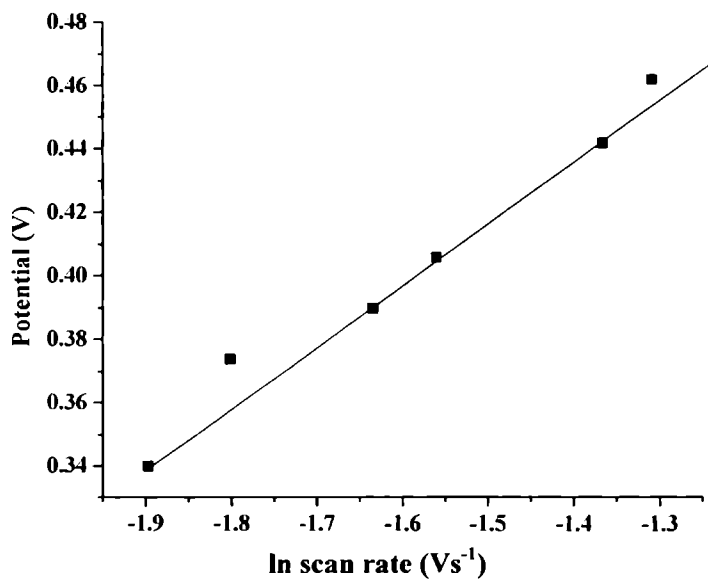


Figure 5.9. Variation of ln scan rate versus anodic potential

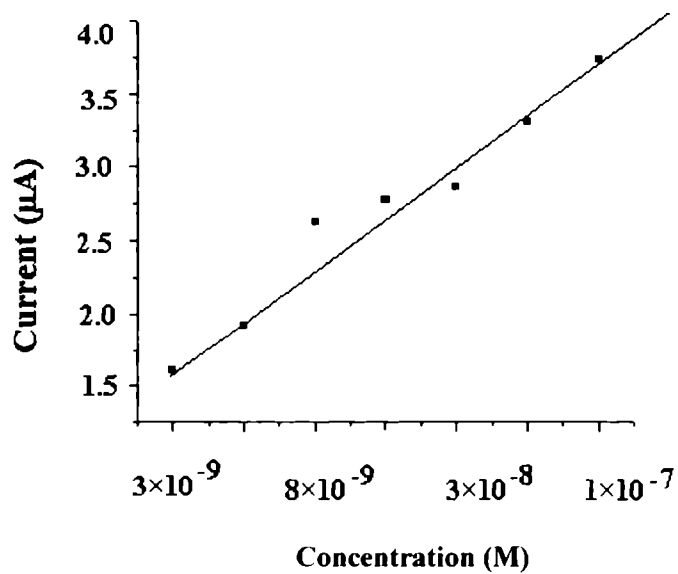
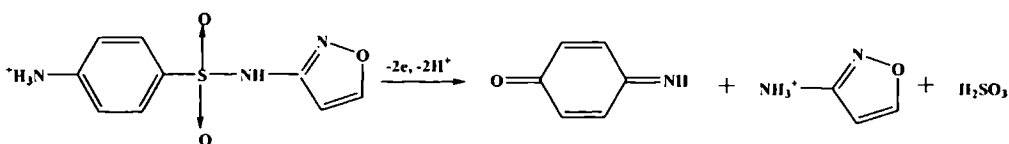


Figure 5.10. Dependence of concentration of SMX on peak current



**Scheme 5.1. Probable mechanism for the electrooxidation of SMX**

.....

## POLY(METHYL RED) MODIFIED GLASSY CARBON ELECTRODE FOR THE VOLTAMMETRIC DETERMINATION OF DOMPERIDONE

- 6.1. Introduction
- 6.2. Experimental
- 6.3. Results and Discussion
- 6.4. Conclusions

Voltammetric determination of domperidone (DOM) on poly(methyl red) modified glassy carbon electrode (PMRE/GCE) is described in this chapter. At the bare GCE, DOM yields an irreversible oxidation peak at 0.784 V and 0.480 V at PMRE/GCE. Various electrochemical characteristics were studied for the determination of DOM. The lower detection limit of DOM is  $9.9 \times 10^{-8}$  M. Analysis of DOM in pharmaceutical formulations and spiked urine sample were performed.

### 6.1 Introduction

Domperidone (DOM) (5-chloro-1-(1-[3-(2-oxo-2,3-dihydro-1*H*-benzo[*d*]imidazol-1-yl)propyl]piperidin-4-yl)-1*H*-benzo[*d*]imidazol-2(3*H*)-one) shown in Figure 6.1 is an antidopaminergic drug, developed by Janssen Pharmaceutica, and used orally or intravenously, generally to suppress nausea and vomiting, as a prokinetic agent and for promoting lactation. DOM is used, together with metoclopramide, cyclizine, and 5HT<sub>3</sub> receptor antagonists. It can be used in patients with Parkinson's disease because, unlike metoclopramide, DOM does not cross the blood–brain barrier. DOM has also been found effective in the treatment of gastroparesis and for paediatric gastroesophageal reflux. The

hormone prolactin stimulates lactation in humans, and its release is inhibited by the dopamine secreted by the hypothalamus. DOM by acting as an anti-dopaminergic, results in increased prolactin secretion and thus promotes lactation. DOM is a first choice antiemetic in some countries. DOM blocks the action of dopamine. It has strong affinities for the D<sub>2</sub> and D<sub>3</sub> dopamine receptors, which are found in the chemoreceptor trigger zone, located just outside the blood brain barrier, which, among others, regulates nausea and vomiting.

However, it is not approved for prescription in the US. In June 2004, the Food and Drug Administration issued a letter warning women not to take DOM, citing unknown risks to parents and infants, and warned pharmacies that domestic sale was illegal and that import shipments from other countries would be searched and seized. DOM is excreted in breast milk. Because this medication enhances movement in the digestive tract, it may affect the absorption and action of other medications.<sup>176-179</sup>

To date numerous methods have been reported for the determination of DOM. It includes spectrophotometry,<sup>180-185</sup> fluorometry,<sup>186,187</sup> LC-MS,<sup>188-190</sup> HPLC,<sup>191-199</sup> RPHPLC,<sup>200-203</sup> potentiometry<sup>204</sup> and voltammetry.<sup>205,206</sup> Most of the methods suffer from disadvantages like lack of sensitivity, involves heating or extraction, requires long time for the completion of reaction, narrow detection limit etc. Hence voltammetric method based on poly(methyl red) modified glassy carbon electrode (PMRE/GCE) is developed for the determination of DOM .

Methyl-red (2-[4-(dimethylamino)phenylazo]benzoicacid) with molecular formula of NC<sub>6</sub>H<sub>4</sub>COOH is an organic dye and typical aromatic azo compound,<sup>207</sup> the structure of which is shown in Figure 6.2.

## **6.2 Experimental**

### **6.2.1 Fabrication of poly(methyl red) modified glassy carbon electrode (PMRE/GCE)**

GCE was cleaned as explained in section 2.3. Then the treated electrode was electroactivated by successive cyclic voltammetric sweeps in 0.1 M sulfuric acid solution between -1.0 V and +2.2 V. Immobilization of methyl red on the surface of GCE was performed by cyclic voltammetry of  $1.0 \times 10^{-3}$  M methyl red in 0.5 M  $\text{NaNO}_3$  solution. The film was grown on GCE by cyclic voltammetric scans between -1.0 V and 2.2 V of 20 cycles.<sup>95</sup> Figure 6.3 is the cyclic voltammogram of electropolymerisation of methyl red. The redox peak current increased with the enhancement of the cyclic number of voltammetric scans, indicating that an electroconductive film formed on the electrode surface. PMRE/GCE was washed with water to remove the remaining methyl red monomers after immobilization. After drying, a thin film could be seen at the electrode surface.

### **6.2.2 Preparation of analyte sample**

Stock solution of DOM ( $1 \times 10^{-2}$  M) was prepared in methanol. Standard solutions of the analyte ( $1 \times 10^{-3}$  M –  $1 \times 10^{-8}$  M) were prepared by serial dilution of the stock solution using acetate buffer solution (ABS).

### **6.2.3 Analysis of sample**

Sample solution was taken in the electrochemical cell. Voltammograms from -0.05 V to +1.30 V were recorded and finally the peak current at about 0.480 V was measured for DOM. Prior to and after each measurement, the PMRE/GCE was activated by successive cyclic voltammetric sweeps between 0 V to 1.3 V at  $100 \text{ mVs}^{-1}$  in ABS until the voltammograms kept unchangeable.

## 6.3 Results and Discussion

### 6.3.1 Surface studies of PMRE/GCE

Surface morphological observations of PMRE/GCE were carried out by scanning electron microscopy (SEM). Figures 6.4a and 6.4b depict the SEM images of the bare GCE and PMRE/GCE at 500 times magnification respectively. The comparison points to the effective modification of the bare GCE. Figure 6.4c and 6.4d show the SEM images of PMRE/GCE at 1000 times and 3000 times magnification. It can be seen that PMRE has a porous nature. Cyclic voltammetry of 2 mM potassiumferricyanide solution was carried out at both bare GCE and PMRE/GCE at different scan rates to calculate the effective surface area of them. The obtained current was plotted against the square root of scan rates in both the cases. The slopes of the straight lines were determined. By using the Randles-Sevcik equation for reversible reaction,

$$i_p = (2.687 \times 10^5) n^{3/2} \nu^{1/2} D^{1/2} A c$$

( $i_p$  refers to peak current,  $n$  is the number of electrons transferred,  $D$  is the diffusion coefficient,  $A$  is the surface area of the electrode,  $c$  is the concentration of potassium ferricyanide solution and  $\nu$  stands for scan rate), effective surface area of bare GCE and PMRE/GCE were calculated. Taking  $n=1$  and  $D= 7.6 \times 10^{-6} \text{ cm}^2 \text{ s}^{-1}$ , the effective surface area of bare GCE and PMRE/GCE was calculated to be  $0.0669 \text{ cm}^2$  and  $0.2882 \text{ cm}^2$  respectively. The large surface area of the modified GCE compared to bare GCE is evident from the resultant values.

### 6.3.2 Investigation of the electrochemical activity of PMRE/GCE

The above fabricated electrode was applied to study the electrocatalytic property of PMRE. The studies showed that PMRE/GCE couldn't sense the

drugs ceftriaxone sodium and alendronate sodium voltammetrically. For the drugs rofecoxib and diclofenac sodium, PMRE/GCE gave the voltammetric response at a higher potential with comparatively lower current than that obtained at bare GCE. But for domperidone, the oxidation occurred at a 300 mV lesser potential on PMRE/GCE than on bare GCE, with a small increase in peak current.

### **6.3.3 Electrochemical behaviour of DOM and the optimization of the developed method**

#### **6.3.3.1 Comparison of the electrochemical behaviour of DOM at bare GCE and PMRE/GCE**

The electrochemical behaviour of DOM at a PMRE/GCE has been investigated using Square Wave Voltammetry (SWV). Figure 6.5 shows the comparison of oxidation peak of  $1 \times 10^{-3}$  M DOM at a scan rate of  $100 \text{ mVs}^{-1}$  with square wave amplitude 25 mV and square wave frequency 15 Hz at bare GCE and PMRE/GCE. At the bare GCE, DOM yields an irreversible oxidation peak at 0.784 V (curve a). Under the same conditions, a well defined irreversible oxidation peak appears at 0.480 V for the PMRE/GCE (curve b). The peak potential of DOM shifts towards a very low potential at PMRE/GCE compared to that at bare GCE and a small increase in anodic peak current is observed. Further electrochemical studies of DOM on PMRE/GCE were carried out.

#### **6.3.3.2 Effect of various supporting electrolyte**

The electrochemical properties of  $10^{-3}$  M DOM in various medium such as PBS, ABS, CBS,  $\text{H}_2\text{SO}_4$ , HCl, KCl,  $\text{KNO}_3$  and NaOH were investigated by SWV. It was observed that the peak current is highest and the peak shape is well defined in ABS. Hence ABS was chosen as the experimental medium for the voltammetric studies of DOM.

### 6.3.3.3 Effect of pH of the medium

The electrochemical studies of  $10^{-3}$  M DOM in ABS were carried out in the pH range of 2 to 10 using SWV, the graphical representation of which is shown in Figure 6.6. The best oxidation response was obtained in pH 10 as the peak current is the highest. Thus pH 10 was fixed as optimal pH.

### 6.3.3.4 Effect of accumulation of DOM

The accumulation step is usually a simple and effective way of enhancing the sensitivity. The influence of the accumulation time on the oxidation peak current of  $10^{-3}$  M DOM was tested using SWV. The results are plotted in Figure 6.7. The oxidation peak current decreased as DOM was allowed to accumulate on the surface of electrode. These results indicate that electrochemical oxidation of DOM on PMRE/GCE is diffusion controlled rather than adsorption controlled.

### 6.3.3.5 Effect of scan rate and nature of electrochemical process

The influence of the scan rate on the oxidative peak current and potential of  $10^{-3}$  M DOM was investigated by Linear Sweep Voltammetry (LSV). Figure 6.8 describes the variation of anodic peak current with scan rate  $20 \text{ mVs}^{-1}$  –  $100 \text{ mVs}^{-1}$  and Figure 6.9 shows the linear behaviour of anodic peak current with square root of scan rate in the range  $20 \text{ mVs}^{-1}$  –  $80 \text{ mVs}^{-1}$ . The linear regression equation for the plot is given by  $i_p = 0.7452v^{1/2} + 2.0030$  ( $r = 0.9904$ )

This again points to the fact that the behaviour of DOM during the electrode reaction is controlled by diffusion rather than adsorption.

### 6.3.3.6 Investigation of the possible mechanistic pathway for the electrooxidation of DOM

Potential plotted against  $\ln$  scan rate gave a linear plot (Figure 6.10), slope of which is 0.0370. Based on the Laviron's equation,<sup>131</sup> the slope of this

plot equals to  $RT/\alpha nF$ , where  $\alpha$  is assumed to be 0.5 for the totally irreversible electrode process. The calculation gave the number of electrons ( $n$ ) involved in the electrochemical reaction to be 1.3. Hence one electron oxidation of DOM can be proposed. It thus seems reasonable to assume that the oxidation of the nitrogen atom of the amide group is most probably involved, with one electron and one proton producing a free radical species.<sup>205</sup>

### **6.3.3.7 Estimation of limit of detection of DOM**

The effect of concentration of DOM in ABS (pH 10) on the modified GCE was studied using SWV. Figure 6.11 shows square wave voltammograms of DOM on PMRE/GCE at various concentrations ( $10^{-3}$  M –  $10^{-7}$  M). The results show that the oxidative peak current has a linear relationship with the concentration in the range  $3 \times 10^{-7}$  M –  $5 \times 10^{-5}$  M which is shown in Figure 6.12. The linear regression equation is  $i_p = 0.5074c + 0.7718$  ( $r = 0.9970$ ,  $c$  in M,  $i_p$  in  $\mu A$ ). The lower detection limit of DOM is  $9.9 \times 10^{-8}$  M ( $4.20 \times 10^{-8}$   $gmL^{-1}$ ).

### **6.3.3.8 Reproducibility and stability of PMRE/GCE**

The reproducibility of the electrode was examined by repetitive voltammetric determination of  $1 \times 10^{-3}$  M DOM using the same PMRE/GCE. Comparable results were obtained with relative standard deviation (RSD) of 4.8% suggesting that the PMRE/GCE has good reproducibility. PMRE/GCE exhibited stable response for 5 days.

### **6.3.4 Influence of foreign species on the oxidation of DOM**

In order to examine the effect of foreign bodies on the anodic current of DOM, 100-fold concentration of NaCl, dextrose, lactose, urea,  $K_2SO_4$ , glycine and ascorbic acid were added to  $10^{-3}$  M DOM. It is found that upto 100-fold concentration of NaCl, dextrose, lactose and  $K_2SO_4$  have no influence on the

signals of  $1 \times 10^{-3}$  M DOM, with deviation below 5%. However, glycine, urea and ascorbic acid do interfere severely. Table 6.1 lists the influence of other substances on the oxidation signal of DOM.

### 6.3.5 Application of the developed method

Commercial formulation containing DOM, Domstal tablet was analysed. After powdering two Domstal tablets, their average mass was determined. Required amount of it to prepare  $10^{-3}$  M was transferred to 25 ml standard flask, dissolved and made up to the mark using methanol. SW voltammograms of the oxidation of DOM in the tablet was recorded and the unknown concentrations were determined from the calibration graph. The recoveries are in the range of 95-97% and C.V for six replicate determinations for domstal tablet was found to be 1.12 ( $\leq 3\%$ ) as shown in Table 6.2.

In order to test the accuracy of the proposed method, several aliquots of DOM were spiked into urine samples in different proportion to get various concentration of DOM ( $10^{-4}$  M to  $10^{-6}$  M). The SW voltammograms were recorded applying the optimal conditions for their analytical determination. Recoveries lie in the range of 96-102% as can be seen from Table 6.3.

### 6.3.6 Comparison with the reported works

A comparison of the present work with the already reported works is tabulated in Table 6.4. It can be inferred that the present work is comparable with the reported works.

## 6.4 Conclusions

In summary, a voltammetric method has been developed for the determination of DOM using PMRE/GCE, evaluated the electrochemical

performance and achieved a sensitive determination of DOM. A lower detection limit of  $9.9 \times 10^{-8}$  M was obtained on the modified GCE. The electrocatalytic nature of PMRE/GCE for the determination of DOM is evident from the favorable reduction in oxidation overpotential of DOM. It is also shown that the developed sensor can be used for the determination of DOM in human urine and pharmaceutical products.

**Table 6.1. Influence of  $10^{-1}$  M of foreign species on the anodic peak current of  $10^{-3}$  M DOM**

| S.No: | Foreign species    | Signal change % |
|-------|--------------------|-----------------|
| 1     | Glycine            | 25.42           |
| 2     | Urea               | 29.75           |
| 3     | Ascorbic acid      | -26.33          |
| 4     | Sodium chloride    | -4.92           |
| 5     | Potassium sulphate | 4.50            |
| 6     | Lactose            | -4.40           |
| 7     | Dextrose           | -3.82           |

**Table 6.2. Determination of DOM in commercial formulation**

| Tablet         | Declared amount (mg/tablet) | Found amount* (mg/tablet) | S.D  | C.V (%) |
|----------------|-----------------------------|---------------------------|------|---------|
| Domstal tablet | 400 mg                      | 367 mg                    | 4.12 | 1.12    |

*Average of six replicates\**

**Table 6.3. Determination of DOM in urine sample**

| Added amount of DOM (M) in urine sample | Found amount of DOM (M) in urine sample | Recovery% |
|---|---|-----------|
| $1.00 \times 10^{-6}$                   | $0.96 \times 10^{-6}$                   | 96.0      |
| $2.00 \times 10^{-7}$                   | $1.97 \times 10^{-7}$                   | 98.4      |
| $8.00 \times 10^{-7}$                   | $8.16 \times 10^{-7}$                   | 102.0     |

**Table 6.4. Comparison of the present work with some of the reported works**

| S.No: | Method   | Lower detection limit                                    |
|-------|--|--|
| 1     | Spectrophotometry <sup>180</sup>                                 | $1.00 \times 10^{-5} \text{ gml}^{-1}$                   |
| 2     | Spetrophotometry <sup>181</sup>                                  | $5.00 \times 10^{-6} \text{ gml}^{-1}$                   |
| 3     | Spectrophotometry <sup>182</sup>                                 | $2.50 \times 10^{-8} \text{ gml}^{-1}$                   |
| 4     | Spectrophotometry <sup>183</sup>                                 | $8.00 \times 10^{-6} \text{ gml}^{-1}$                   |
| 5     | Spectrophotometry <sup>184</sup>                                 | $5.00 \times 10^{-6} \text{ gml}^{-1}$                   |
| 6     | Spectrophotometry <sup>185</sup>                                 | $8.00 \times 10^{-6} \text{ gml}^{-1}$                   |
| 7     | Flourometry <sup>186</sup>                                       | $1.00 \times 10^{-8} \text{ gml}^{-1}$                   |
| 8     | Flourometry <sup>187</sup>                                       | $5.00 \times 10^{-9} \text{ gml}^{-1}$                   |
| 9     | LC-MS <sup>188</sup>   | $1.00 \times 10^{-9} \text{ gml}^{-1}$                   |
| 10    | LC-MS <sup>189</sup>   | $1.89 \times 10^{-10} \text{ gml}^{-1}$                  |
| 11    | LC-MS <sup>190</sup>   | $1.00 \times 10^{-9} \text{ gml}^{-1}$                   |
| 12    | HPLC <sup>191</sup>  | $1.00 \times 10^{-9} \text{ gml}^{-1}$                   |
| 13    | HPLC <sup>192</sup>  | $5.00 \times 10^{-10} \text{ gml}^{-1}$                  |
| 14    | HPLC <sup>193</sup>  | $5.00 \times 10^{-5} \text{ gml}^{-1}$                   |
| 15    | HPLC <sup>194</sup>  | $3.86 \times 10^{-9} \text{ gml}^{-1}$                   |
| 16    | HPLC <sup>195</sup>  | $9.83 \times 10^{-7} \text{ gml}^{-1}$                   |
| 17    | HPLC <sup>196</sup>  | $1.00 \times 10^{-5} \text{ gml}^{-1}$                   |
| 18    | HPLC <sup>197</sup>  | $5.00 \times 10^{-6} \text{ gml}^{-1}$                   |
| 19    | HPLC <sup>198</sup>  | $1.00 \times 10^{-9} \text{ gml}^{-1}$                   |
| 20    | HPLC <sup>199</sup>  | $6.00 \times 10^{-8} \text{ gml}^{-1}$                   |
| 21    | RPHPLC <sup>200</sup>  | $1.53 \times 10^{-8} \text{ gml}^{-1}$                   |
| 22    | RPHPLC <sup>201</sup>  | $2.30 \times 10^{-7} \text{ gml}^{-1}$                   |
| 23    | RPHPLC <sup>202</sup>  | $1.00 \times 10^{-9} \text{ gml}^{-1}$                   |
| 24    | RPHPLC <sup>203</sup>  | $5.00 \times 10^{-6} \text{ gml}^{-1}$                   |
| 25    | Potentiometry <sup>204</sup>                                     | $4.26 \times 10^{-7} \text{ gml}^{-1}$                   |
| 26    | Voltammetry <sup>205</sup>                                       | $2.60 \times 10^{-7} \text{ gml}^{-1}$                   |
| 27    | Voltammetry <sup>206</sup>                                       | $1.70 \times 10^{-7} \text{ gml}^{-1}$                   |
| 28    | <b>Voltammetry at PMRE/GCE modified electrode (Present work)</b> | <b><math>4.20 \times 10^{-8} \text{ gml}^{-1}</math></b> |

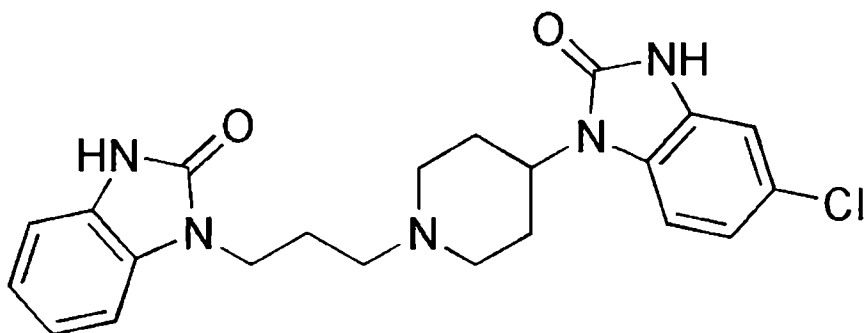


Figure 6.1. Structure of Domperidone

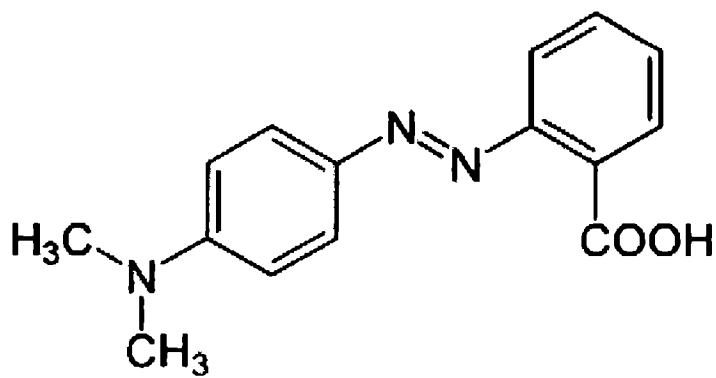
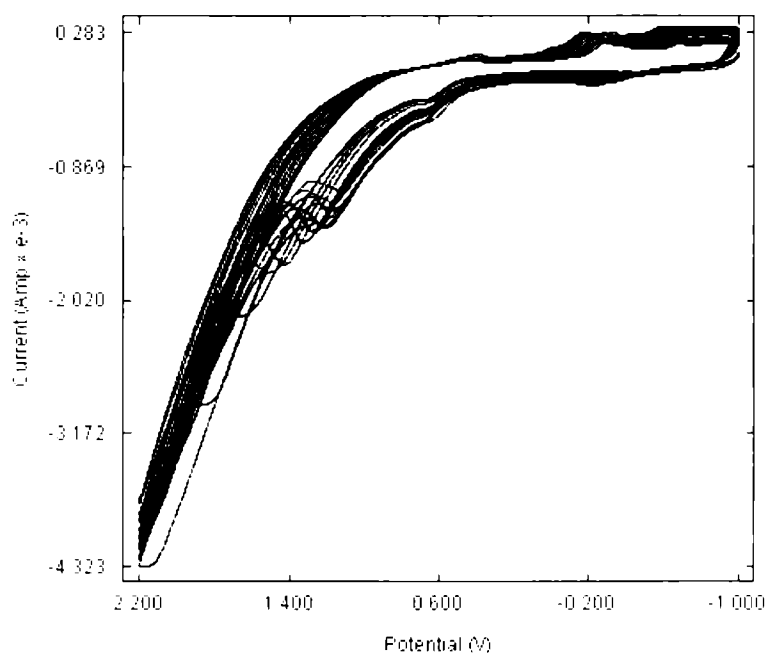
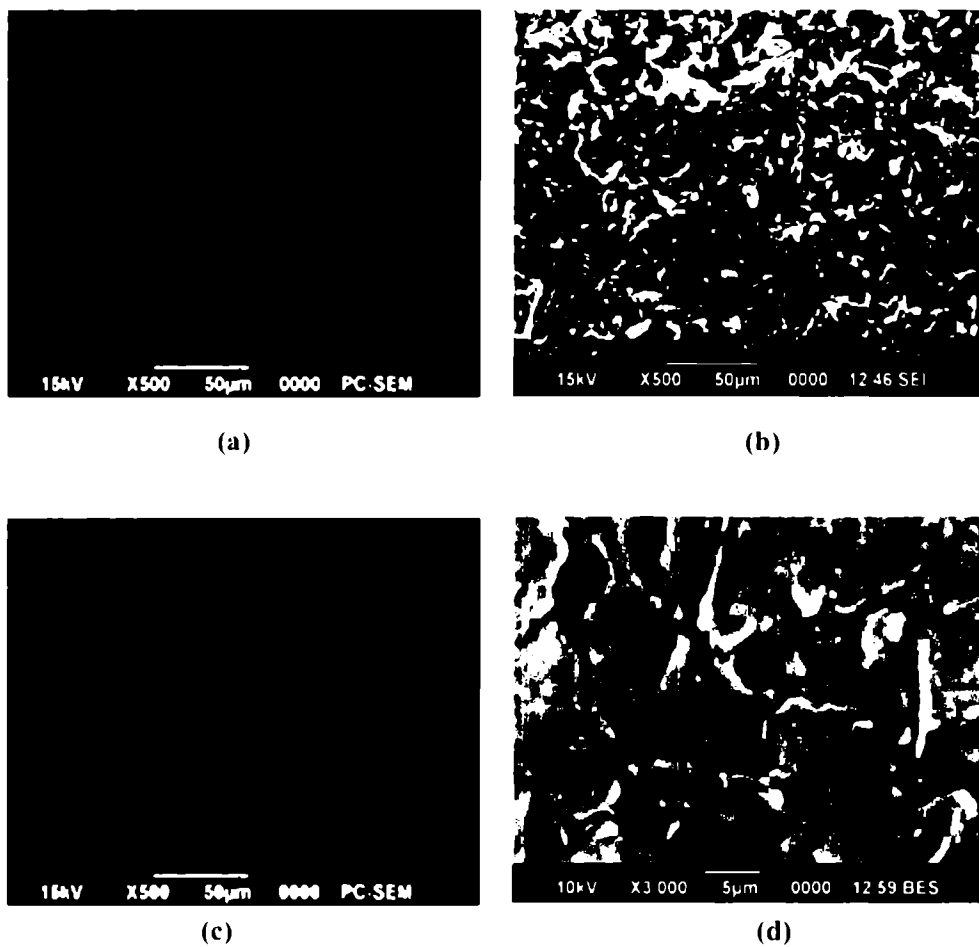


Figure 6.2. Structure of methyl red



**Figure 6.3.** Cyclic voltammograms of polymerisation of methyl red on GCE at a scan rate of  $100 \text{ mVs}^{-1}$



**Figure 6.4.** SEM images of (a) bare GCE at 500× magnification (b) PMRE/GCE at 500× magnification (c) PMRE/GCE at 1000 × magnification (d) PMRE/GCE at 3000 × magnification

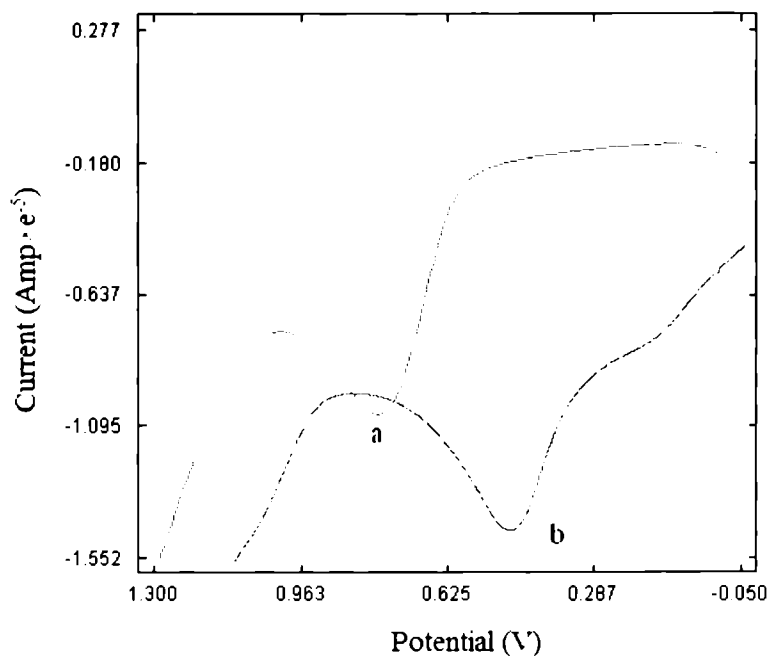


**Figure 6.5.** Square wave voltammograms of electrochemical oxidation of  $1 \times 10^{-3}$  M DOM on (a) bare GCE and (b) PMRE/GCE

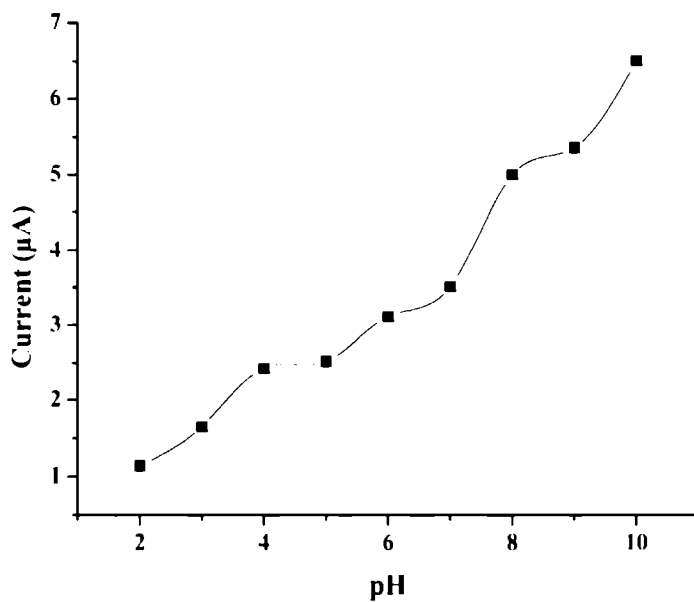


**Figure 6.6.** Variation of anodic peak current with pH

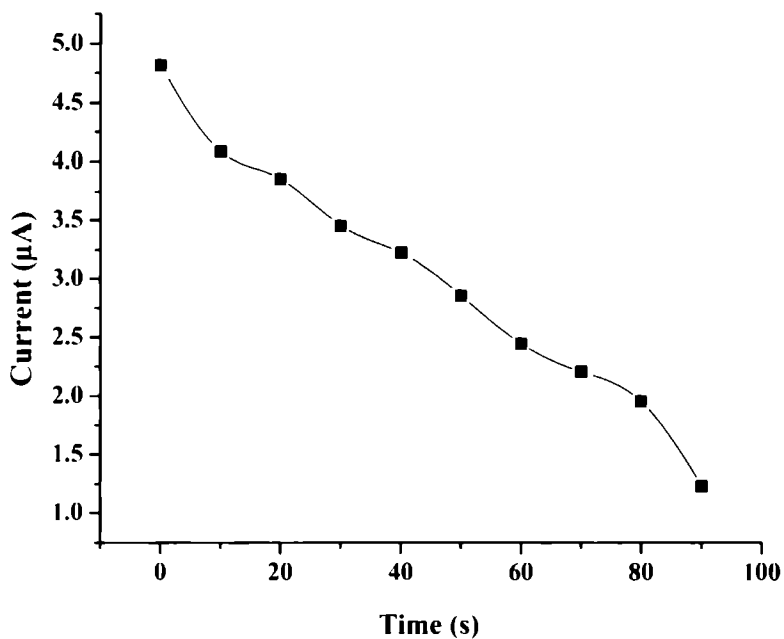


Figure 6.7. Effect of accumulation time of DOM on the anodic peak current

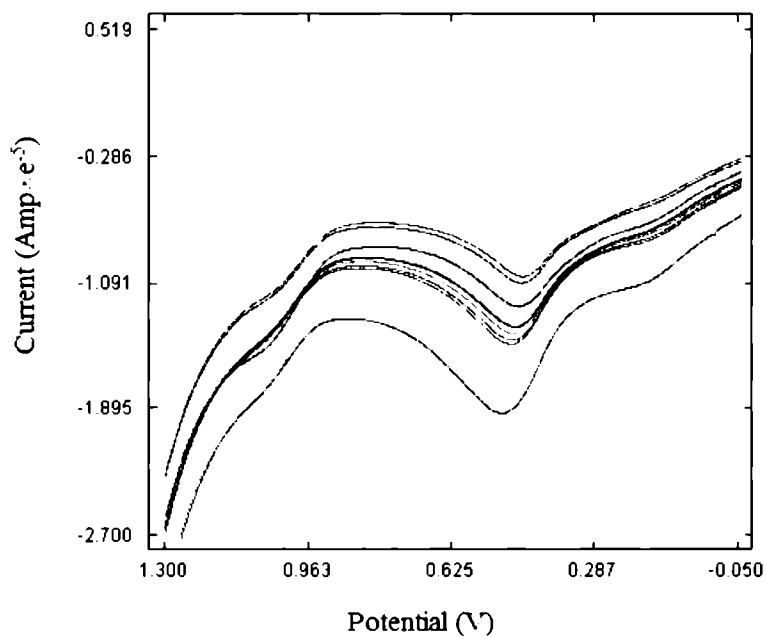
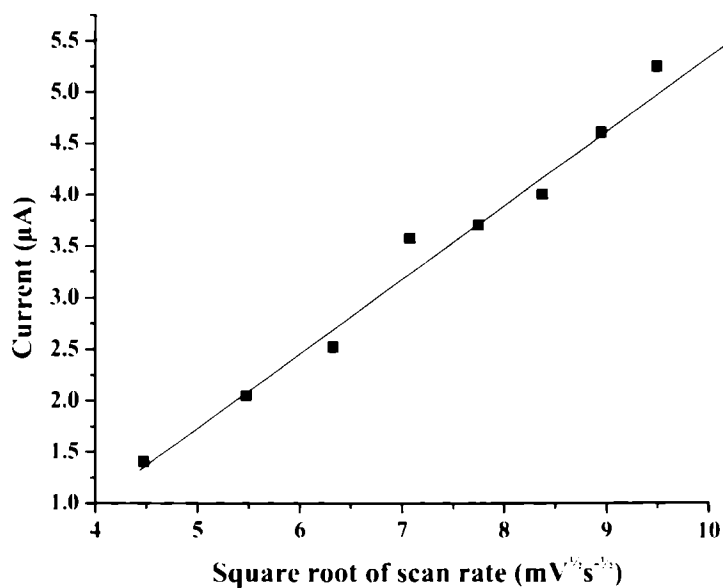
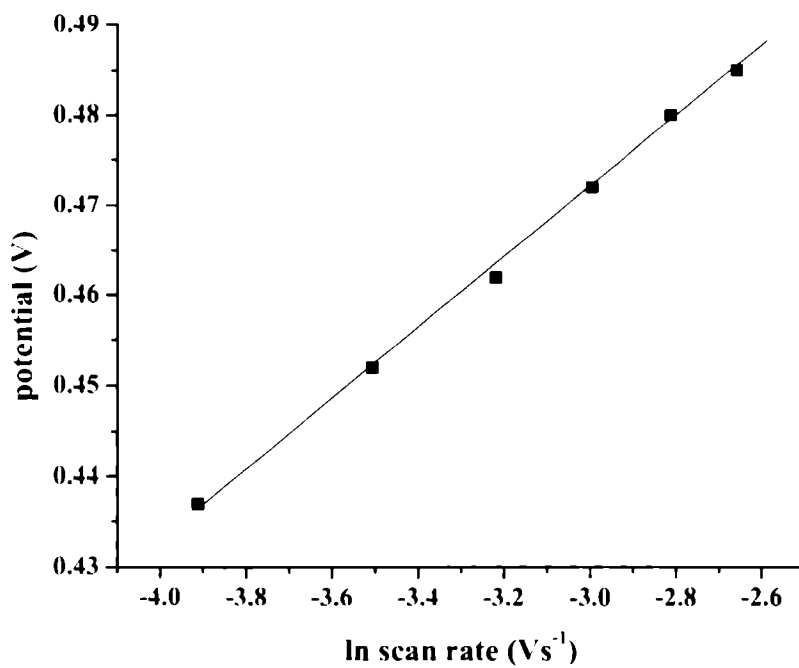


Figure 6.8. Linear sweep voltammograms of  $10^{-3}$  M DOM at scan rates 20, 30, 40, 50, 60, 70, 80, 90, 100  $\text{mVs}^{-1}$  (from top to bottom)



**Figure 6.9.** Variation of the anodic peak current of DOM as a function of square root of scan rate



**Figure 6.10.** Variation of ln scan rate versus anodic potential

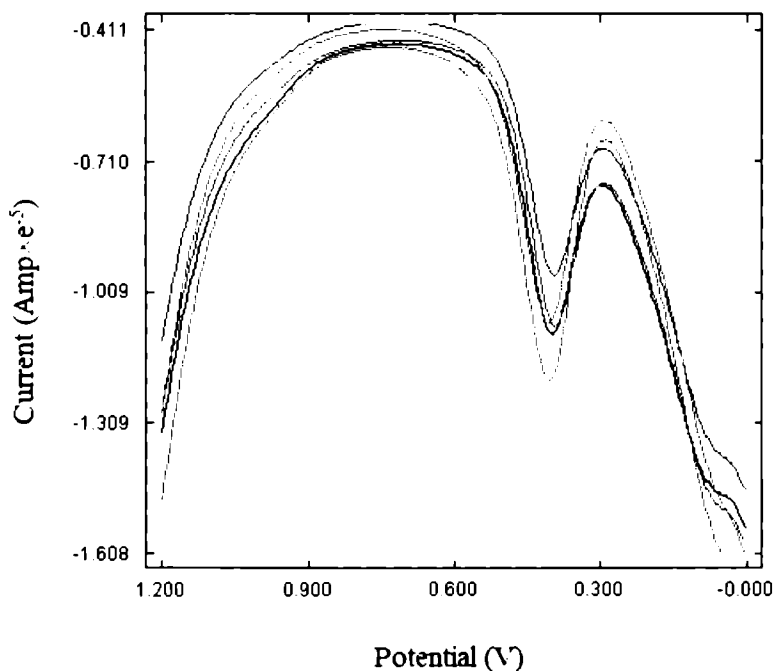


Figure 6.11. Square wave voltammograms of concentrations  $10^{-3}$ ,  $10^{-4}$ ,  $10^{-5}$ ,  $10^{-6}$ ,  $10^{-7}$  M of DOM (from bottom to top)

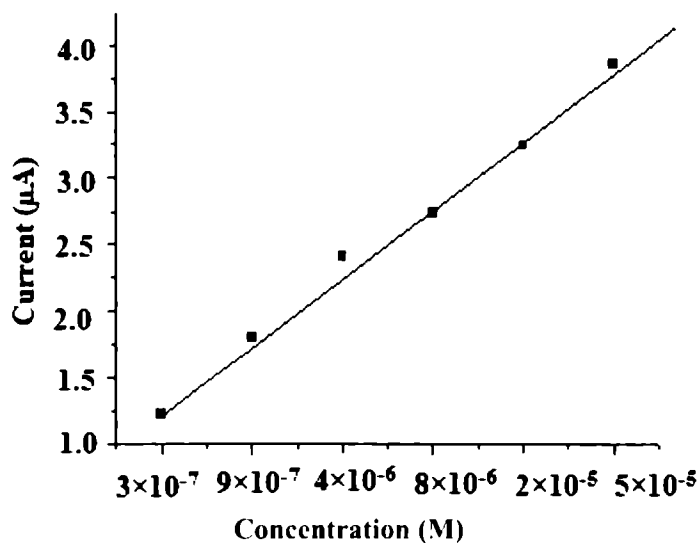


Figure 6.12. Dependence of concentration of DOM on peak current

.....S(2)R.....

## POLY(ERIOCHROME BLACK T) MODIFIED ELECTRODE FOR THE VOLTAMMETRIC DETERMINATION OF TINIDAZOLE

|                 |                                    |
|-----------------|------------------------------------|
| <b>Contents</b> | 7.1. <i>Introduction</i>           |
|                 | 7.2. <i>Experimental</i>           |
|                 | 7.3. <i>Results and Discussion</i> |
|                 | 7.4. <i>Conclusions</i>            |

---

This chapter discusses the voltammetric determination of tinidazole (TNZ) on poly(eriochrome black T) modified glassy carbon electrode (PEBT/GCE). Electroreduction of TNZ occurs at -708 mV on bare GCE and at -608 mV on PEBT/GCE. Optimum conditions for the determination of TNZ were probed for. A lower detection limit of  $8.9 \times 10^{-9}$  M could be achieved using the sensor. PEBT/GCE was used for the determination of TNZ in pharmaceutical formulation and urine sample.

### 7.1 Introduction

Developed in 1972, tinidazole (TNZ) shown in Figure 7.1 is an anti-parasitic drug used against protozoan infections. It is widely known throughout Europe and the developing world for the treatment of a variety of amoebic and parasitic infections. It is used to treat trichomoniasis, giardiasis and amebiasis. It is chemically similar to metronidazole a drug with some unpleasant side effects that is used in the United States as first-line therapy for amoebae. TNZ has similar side effects but has a shorter treatment course. TNZ.

may be a therapeutic alternative in the setting of metronidazole intolerance. The most common side effects reported with TNZ are upset stomach, diarrhea and itchiness. Other side effects which occur are headache, physical fatigue and dizziness. Oncologic side effects include mutagenicity in animal studies. TNZ has been tested positive for genotoxicity in vivo studies.<sup>208, 209</sup>

Many methods have been reported for the determination of TNZ which include spectrophotometry,<sup>210-215</sup> HPLC,<sup>216-220</sup> capillary electrophoresis,<sup>221,222</sup> micellar liquid chromatography,<sup>223</sup> voltammetry<sup>224-230</sup> etc. To overcome the difficulties and disadvantages of these methods, voltammetry based method is developed, which comprises poly(eriochrome black T) modified glassy carbon electrode (PEBT/GCE) as the working electrode. Eriochrome black T (EBT) shown in Figure 7.2 is an azonaphthol dye well known as metalochromic indicator in EDTA titrations and in spectrophotometric determinations, but scarcely involved in electrochemical procedures. PEBT film on the surface of GCE can increase the current response of the analytes due to the high concentration of negatively charged functional group  $-SO_3^-$  and the electron-rich oxygen atom. Due to the rich electroactive center and three-dimensional available field potential, the polymerized film modified electrode has stable performance with good infusible and insoluble capability.<sup>231-239, 101</sup>

## 7.2 Experimental

### 7.2.1 Fabrication of poly(eriochrome black T) modified glassy carbon electrode (PEBT/GCE)

The GCE was cleaned as detailed in section 2.3. The polished electrode was electrochemically pretreated by cycling in 0.1 M  $H_2SO_4$  in the potential range  $-0.4$  V and 0.8 V at a scan rate of  $100\text{ mVs}^{-1}$  for 25 times and then the electrode was treated in 0.1 M NaOH under the same conditions for 25 times. The poly(EBT) coated electrode (PEBT/GCE) was fabricated under the same

conditions with the pretreated electrode in 0.5 mM EBT solution containing 0.1 M NaOH. Cyclic voltammograms of polymerization of 0.5 mM EBT on the surface of GCE is shown in Figure 7.3. After polymerization, the film was washed with water and cycled in pH 4 PBS between  $-0.2$  V and  $0.8$  V to eliminate unreacted EBT at  $100 \text{ mVs}^{-1}$  for five cycles.<sup>101</sup>

### **7.2.2 Preparation of analyte sample**

Stock solution of TNZ ( $1 \times 10^{-2}$  M) was prepared in methanol. Standard solutions of the analyte ( $1 \times 10^{-3}$  M –  $1 \times 10^{-8}$  M) were prepared by serial dilution of the stock solution using phosphate buffer.

### **7.2.3 Electrochemical measurements of TNZ**

TNZ in phosphate buffer solution was taken in the electrochemical cell and was analysed using various voltammetric techniques. Differential pulse voltammograms of TNZ from 0 mV to  $-1000$  mV were recorded.

## **7.3 Results and discussion**

### **7.3.1 Surface studies of PEBT/GCE**

Surface morphological observations of PEBT/GCE were carried out by scanning electron microscopy (SEM). Figures 7.4a and 7.4b depict the SEM images of the bare GCE and PEBT/GCE at 500 times magnification respectively. The comparison points to the effective modification of the bare GCE. Figures 7.4c and 7.4d show the SEM images of PEBT/GCE at 1000 times and 3000 times magnification. Cyclic voltammetry of 2 mM potassium ferricyanide solution was carried out at both bare GCE and PEBT/GCE at different scan rates to calculate the effective surface area of them. The obtained current was plotted against the square root of scan rates in both the

cases. The slopes of the straight lines were determined. By using the Randles-Sevcik equation for reversible reaction,

$$i_p = (2.687 \times 10^5) n^{3/2} \nu^{1/2} D^{1/2} A c$$

( $i_p$  refers to peak current,  $n$  is the number of electrons transferred,  $D$  is the diffusion coefficient,  $A$  is the surface area of the electrode,  $c$  is the concentration of potassium ferricyanide solution and  $\nu$  stands for scan rate), effective surface area of bare GCE and PEPT/GCE were calculated. Taking  $n=1$  and  $D=7.6 \times 10^{-6} \text{ cm}^2 \text{ s}^{-1}$ , the effective surface area of bare GCE and PEPT/GCE was calculated to be  $0.0669 \text{ cm}^2$  and  $0.2443 \text{ cm}^2$  respectively. The large surface area of the modified GCE compared to bare GCE is evident from the resultant values.

### 7.3.2 Investigation of the electrochemical activity of PEPT/GCE

PEPT/GCE was used for sensing various drugs like diclofenac sodium, tinidazole, sulfamethoxazole, acyclovir etc. For diclofenac sodium no considerable shift for the oxidation potential was observed compared to the bare electrode. In the case of sulfamethoxazole and acyclovir, increase in oxidation potential at PEPT/GCE compared to that at bare GCE was recorded. The reduction of tinidazole occurred at lower potential at PEPT/GCE than that at bare GCE.

### 7.3.3 Electrocatalytic reduction of TNZ on PEPT/GCE and optimization of the developed method

#### 7.3.3.1 Comparison of the electrochemical behaviour of TNZ at bare GCE and PEPT/GCE

The electrochemical behaviour of TNZ at a PEPT/GCE has been investigated using Differential Pulse Voltammetry (DPV) and Linear Sweep Voltammetry (LSV). Figure 7.5 shows the differential pulse (DP)

voltammograms of  $10^{-3}$  M TNZ in PBS of pH 7 at bare GCE (curve a) and PEBT/GCE (curve b) respectively. All the DPV experiments of TNZ were performed at pulse width 50 ms, pulse period 200 ms and pulse amplitude 50 mV. It is evident that the electroreduction of TNZ occurs at -708 mV on bare GCE. The reduction of TNZ at the modified GCE occurs at -608 mV. The cathodic potential of TNZ shifts to a lower value considerably at PEBT/GCE compared to that at bare GCE. Also the cathodic current gets boosted up at the modified GCE. Optimisation studies for the determination of TNZ at PEBT/GCE were carried out.

### **7.3.3.2 Influence of various supporting electrolyte**

The voltammetric behavior of TNZ was tested in various supporting electrolytes like acetate buffer, citrate buffer, phosphate buffer, lithium perchlorate, potassium nitrate, sulphuric acid and sodium hydroxide to investigate which of them yielded the best sensor response using DPV. It was observed that the reduction of TNZ at the modified electrode is much better in phosphate buffer than that in other medium on the basis of lower reduction potential, higher current and reproducibility. Thus phosphate buffer was used as the experimental medium for the further studies of TNZ.

### **7.3.3.3 Effect of pH of the medium**

Figure 7.6 and Figure 7.7 demonstrate the effect of pH on the electroreduction of TNZ at PEBT/GCE. As pH increases, the value of the reduction potential increases. Lowest potential is recorded at pH 2. But the relation of pH to current shows no regular trend. Maximum current response is obtained at pH 5, followed by pH 3. Taking into account the lower cathodic potential and good current response, pH 3 is considered as optimum pH.

### 7.3.3.4 Effect of preconcentration of TNZ

As time is given for TNZ to adsorb onto the surface of PEBT/GCE, its response towards electroreduction decreases which is depicted in Figure 7.8. Hence it can be deduced that the electroreduction of TNZ at PEBT/GCE doesn't follow an adsorption process.

### 7.3.3.5 Effect of scan rate on the reduction of TNZ

The effect of the linear sweep potential rate upon the voltammetric response of  $10^{-3}$  M TNZ in phosphate buffer of pH 7 was studied. Scan rate was varied from 20 to 100  $\text{mVs}^{-1}$ . Figure 7.9 is the overlay of the linear sweep voltammograms of the electroreduction of TNZ at PEBT/GCE at scan rates ranging from 20 to 80  $\text{mVs}^{-1}$ . The peak current increases with the scan rate and in addition exhibited a linear relation to square root of scan rate as described in Figure 7.10 with the linear regression equation  $i_p = 2.4495v^{1/2} + 8.0671$ , where  $v^{1/2}$  stands for square root of scan rate ( $r = 0.9904$ ). This again confirms that electroreduction of TNZ at PEBT/GCE is not adsorption controlled, but it is diffusion controlled.

### 7.3.3.6 Investigation of the possible mechanistic pathway for the electroreduction of TNZ

$\ln$  scan rate was plotted against the cathodic potential of TNZ which resulted in a linear graph as shown in Figure 7.11 with a slope of 0.0333. Based on the Laviron's equation,<sup>131</sup> the slope of this plot equals to  $RT/\alpha nF$ , where  $\alpha$  is assumed to be 0.5 for the totally irreversible electrode process. The calculation gave the number of electrons involved in the electrochemical reaction ( $n$ ) to be 1.6. Hence number of electrons involved in the electroreduction of TNZ can be considered to be 2. The mechanism of electroreduction of TNZ<sup>240</sup> is described in scheme 7.1.

### 7.3.3.7 Quantification of TNZ

The differential pulse voltammetric behavior of various concentration of TNZ was analysed. Figure 7.12 shows the DP voltammograms of electroreduction of TNZ of concentrations in the range  $10^{-3}$  M –  $10^{-8}$  M in phosphate buffer of pH 3. The cathodic current showed linearity with increasing concentration of TNZ in the range  $1 \times 10^{-8}$  M -  $8 \times 10^{-7}$  M and the linear regression equation is given as  $i_p = 0.1986c + 0.8365$ , where  $c$  stands for concentration ( $r = 0.9993$ ,  $n=8$ ). From the calibration curve, shown in Figure 7.13, detection limit of  $8.9 \times 10^{-9}$  M ( $2.18 \times 10^{-12}$  gml<sup>-1</sup>) could be achieved.

### 7.3.3.8 Reproducibility and stability

Relative standard deviation of 2.9% for the current response of  $10^{-3}$  M TNZ ( $n=10$ ) shows excellent reproducibility. The long term stability of PEBT/GCE was evaluated by measuring the current responses at a fixed TNZ concentration of  $10^{-3}$  M over a period of 3 weeks. The electrode was used daily and was stored in distilled water after use. The experimental results indicated that the current responses deviated only 3.8% revealing that the fabricated sensor possesses long term stability.

### 7.3.4 Selectivity

The additions of upto  $10^{-1}$  M of urea, ascorbic acid, NaCl, K<sub>2</sub>SO<sub>4</sub>, dextrose, lactose and metronidazole benzoate were tested on the differential pulse voltammetric behavior of  $10^{-3}$  M TNZ. Upto 100 fold concentration of urea, NaCl, K<sub>2</sub>SO<sub>4</sub>, dextrose and lactose do not interfere, whereas ascorbic acid is found to interfere slightly and metronidazole benzoate is found to interfere severely. The results are tabulated in Table 7.1. Equimolar concentration of metronidazole benzoate with TNZ reduces the signal change

percentage by 15.9% which means that it interferes with the determination of TNZ.

### 7.3.5 Application potential of the sensor

Experiments were performed analyzing commercial formulation containing TNZ, Tinidal. After powdering five tablets, their average mass was determined. Required amount of it to prepare  $10^{-3}$  M was transferred to 25 ml standard flask and made up to the mark using methanol. The solution was filtered. Solutions of different concentrations were made by taking suitable aliquots of the clear filtrate and diluting them with phosphate buffer. DP voltammograms of the reduction of various concentrations of the tablet were recorded and the unknown concentrations were determined from the calibration graph. C.V for six replicate determinations was found to be 1.50 and the results are tabulated in Table 7.2.

The urine sample was spiked with TNZ by adding several aliquots of TNZ in different proportion to get various concentration of TNZ ( $10^{-4}$  M to  $10^{-6}$  M). The DP voltammograms were recorded applying the optimal conditions for their analytical determination. Recoveries lie in the range of 95-104%. The results of the voltammetric analysis of spiked samples of urine shows good recovery as can be seen from Table 7.3.

### 7.3.6 Comparison with the reported works

A comparison of the reported works with the present work is tabulated in Table 7.4. Lowest detection limit is obtained using the present work compared to other reported works.

## 7.4 Conclusions

A conducting polymer film of eriochrome black T was coated on the surface of GCE. PEBT/GCE thus formed was used for the voltammetric studies of TNZ. The reduction of TNZ on PEBT/GCE was found to be highly facilitated than at bare GCE in terms of lower potential and higher current. The reduction of TNZ is pH dependent and the reduction potential drastically shifts to lower value in acidic medium. The electrochemical process is found to be diffusion controlled. It is interpreted that the electroreduction of TNZ at PEBT/GCE proceeds through a 2 electron process. The detection limit of TNZ using the proposed method is  $8.9 \times 10^{-9}$  M. Selectivity of the PEBT/GCE towards TNZ is highly interrupted by the presence of metronidazole benzoate. The sensor exhibits stable response towards TNZ for long time. The method was extended for the determination of drug in tablet and in spiked samples.

**Table 7.1. Influence of  $10^{-1}$  M of foreign species on the cathodic peak current of  $10^{-3}$  M TNZ**

| S.No: | Foreign species        | Signal change % |
|-------|------------------------|-----------------|
| 1     | Urea                   | 4.92            |
| 2     | Ascorbic acid          | 13.88           |
| 3     | Sodium chloride        | -3.40           |
| 4     | Potassium sulphate     | -3.50           |
| 5     | Lactose                | -4.20           |
| 6     | Dextrose               | -3.82           |
| 7     | Metronidazole benzoate | -69.31          |

**Table 7.2. Determination of TNZ in commercial formulations**

| Tablet  | Declared amount (mg/tablet) | Found amount* (mg/tablet) | S.D  | C.V (%) |
|---------|-----------------------------|---------------------------|------|---------|
| Tinidal | 300 mg                      | 287 mg                    | 4.20 | 1.50    |

*Average of six replicates\**

**Table 7.3. Determination of TNZ in urine sample**

| Added amount of TNZ (M) in urine sample | Found amount of TNZ (M) in urine sample | Recovery% |
|---|---|-----------|
| $3.00 \times 10^{-6}$                   | $2.86 \times 10^{-6}$                   | 95.3      |
| $5.00 \times 10^{-6}$                   | $4.97 \times 10^{-6}$                   | 99.4      |
| $7.00 \times 10^{-6}$                   | $7.26 \times 10^{-6}$                   | 103.7     |

**Table 7.4. Comparison of the developed method with other reported works for the determination of TNZ**

| S.No: | Method  | Lower detection limit                                     |
|-------|---|---|
| 1     | Spectrophotometry <sup>210</sup>                  | $7.40 \times 10^{-7}$ gml <sup>-1</sup>                   |
| 2     | Spectrophotometry <sup>211</sup>                  | $7.00 \times 10^{-8}$ gml <sup>-1</sup>                   |
| 3     | Spectrophotometry <sup>212</sup>                  | $4.72 \times 10^{-7}$ gml <sup>-1</sup>                   |
| 4     | Spetrophotometry <sup>213</sup>                   | $4.40 \times 10^{-7}$ gml <sup>-1</sup>                   |
| 5     | Spectrophotometry <sup>214</sup>                  | $1.94 \times 10^{-6}$ gml <sup>-1</sup>                   |
| 6     | Spectrophotometry <sup>215</sup>                  | $2.00 \times 10^{-8}$ gml <sup>-1</sup>                   |
| 7     | HPLC <sup>216</sup>                               | $5.00 \times 10^{-8}$ gml <sup>-1</sup>                   |
| 8     | HPLC <sup>217</sup>                               | $9.20 \times 10^{-8}$ gml <sup>-1</sup>                   |
| 9     | HPLC <sup>218</sup>                               | $1.00 \times 10^{-5}$ gml <sup>-1</sup>                   |
| 10    | RPHPLC <sup>219</sup>                             | $3.00 \times 10^{-7}$ gml <sup>-1</sup>                   |
| 11    | RPHPLC <sup>220</sup>                             | $1.00 \times 10^{-8}$ g ml <sup>-1</sup>                  |
| 12    | Capillary electrophoresis <sup>221</sup>          | $1.00 \times 10^{-6}$ gml <sup>-1</sup>                   |
| 13    | Capillary electrophoresis <sup>222</sup>          | $6.00 \times 10^{-7}$ gml <sup>-1</sup>                   |
| 14    | Micellar Liquid Chromatography <sup>223</sup>     | $1.00 \times 10^{-13}$ gml <sup>-1</sup>                  |
| 15    | Differential Pulse Voltammetry <sup>224</sup>     | $6.70 \times 10^{-9}$ gml <sup>-1</sup>                   |
| 16    | Differential Pulse Voltammetry <sup>225</sup>     | $2.40 \times 10^{-6}$ gml <sup>-1</sup>                   |
| 17    | Stripping Voltammetry <sup>226</sup>              | $1.11 \times 10^{-10}$ gml <sup>-1</sup>                  |
| 18    | Gold nanoparticles/CNT Voltammetry <sup>227</sup> | $2.47 \times 10^{-9}$ gml <sup>-1</sup>                   |
| 19    | Voltammetry <sup>228</sup>                        | $3.00 \times 10^{-8}$ gml <sup>-1</sup>                   |
| 20    | Voltammetry <sup>229</sup>                        | $2.47 \times 10^{-9}$ gml <sup>-1</sup>                   |
| 21    | Voltammetry <sup>230</sup>                        | $2.47 \times 10^{-9}$ gml <sup>-1</sup>                   |
| 22    | <b>Voltammetry at PEBT/GCE<br/>(Present work)</b> | <b><math>2.18 \times 10^{-12}</math> gml<sup>-1</sup></b> |

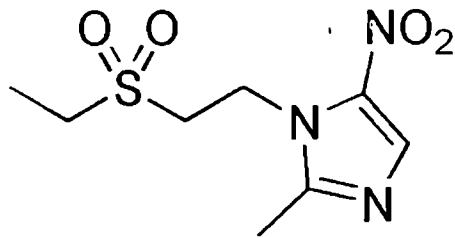


Figure 7.1. Structure of TNZ

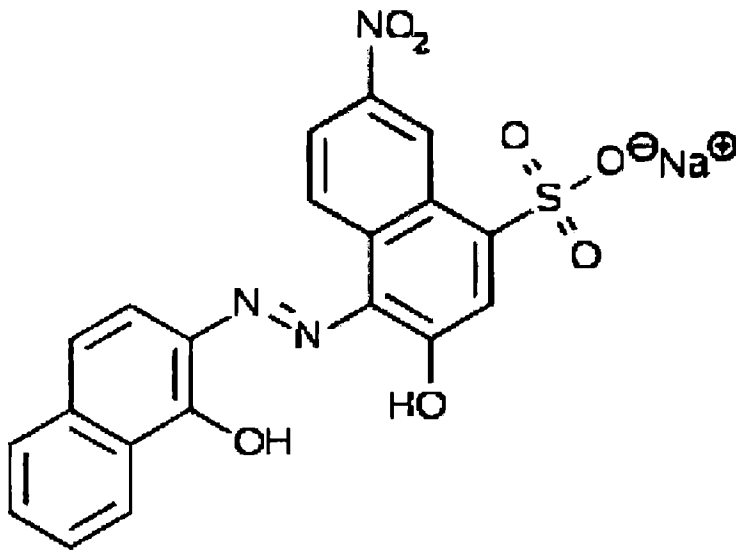
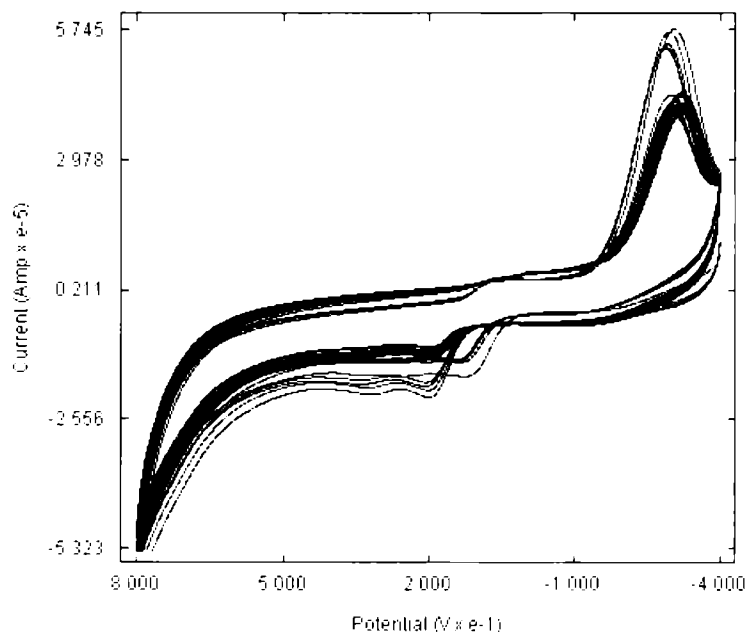
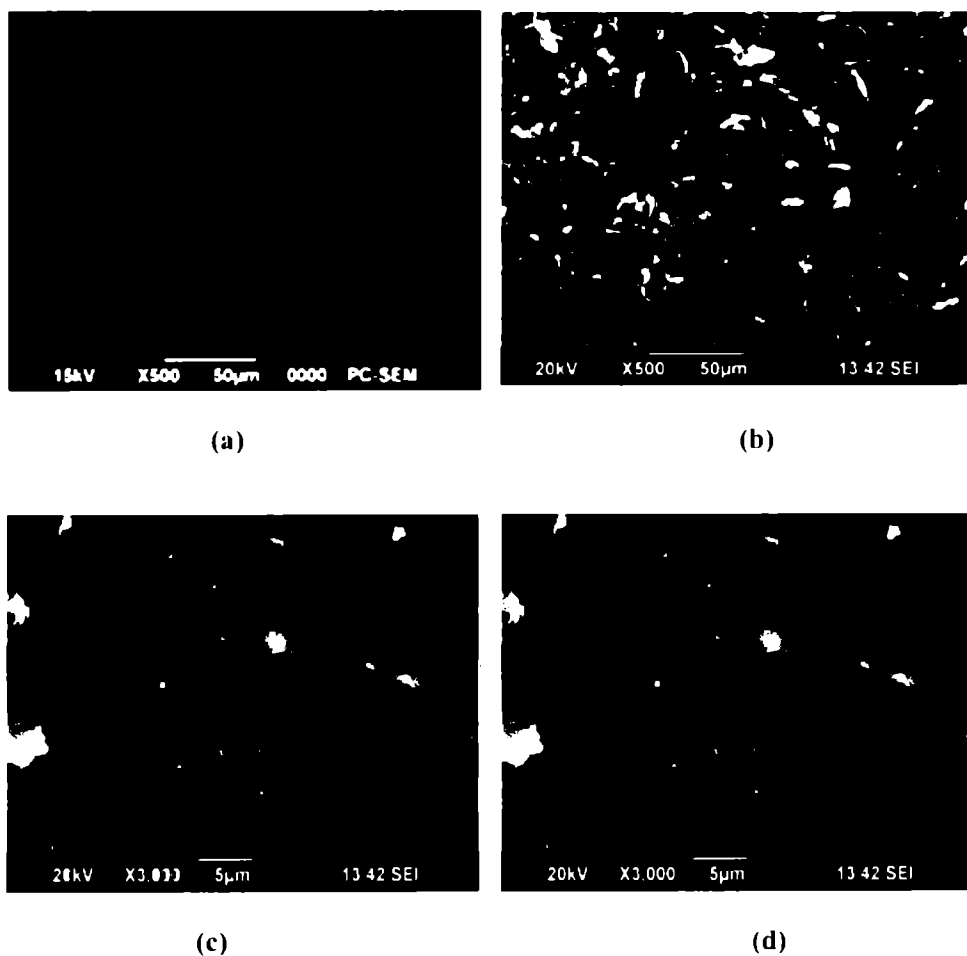


Figure 7.2. Structure of EBT



**Figure 7.3.** Cyclic voltammograms of polymerisation of eriochrome black T on GCE at a scan rate of  $100 \text{ mVs}^{-1}$



**Figure 7.4. SEM images of (a) bare GCE at 500× magnification (b) PEPT/GCE at 500× magnification (c) PEPT/GCE at 1000 × magnification (d) PEPT/GCE at 3000 × magnification**

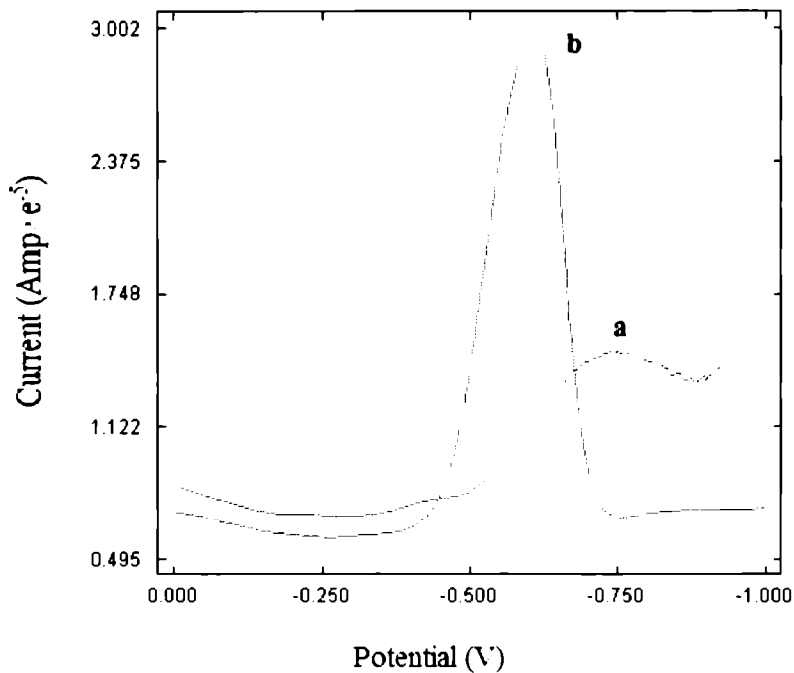


**Figure 7.5. Differential pulse voltammograms of the reduction of  $10^{-3}$  M TNZ at a) bare GCE b) PEBT/GCE**

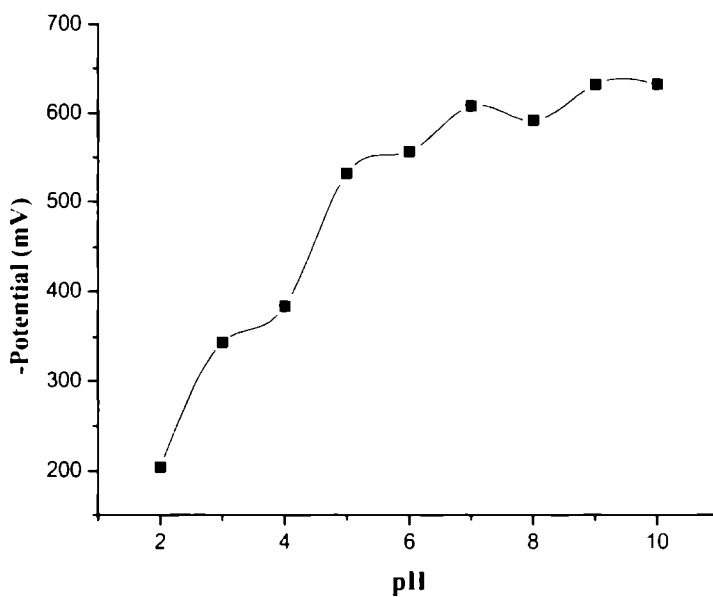


**Figure 7.6. Plot of pH versus potential**

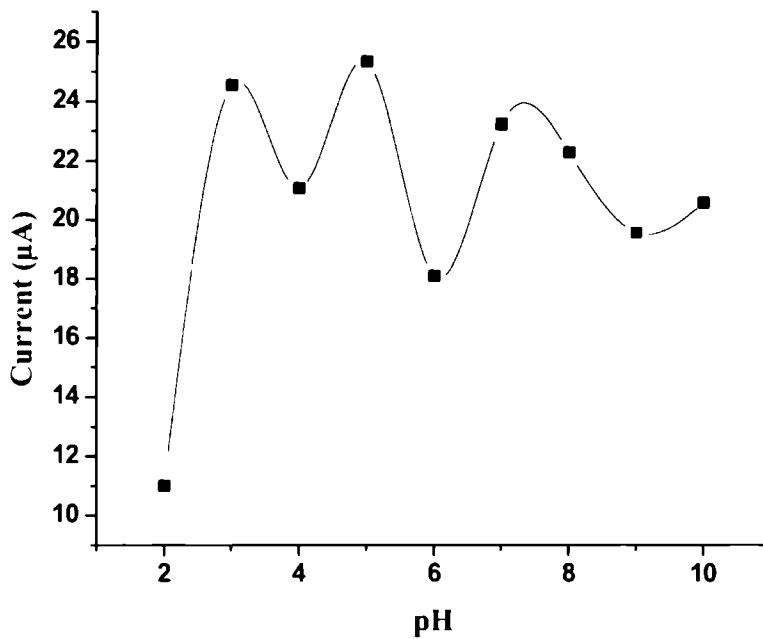


Figure 7.7. Plot of pH versus current

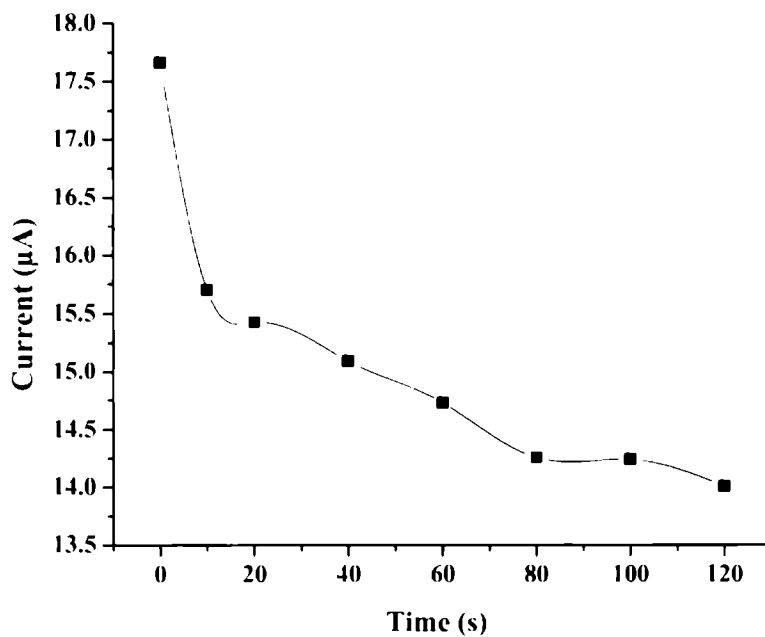
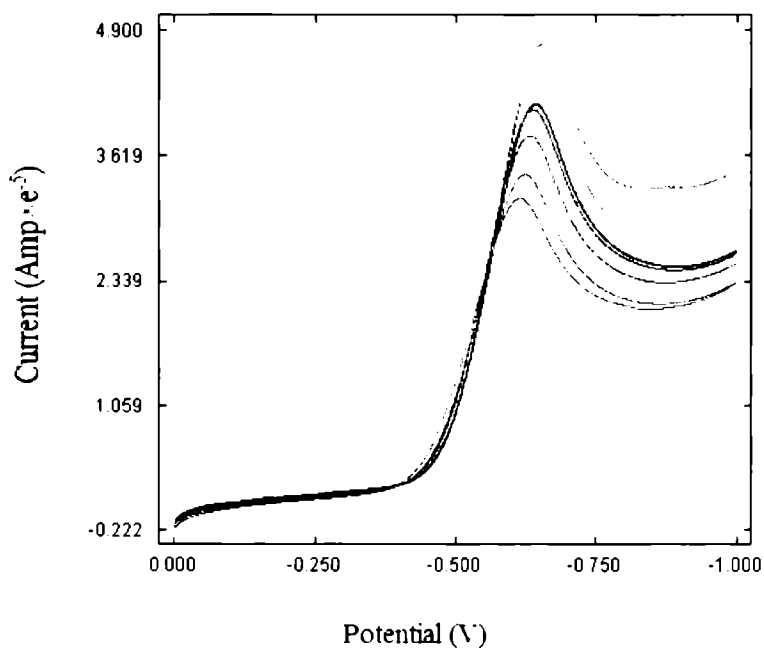
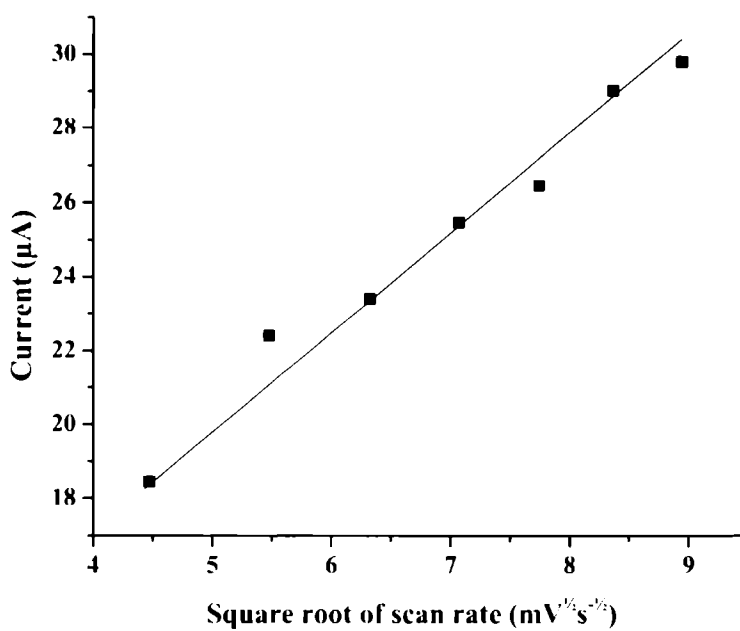


Figure 7.8. Relationship between cathodic peak current and accumulation time



**Figure 7.9.** Linear sweep voltammograms of 10<sup>-3</sup> M of TNZ at scan rates 20, 30, 40, 50, 60, 70, 80 mVs<sup>-1</sup> (from bottom to top)



**Figure 7.10.** Variance of cathodic peak current of 10<sup>-3</sup> M of TNZ with square root of scan rate

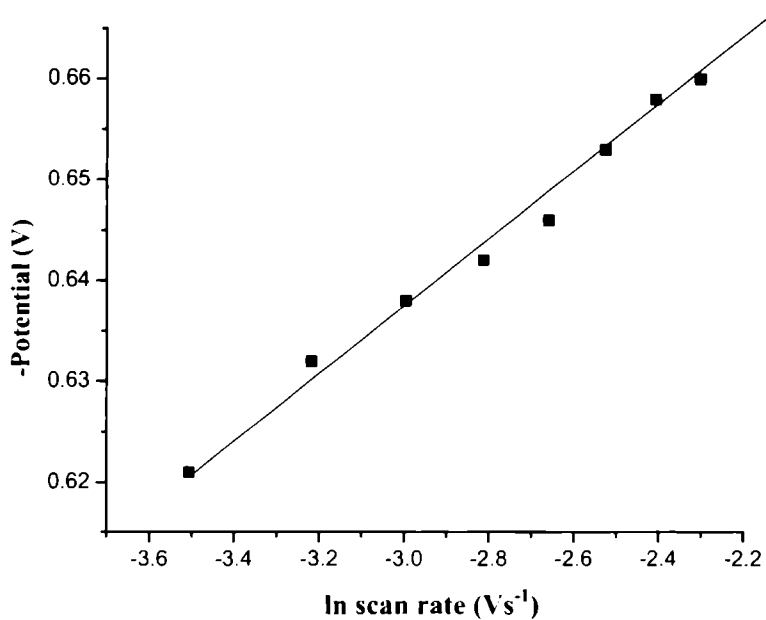


Figure 7.11. Plot of ln scan rate versus cathodic potential

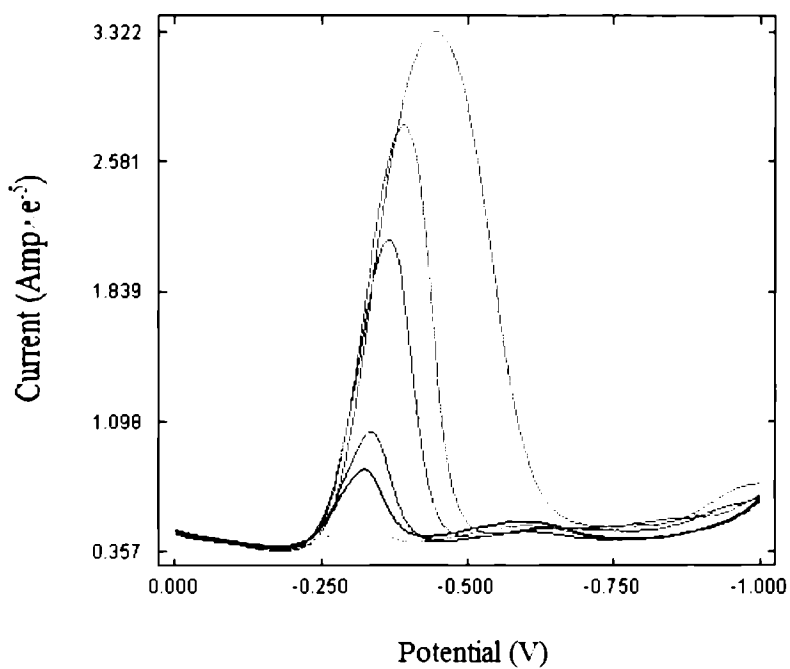
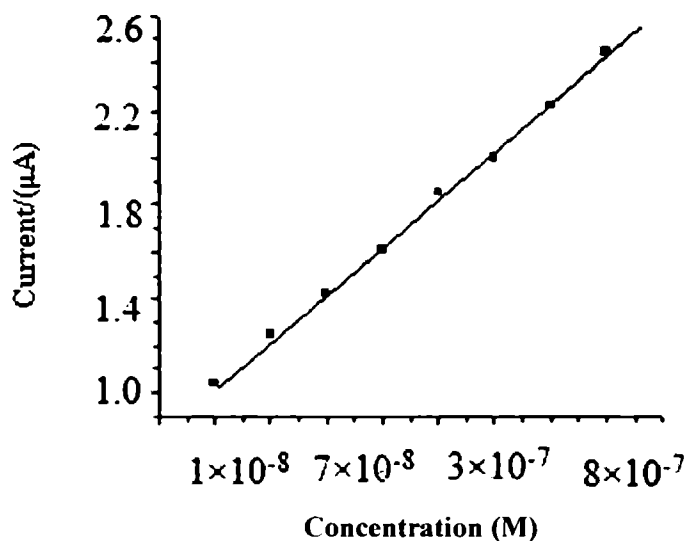
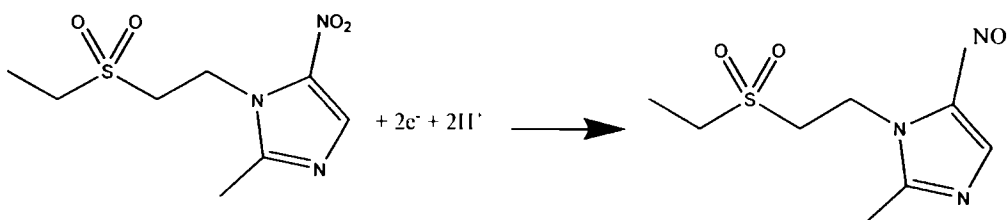


Figure 7.12. Differential pulse voltammograms of reduction of TNZ of concentrations  $10^{-3}$ ,  $10^{-4}$ ,  $10^{-5}$ ,  $10^{-6}$ ,  $10^{-7}$ ,  $10^{-8}$  M (from top to bottom)



**Figure 7.13.** Dependence of peak current on the concentrations of TNZ in the range  $1 \times 10^{-8}$  M -  $8 \times 10^{-7}$  M



**Scheme 7.1.** Mechanism of electroreduction of TNZ

.....

## COMPUTATIONAL STUDIES OF THE ELECTROOXIDATION OF TRIMETHOPRIM

|                 |                                    |
|-----------------|------------------------------------|
| <b>Contents</b> | <i>8.1. Introduction</i>           |
|                 | <i>8.2. Computational method</i>   |
|                 | <i>8.3. Results and Discussion</i> |
|                 | <i>8.4. Conclusions</i>            |

This chapter explains the investigation of electrocatalysis of [5,10,15,20-tetrakis(4-methoxyphenyl)porphyrinato]Mn(III)chloride (TMOPPMn(III)Cl) towards the oxidation of trimethoprim (TMP) by computational methods. DFT calculations were performed at the B3LYP level to detect the site of oxidation as well as to survey the role of manganese porphyrin in the facile oxidation of TMP. Atoms in molecule (AIM) analysis and natural bond orbital (NBO) analysis also substantiate the utility of TMOPPMn(III)Cl in TMP oxidation by confirming the co-ordination of trimethoprim to manganese porphyrin on removal of proton.

### 8.1 Introduction

The search for accurate electronic wave functions of polyatomic molecules uses mainly the molecular orbital method. The presence of several nuclei causes greater computational difficulties than for diatomic molecules. Molecular quantum mechanical methods are classified as either *ab initio* or semiempirical. Semiempirical methods use a simpler Hamiltonian than the correct molecular Hamiltonian and use parameters whose values are adjusted to fit experimental data or the results of *ab initio* calculations. In contrast, *ab*

initio calculation uses the correct Hamiltonian and does not use experimental data other than the values of the fundamental physical constants. An ab initio self consistent field calculation uses the approximation of taking  $\Psi$  as an antisymmetrized product of one electron spin orbitals and uses a finite and hence incomplete basis set.<sup>241,242</sup>

A basis set is a set of functions used to create the molecular orbitals which are expanded as a linear combination of such functions with the weights or coefficients to be determined. Usually these functions are atomic orbitals in that they are centered on atoms. Otherwise the functions are centered on bonds or lone pairs. In modern computational chemistry, quantum chemical calculations are typically performed within a finite set of basis functions. The wave functions under consideration are all represented as vectors, the components of which correspond to coefficients in a linear combination of the basis functions in the basis set used. The operators are then represented as matrices. The basis functions are usually not exactly the exact atomic orbitals. Initially these atomic orbitals were typically Slater orbitals which correspond to a set of functions which decayed exponentially with distance from the nuclei, later it was realized by Franck boys that these slater type orbitals could be approximated as linear combinations of Gaussian orbitals instead.<sup>241,243</sup>

Minimal basis sets are composed of minimum number of basis functions required to represent all the electrons on each atom. Eg: STO-3G, STO-4G, STO-3G\*, STO-6G.

The minimal basis sets suffer from several deficiencies. The atoms at the end of a period of the periodic table are described using the same number of basis functions as the atoms at the beginning of the period. A minimal basis set only contains one contraction per atomic orbital and as the radial exponents

are not allowed to vary during the calculation, the functions cannot expand or contract in size in accordance with the molecular environment. The third drawback is that a minimal basis set cannot describe non spherical aspects of the electronic distribution.

These problems with minimal basis sets can be addressed if more than one function is used for each orbital. A basis set which doubles the number of functions in the minimal basis set is called a double zeta basis set. An alternative to the double zeta basis approach is to double the number of functions used to describe the valence electrons but to keep a single function for the inner shells and is called split basis set. Three Gaussian functions are used to describe the core orbitals. The valence electrons are also represented by three Gaussians, the contracted part by two Gaussians and the diffuse part by one Gaussian. Eg: 3-21 G, 4-21 G, 6-21 G, 6-31 G.

The use of split valence basis set can help to surmount the problems with non isotropic charge distribution but not completely. This problem can be overcome by introducing polarization functions into the basis set. The polarization functions have a higher angular quantum number and hence correspond to p orbitals for hydrogen and d orbitals for the first and second row elements. Eg: 6-31G\*. The inability to deal with species such as anions and molecules containing lone pairs which have a significant amount of electron density away from the nuclear centres can be overcome by adding highly diffuse functions to the basis set. Eg: 3-21+G. Diffuse functions can also be included for hydrogen as well as for heavy atoms. Eg: 6-31+G(d).<sup>244,245</sup>

### **8.1.1 Density functional theory**

Density Functional theory (DFT) is an approach to the electronic structure of atoms and molecules which has enjoyed a dramatic surge of

interest since the late 1980's and 1990's. In Hartree Fock (HF) theory, the multi electron wave function is expressed as a Slater determinant which is constructed from a set of N single electron wave functions. DFT also considers single electron functions. Whereas HF theory does calculate the full N electron wave function, DFT only attempts to calculate the total electronic energy and the overall electronic distribution. The idea of DFT is that there is a relationship between the total electronic energy and the overall electronic density. Hohenberg and Kohn showed that the ground state energy and other properties of a system were defined by the electron density. In DFT, the energy functional is written as a sum of two terms

$$E[\rho(\mathbf{r})] = \int V_{\text{ext}}(\mathbf{r})\rho(\mathbf{r}) d\mathbf{r} + F[\rho(\mathbf{r})] \quad \text{----- (8.1)}$$

The first term arises from the interaction of the electrons with an external potential  $V_{\text{ext}}$  typically due to the Coulomb interaction with the nuclei.  $F[\rho(\mathbf{r})]$  is the sum of kinetic energy of the electrons and the contribution from interelectronic interactions. The minimum value in the energy corresponds to the exact ground state electron density so enabling a variational approach to be used. The best solution corresponds to the minimum of energy and an incorrect density gives an energy above the true energy.

In order to minimize the energy, a Lagrangian multiplier,  $(-\mu)$  is introduced leading to the following equation:

$$\frac{\delta}{\delta\rho(\mathbf{r})} \left[ E[\rho(\mathbf{r})] - \mu \int \rho(\mathbf{r}) d\mathbf{r} \right] = 0 \quad \text{----- (8.2)}$$

$$\left( \frac{\delta E[\rho(\mathbf{r})]}{\delta\rho(\mathbf{r})} \right)_{V_{\text{ext}}} = \mu \quad \text{----- (8.3)}$$

Equation (8.3) is the DFT equivalent of the Schrodinger equation.

Kohn and Sham suggested a practical way to solve the Hohnberg-Kohn theorem for a set of interacting electrons. The difficulty with equation (8.1) is that we do not know what the function  $F[\rho(\mathbf{r})]$  is.

$F[\rho(\mathbf{r})]$  should be approximated as the sum of three terms.

$$F[\rho(\mathbf{r})] = E_{KE}[\rho(\mathbf{r})] + E_H[\rho(\mathbf{r})] + E_{XC}[\rho(\mathbf{r})]$$

where  $E_{KE}[\rho(\mathbf{r})]$  is the kinetic energy,  $E_H[\rho(\mathbf{r})]$  is the electron electron Coulombic energy and  $E_{XC}[\rho(\mathbf{r})]$  contains contributions from exchange and correlation.

Adding the electron-nuclear interaction leads to the full expression for the energy of an N electron system within the Kohn-Sham scheme:

$$E[\rho(\mathbf{r})] = \sum_{i=1}^N \int \psi_i(\mathbf{r}) \left( -\frac{\nabla^2}{2} \right) \psi_i(\mathbf{r}) d\mathbf{r} + \frac{1}{2} \iint \frac{\rho(\mathbf{r}_1)\rho(\mathbf{r}_2)}{|\mathbf{r}_1 - \mathbf{r}_2|} d\mathbf{r}_1 d\mathbf{r}_2 + E_{XC}[\rho(\mathbf{r})] - \sum_{A=1}^M \int \frac{Z_A}{|\mathbf{r} - \mathbf{R}_A|} \rho(\mathbf{r}) d\mathbf{r}$$

where  $E_{XC}[\rho(\mathbf{r})]$  is the exchange correlation functional, which thus not only contains contributions due to exchange and correlation but also a contribution due to the difference between the true kinetic energy of the system and  $E_{KE}[\rho(\mathbf{r})]$ .

The density  $\rho(\mathbf{r})$  of the system is written as the sum of the square moduli of a set of one electron orthonormal orbitals<sup>243,245</sup>

$$\rho(\mathbf{r}) = \sum_{i=1}^N |\psi_i(\mathbf{r})|^2$$

Correlation effects are incorporated from the beginning in DFT. The exchange correlation energy is written as a sum of the exact exchange term together with the correlation component from the local density approximation. Hybrid functionals are a class of approximations to the exchange-correlation energy functional in DFT that incorporate a portion of exact exchange from HF theory with exchange and correlation from other sources (ab initio or empirical). The exact exchange energy functional is expressed in terms of the Kohn-Sham orbitals rather than the density, so is termed an implicit density functional. One of the most commonly used versions is B3LYP, which stands for Becke, 3-parameter, Lee-Yang-Parr.<sup>246</sup>

The popular B3LYP (Becke, three-parameter, Lee-Yang-Parr)<sup>247,248</sup> exchange-correlation functional is:

$$E_{XC}^{B3LYP} = (1 - a_0)E_X^{LSDA} + a_0E_X^{HF} + a_X\Delta E_X^{B88} + a_C E_C^{LYP} + (1 - a_C)E_C^{VWN}$$

where  $E_X^{LSDA}$  is the exchange energy under the local spin density approximation,  $E_X^{HF}$  is the exact exchange from Hartree Fock theory,  $\Delta E_X^{B88}$  is the Becke 88 exchange functional,<sup>249</sup>  $E_C^{LYP}$  is the correlation functional of Lee, Yang and Parr,<sup>250</sup>  $E_C^{VWN}$  is the Vosko, Wilk and Nusair local-density approximation to the correlation functional.<sup>251</sup>  $a_0 = 0.20$ ,  $a_X = 0.72$  and  $a_C = 0.81$  are the three empirical parameters determined by fitting the predicted values to a set of atomization energies, ionization potentials, proton affinities and total atomic energies<sup>252</sup> and are generalized gradient approximations.

Density functional methods using gradient corrected functionals can give results for a wide variety of properties that are competitive with and in some cases superior to ab initio calculations using correlation like in MP2. Calculations have been carried out only for the species involved in the reaction, omitting

the electrode. Barth et al. have shown by ab initio calculations and scanning tunneling microscopy (STM) observations of tetrapyridyl and Fe(II)-tetrafluoride-porphyrin molecules on the Ag(111) surface that the molecular structure remains largely unaffected by the adsorption on the silver surface.<sup>253</sup> Many studies have been carried out in which DFT has been used as a tool to investigate mechanisms of reactions occurring on surfaces, without considering the electrode or the surface on which these reactions occur.<sup>254</sup> D'Souza et al. also showed that the HOMO-LUMO energy gaps obtained for porphyrin systems by DFT calculations follow the trends of the electrochemical results. Their studies revealed good agreement between the experimental results and computational predictions.<sup>255-257</sup> However, it is important to note that these in vacuo calculations provide a qualitative idea about the oxidation mechanism, and a quantitative estimation will require an explicit consideration for the presence of the electrode and solvation effects.

The AIM approach relies on an analysis of the topological properties of the charge density,  $\rho(r)$  and its quality depends on the computational level chosen. Both the gradient and the Laplacian of the charge density,  $\nabla\rho$  and  $\nabla^2\rho$  respectively, can be analyzed and provide complementary information on bonds. The critical points of  $\nabla\rho$  give information about the existence of bonds, while the sign of  $\nabla^2\rho$  at that point reflects the kind of interaction. Nuclei attract the charge density so that maxima of  $\nabla\rho$  are found there. A bond corresponds to a saddle point (the bond critical point), where  $\nabla\rho$  becomes zero, a maximum only in one plane of space and is found joining two trajectories of maximum  $r$  along the space, toward the nuclei.<sup>258-264</sup> NBO analysis is based on a method for optimally transforming a given wave function into localized form. In NBO analysis, the input atomic orbital basis set is transformed via natural atomic

orbitals (NAOs) and natural hybrid orbitals (NHOs) into natural bond orbitals (NBOs). The NBOs obtained in this fashion correspond to the widely used Lewis picture, in which two-center bonds and lone pairs are localized.<sup>265</sup>

## 8.2 Computational method

Quantum chemical calculations have been performed using the Gaussian 03 suite of programs.<sup>266</sup> All the geometries were fully optimized by density functional theory (DFT) using the Becke, three-parameter, Lee-Yang-Parr (B3LYP) hybrid functional theory.<sup>250,267</sup> 6-31+G(d) basis set<sup>268,269</sup> was used to optimize all the structures involved in the uncatalyzed reaction of trimethoprim at bare glassy carbon electrode (GCE). For the optimization of the geometries involved in the catalyzed reaction on TMOPPMn(III)Cl/GCE, split basis set method with 6-31+G(d) for the main group elements and compact effective potentials split valence set (CEP-31G)<sup>270,271</sup> for manganese was utilized. These geometries were also optimized using Los Alamos 19 electron shape consistent relativistic ECP (LANL2DZ) basis set<sup>272,273</sup> to carry out natural bond orbital (NBO) and atoms-in-molecules (AIM) analysis. [Mn(III) porphyrin]Cl is chosen as a model for TMOPPMn(III)Cl in the computational investigation of the catalyzed reaction. All minimum energy structures have been characterized through frequency calculations to ensure that there are no saddle points corresponding to imaginary frequencies.

## 8.3 Results and Discussion

Voltammetric behavior of trimethoprim investigated at bare GCE and at TMOPPMn(III)Cl/GCE demonstrates the electrocatalytic ability of TMOPPMn(III)Cl. The details of the voltammetric experiment of the oxidation of trimethoprim on TMOPPMn(III)Cl/GCE is already described in Chapter 3. Figure 3.4 shows the differential pulse voltammograms of  $10^{-3}$  M trimethoprim

in phosphate buffer solution at bare GCE (curve a) and TMOPPMn(III)Cl/GCE (curve b). Obviously, the peak potential shifts towards a more negative potential compared to that of a bare GCE. The electrochemical studies of  $10^{-3}$  M of TMP carried out in the pH range 3-10 shows that the peak current is highest at pH 5, which can be seen from Figure 3.5. However, the anodic potential decreases with increase in pH value as can be seen from Figure 8.1. The number of electrons involved in the electrochemical reaction of trimethoprim was calculated to be 3.8. Based on this experimental finding, the proposed possible mechanism is shown in Scheme 3.1.

The optimized structure of trimethoprim is shown in Figure 8.2. There are two amino groups, one at position 4 of the pyrimidine ring and the other at position 2 of the stable pyrimidine system.<sup>132</sup> Deprotonation of  $\text{NH}_2$  group attached to either C4 or C2 of trimethoprim can occur and thus both of these possibilities were investigated computationally. The internal energy change ( $\Delta E$ ), enthalpy change ( $\Delta H$ ) and free energy change ( $\Delta G$ ) of the deprotonation of  $\text{NH}_2$  attached to C4 are -35.9, -30.8 and -31.4 kcal/mol respectively, while that attached to C2 are -26.4, -27.3 and -28.3 kcal/mol respectively. Clearly, deprotonation of the former is more facile than that of latter. Thus for further calculations, we have considered the removal of proton from the C4 amino group. The detailed mechanism<sup>132, 274-276</sup> is outlined in Scheme 8.1. The first step involved in the conversion of trimethoprim (**I**) to nitroso derivative (**IX**) is the deprotonation of  $\text{NH}_2$  group at the 4<sup>th</sup> position to give trimethoprim anion (**II**). The formation of (**II**) from (**I**) is an exothermic process ( $\Delta H = -30.8$  kcal/mol). The distance between C4 and N8 in (**I**) and (**II**) are 1.38 and 1.32 Å<sup>0</sup> respectively as shown in Figure 8.3.

Mn(III)porphyrin]Cl $\cdots$ trimethoprim was optimized with 0, 1 and 2 spin states to analyze their relative stabilities. The geometry with spin state 2

(multiplicity=5) was found to have lowest energy and hence is the most stable one. Hence all the further studies were carried out using [Mn(III)porphyrin]Cl···trimethoprim with spin state 2. The optimized structure of [Mn(III)porphyrin]Cl···trimethoprim with spin state 2 is shown in Figure 8.4. As for the uncatalyzed reaction, the deprotonation of NH<sub>2</sub> of trimethoprim attached to C4 and C2 for the [Mn(III)porphyrin]Cl catalyzed reaction was also investigated.  $\Delta E$ ,  $\Delta H$  and  $\Delta G$  corresponding to the deprotonation of NH<sub>2</sub> attached to C4 are found to be -48.3, -48.4 and -48.4 kcal/mol respectively, while that attached to C2 are -43.4, -45.0 and -42.2 respectively. The values of thermodynamic properties suggest that deprotonation at 4<sup>th</sup> position is more favorable than that at 2<sup>nd</sup> position. Compared to the uncatalyzed reaction, the coordination of [Mn(III)porphyrin]Cl with trimethoprim anion increases the exothermicity of the deprotonation. This suggests that [Mn(III)porphyrin]Cl···trimethoprim (A) gets further stabilized by deprotonation. It is interesting to note that the distance between N46 and Mn is 3.64 Å<sup>0</sup> in (A), whereas in [Mn(III)porphyrin]Cl···trimethoprim anion (B), it is 2.23 Å<sup>0</sup> as shown in Figure 8.5.

Trimethoprim anion gets stabilized by the interaction of Mn(III) of the metalloporphyrin with N of the NH<sub>2</sub> group at the 4<sup>th</sup> position of trimethoprim which carries the reaction forward. Selected bond lengths of structures (A) and (B) are summarized in Table 8.1. HOMO-LUMO for (A) and (B) shown in Figure 8.6 reveals that HOMO - LUMO of (B) is interacting, whereas that of (A) is not. Thus, on deprotonation, trimethoprim anion co-ordinates to [Mn(III)porphyrin]Cl thus facilitating further oxidation.

The plot of the gradient of the charge density  $\rho$  in [Mn(III)porphyrin]Cl···trimethoprim and [Mn(III)porphyrin]Cl···trimethoprim anion is depicted in Figure 8.7 (A) and (B) respectively. The most striking feature of the plots is the absence of critical points between N46 and Mn in [Mn(III)

porphyrin]Cl...trimethoprim, whereas in [Mn(III)porphyrin]Cl...trimethoprim anion, there exists a bond critical point between these atoms, with charge density,  $\nabla\rho = 0.0814$  and Laplacian of charge density,  $\nabla^2\rho = -0.0786$ . The value of  $\nabla\rho$  shows that there is substantial charge density in between N46 and Mn bond. The negative Laplacian for the bond critical points suggests stabilization through intermolecular interactions.

NBO analysis points out a bond order of 0.02 and 0.45 between N46 and Mn in (A) and (B) respectively. This is a further evidence for the fact that trimethoprim coordinates with the Mn of the [Mn(III)porphyrin]Cl only when it is converted to its anionic form on deprotonation.

#### **8.4 Conclusions**

Electrochemical experiments and computational methods show that TMOPPMn(III)Cl acts as an electrocatalyst for the oxidation of trimethoprim. From the voltammetric oxidation of trimethoprim investigated at bare and TMOPPMn(III)Cl modified GCE, it is inferred that the anodic potential required for the oxidation of trimethoprim gets lowered on the TMOPPMn(III)Cl/GCE compared to that on bare GCE. Quantum mechanical calculations explain the role of manganese porphyrin in the easy oxidation of trimethoprim. The calculations show that the oxidation of amino group attached to C4 of trimethoprim is easier than that attached to C2. In comparison to the uncatalyzed, the catalyzed deprotonation, which is the preliminary step in the oxidative mechanism, is energetically more favorable. AIM analysis shows the existence of a bond critical point between manganese and the nitrogen of the trimethoprim anion. NBO analysis further supports the interaction between trimethoprim anion and manganese porphyrin. A bond order of 0.45 is calculated between N46 of trimethoprim anion and manganese

of metalloporphyrin. It is thus deduced that trimethoprim anion interacts with the manganese of the metalloporphyrin. The facile oxidation of trimethoprim in the presence of TMOPPMn(III)Cl can be attributed to the interaction between the metal ion and deprotonated trimethoprim, which assists the transfer of electron in the first step of the reaction. Thus the computational calculations shed light on the role of manganese porphyrin in the easy oxidation of trimethoprim.

**Table 8.1. Selected bond lengths of [Mn(II)porphyrin]Cl...trimethoprim and [Mn(II)porphyrin]Cl...trimethoprimanion computed at B3LYP/6-31+G(d), CEP-31G level of theory.**

The bond lengths are in Angstroms

| Species   | [Mn(II)porphyrin]Cl...<br>trimethoprim | [Mn(II)porphyrin]Cl...<br>trimethoprim anion |
|-----------|--|--|
| N46 - Mn  | 3.64                                   | 2.23   |
| C42 - N46 | 1.38                                   | 1.33   |
| Mn - Cl   | 2.35                                   | 2.58   |

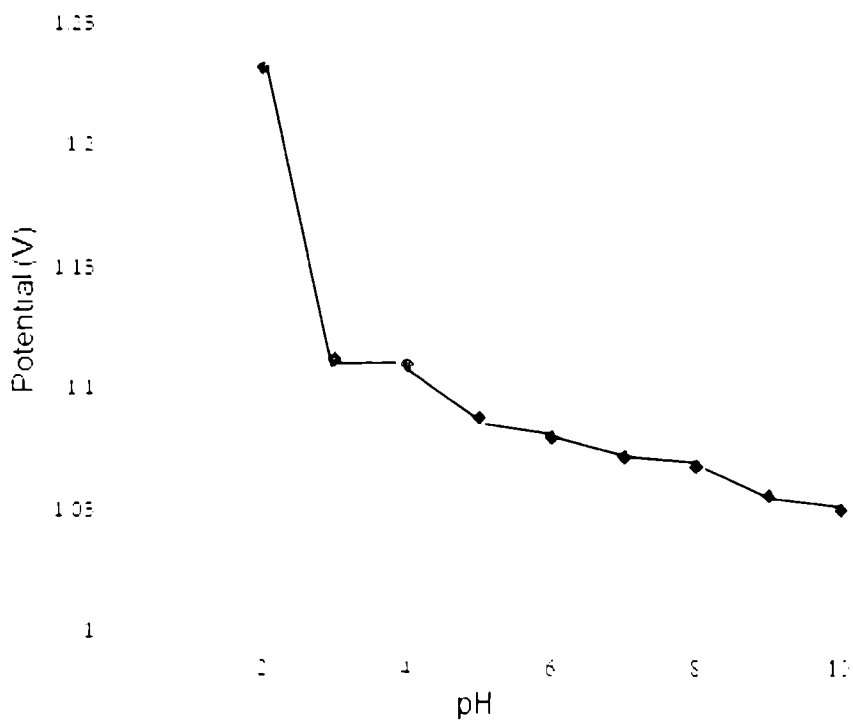


Figure 8.1. Variation of anodic peak potential of  $10^{-3}$  M of Trimethoprim with pH

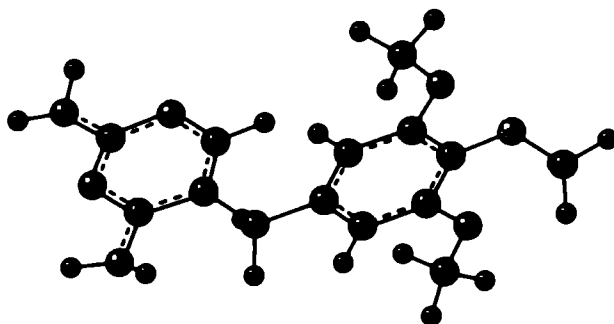


Figure 8.2. Optimised structure of Trimethoprim

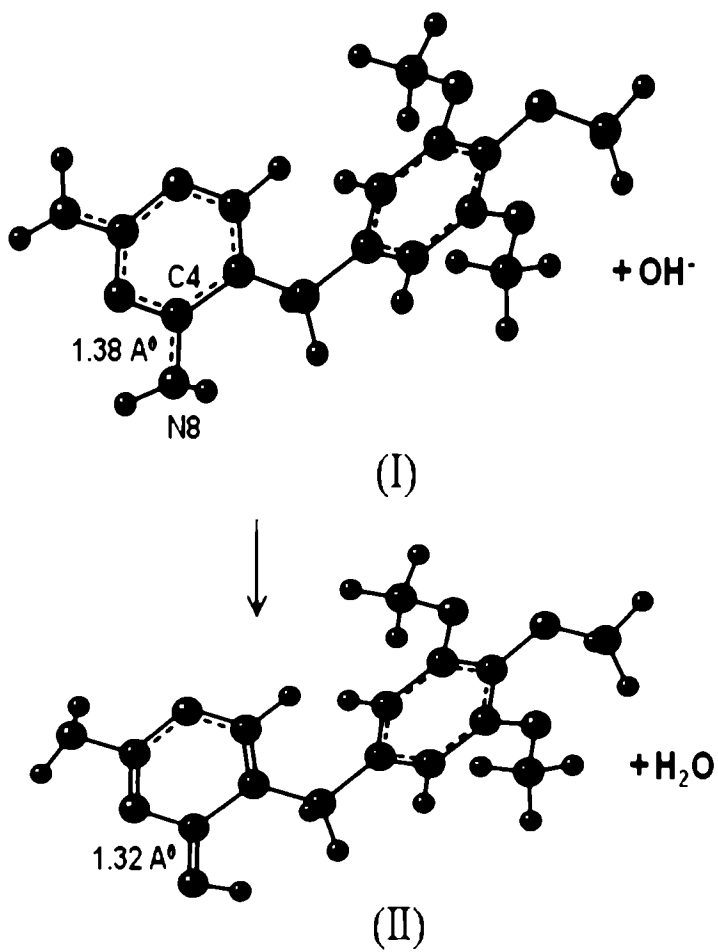


Figure 8.3. Deprotonation of Trimethoprim

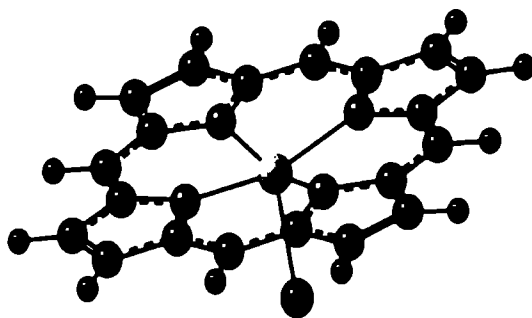


Figure 8.4. Optimised structure of [Mn(III)porphyrin]Cl

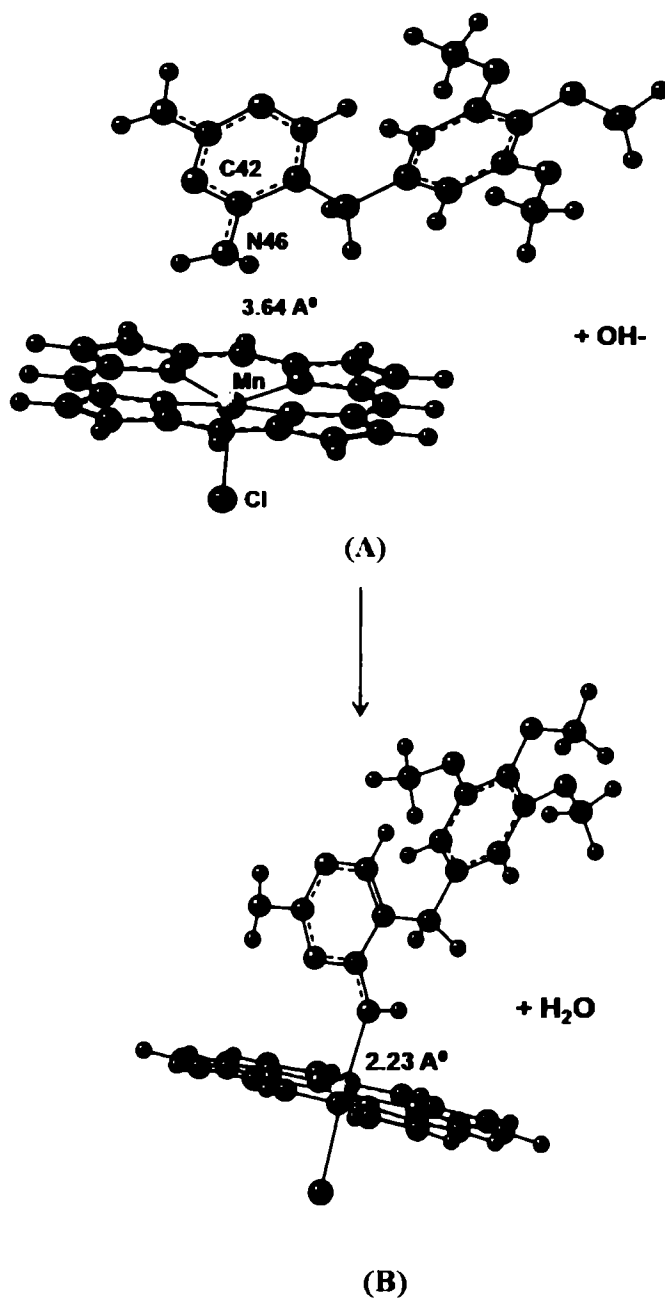
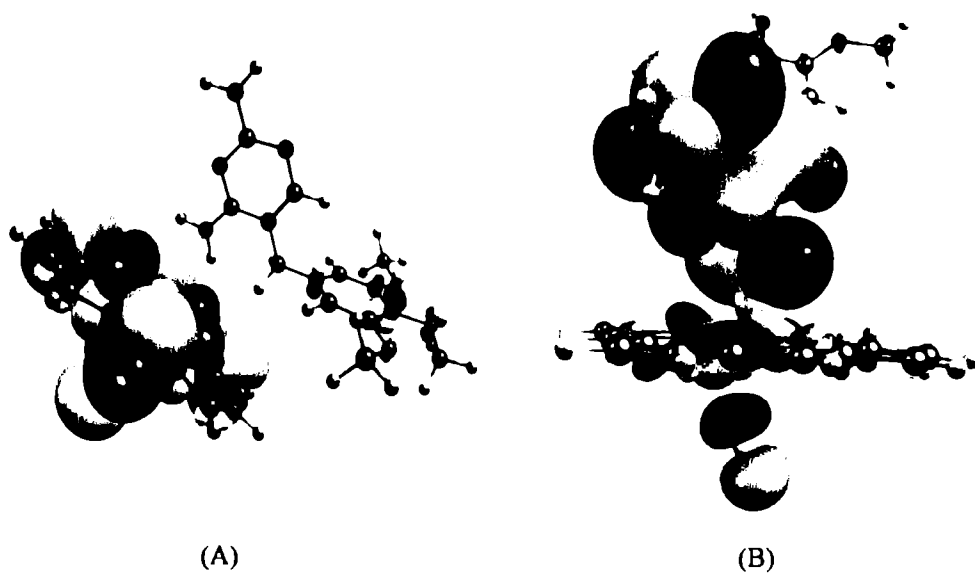
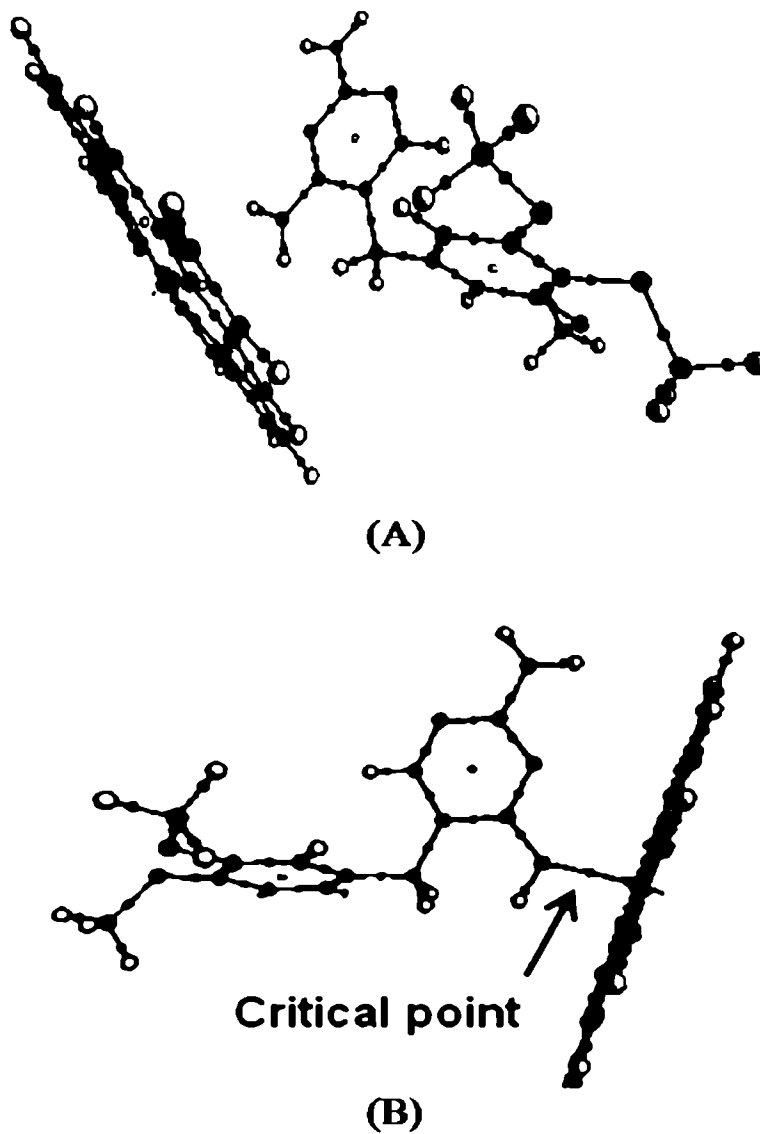


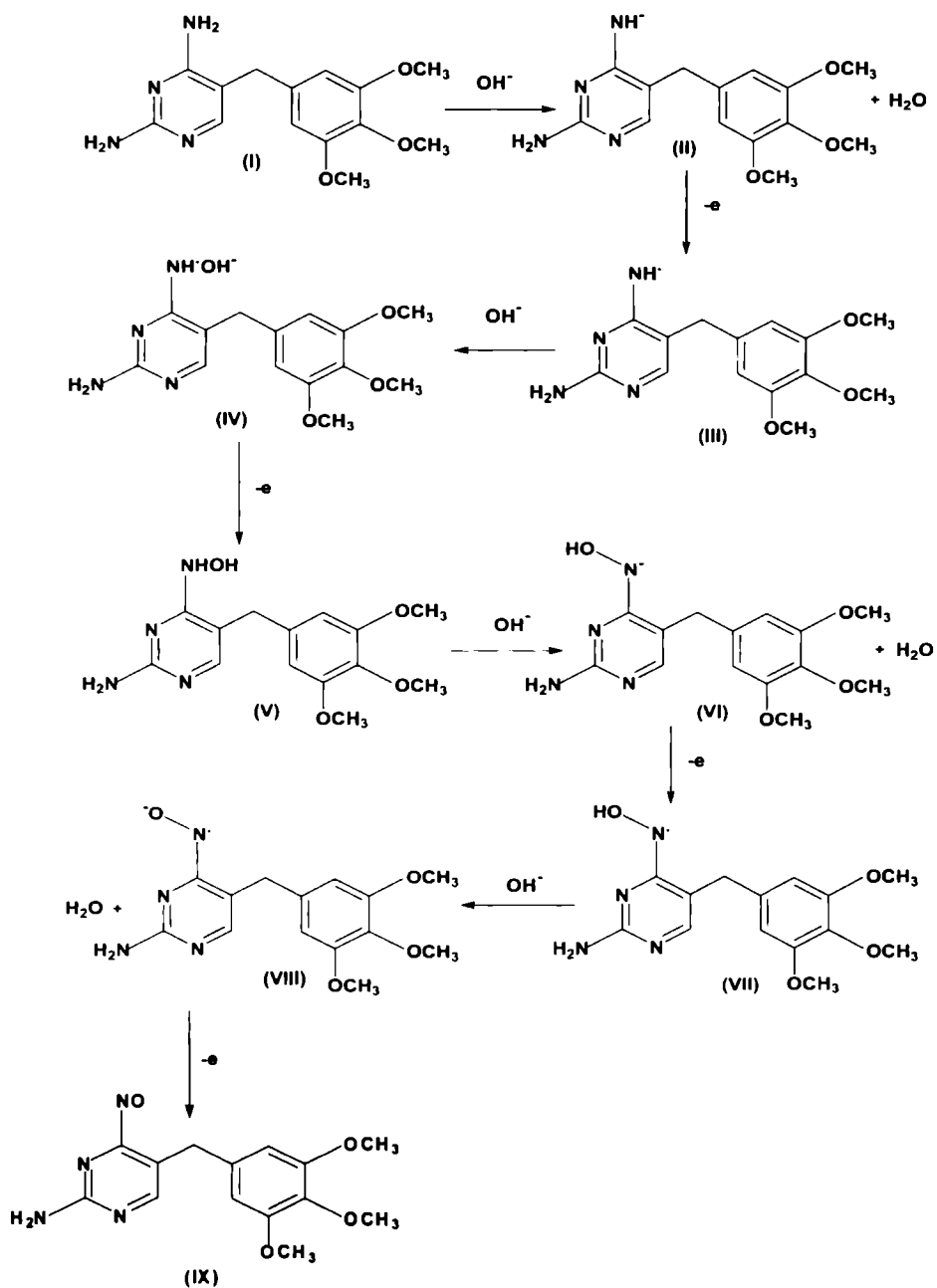
Figure 8.5. Deprotonation in [Mn(III)porphyrin][Cl...trimethoprim



**Figure 8.6. HOMO-LUMO of (A) [Mn(III)porphyrin][Cl<sup>-</sup>·trimethoprim and (B) [Mn(III)porphyrin][Cl<sup>-</sup>·trimethoprim anion**



**Figure 8.7.** Plots of the gradient of charge density in (A) [Mn(III)porphyrin]Cl·trimethoprim and (B) [Mn(III)porphyrin]Cl·trimethoprim anion



Scheme 8.1. Detailed mechanism of oxidation of TMP

.....FOCR.....

- 9.1. *Objectives of the work*
- 9.2. *Summary of the work done*
- 9.3. *Future outlook*

This chapter presents the objectives of the investigation and the summary of the work done. Future outlook is also described. As part of the present investigation glassy carbon electrode was modified using metalloporphyrin and dyes. The modified electrodes were subsequently used for the determination of various pharmaceuticals.

## 9.1 Objectives of the work

The prime objectives of the work include:

- 1) Chemical modification of glassy carbon electrode (GCE).
- 2) Surface studies of the bare and modified electrode by examining the morphology of the surfaces and calculating the effective surface area.
- 3) Applying the modified electrode for the voltammetric determination of pharmaceuticals.
- 4) Comparing the voltammetric response of the drug at bare GCE and modified GCE.

- 5) Optimisation of electrochemical parameters for the determination of different drugs.
- 6) Applying the modified electrode for the voltammetric determination of drug in real samples.
- 7) Computational study of the interaction of the manganese porphyrin with trimethoprim as part of the theoretical investigation of the role of electrode modifier in facilitating the electrochemical reaction of the drug.

## 9.2 Summary of the work done

Various modified electrodes prepared and the respective drugs they sense are listed below:

|  |                         |
|--|-------------------------|
| [5,10,15,20-tetrakis(4-methoxyphenyl)porphyrinato] manganese(III)chloride modified GCE | Trimethoprim & Ambroxol |
| Poly(malachite green) modified GCE   | Sulfamethoxazole        |
| Poy(methyl red) modified GCE   | Domperidone             |
| Poly(criochrome black T) modified GCE  | Tinidazole              |

## 9.3 Future outlook

Electrochemical sensors are used extensively either as a whole or an integral part of a chemical and biomedical sensing element. The fundamentals of this sensing technique are well established and the critical issue is the applicability of the technique to a complex environment such as in blood or other biological fluids. There lies exciting challenge of designing a biosensor using voltammetric and amperometric principles. Further, computational

studies can predict the role of a modifier in catalysing an electrochemical reaction and suggest a possible mechanism for this. Simulation techniques in computational chemistry can provide more accurate results by mimicking an electrode and the real electrochemical situation.

.....EOR.....

- [1] Bockris, J. O. M.; Reddy, A. K. N. *Modern Electrochemistry, Volume 1, Ionics*; Kluwer Academic/Plenum Publishers: New York, 1998.
- [2] Bockris, J. O. M.; Reddy, A. K. N. *Modern Electrochemistry, Volume 2A, Fundamentals of Electrode Processes*; Kluwer Academic/Plenum Publishers: New York, 1998.
- [3] Bard, A. J.; Faulkner, L. R. *Electrochemical Methods—Fundamentals and Applications*; Wiley: New York, 1980.
- [4] Monk, P. M. S. *Fundamentals of Electroanalytical Chemistry*; Wiley: Chichester, 2001.
- [5] Mendham, J.; Denney, R. C.; Barnes, J. D.; Thomas, M. J. K. *Vogel's Textbook of Quantitative Chemical Analysis*; 6<sup>th</sup> Edn, Pearson Education Ltd: Singapore, 2000.
- [6] Brett, C. M. A.; Brett, A. M. O. *Electroanalysis*; Oxford Science Publications: New York, 1998.
- [7] Skoog, D. A.; Holler, F. J.; Crouch, S. R. *Instrumental Analysis*; Brooks/Cole: California, 2009.
- [8] Willard, H. H.; Merritt, L. L.; Dean, J. A.; Settle, F. A. *Instrumental Methods of Analysis*; 6<sup>th</sup> Edn, D. Van Nostrand Co: New York, 1981.
- [9] Vassos, B. H.; Ewing, G. W. *Electroanalytical Chemistry*; John Wiley & Sons: New York, 1983.
- [10] Murray, R. W.; Ewing, A. G.; Durst, R. A. *Anal. Chem.* **1987**, *59*, 379.
- [11] Kellner, R.; Mermet, J. M.; Otto, M.; Valcarcel, M.; Widmer, H. M. *Analytical Chemistry*; Wiley VCH: Weinheim, 2004.
- [12] Markas, A.; Gilmartin, T.; Hart, J. P. *Analyst* **1995**, *120*, 1029.

- [13] Csoregi, E.; Gorton, L.; Marko-Varga, G. *Anal. Chim. Acta* **1993**, *273*, 59.
- [14] Ruiz, B. L.; Dempsey, E.; Hua, C.; Smyth, M. R.; Wang, J. *Anal. Chim. Acta* **1993**, *273*, 425.
- [15] Adams, R. N. *Anal. Chem.* **1958**, *30*, 1576.
- [16] Cespedes, F.; Fabregas, M. J.; Bartroli, J.; Alegrats, S. *Anal. Chim. Acta* **1993**, *273*, 409.
- [17] Kinoshita, K. *Carbon-Electrochemical and Physiochemical Properties*; Wiley: New York, 1988.
- [18] McCreery, R. L. *Electroanalytical Chemistry*; Dekker: New York, 1991.
- [19] Issac, S.; Girish Kumar, K. *Drug Test. Analysis* **2009**, *1*, 350.
- [20] Aubeck, R.; Brauchle, C.; Hampp, N. *Analyst* **1991**, *116*, 811.
- [21] Wang, J. *Electroanalysis* **1991**, *3*, 255.
- [22] Skoog, D. A.; West, D. M.; Holler, F. J.; Crouch, S. R. *Fundamentals of Analytical Chemistry*; Brooks/Cole: California, 2004.
- [23] Valcarcel, M. *Principles of Analytical Chemistry*; Springer: New York, 2000.
- [24] Skoog, D. A.; Holler, F. J.; Nieman, T. A. *Principles of Instrumental Analysis*; Brooks/Cole: California, 2004.
- [25] Christian, G. D. *Analytical Chemistry*; John Wiley & Sons: New York, 1977.
- [26] Fifield, F. W.; Kealey, D. *Principles and Practice of Analytical Chemistry*; Blackwell Science Ltd: Paris, 2000.
- [27] Janata, J. *Principles of Chemical Sensors*; Plenum Press: New York, 1989.
- [28] Cattrall, R. W. *Chemical Sensors*; Oxford University Press: Oxford, 1997.
- [29] Kutner, W.; Wang, J.; L'Her, M.; Buck, R. P. *Pure & Appl. Chem.* **1998**, *70*, 1301.

- [30] Suslick, K. S.; Jeffries, S. D. *Comprehensive Supramolecular Chemistry*; Elsevier: Oxford, 1996.
- [31] Kadish, K. M.; Smith, K. M.; Guillard, R. *The Porphrin Handbook, Volume 3, Inorganic, Organometallic and Coordination Chemistry*; Academic Press: San Deigo, 2000.
- [32] Beletskaya, I.; Tyurin, V. S.; Tsivadze, A. Y.; Guillard, R.; Stern, C. *Chem. Rev.* **2009**, *109*, 1659.
- [33] Chiang, C. K.; Fincher, C. R.; Park, Y. W.; Heeger, A. J.; Shirakawa, H.; Louis, E. J.; Gau, S. C.; McDiarmid, A. G. *Phys. Rev. Lett.* **1977**, *39*, 1098.
- [34] Letheby, H. *J. Chem. Soc.* **1862**, *15*, 161.
- [35] Hush, N. S. *Ann. N. Y. Acad. Sci.* **2003**, *1006*, 1.
- [36] Heeger, A. J. *Appl. Phys.* **2001**, *1*, 247.
- [37] Macdiarmid, A. G. *Curr. Appl. Phys.* **2001**, *1*, 269.
- [38] Shirakawa, H. *Curr. Appl. Phys.* **2001**, *1*, 281.
- [39] Scott, J. C. *Nanostructured Conductive Polymers*; John Wiley & Sons: New York, 2010.
- [40] Diaz, A.; Kanazawa, K.; Gardini, G. *Chem. Commun.* **1979**, *14*, 635.
- [41] Diaz, A. F.; Logan, J. A. *J. Electroanal. Chem.* **1980**, *111*, 111.
- [42] Bockris, J. O. M.; Reddy, A. K. N. *Modern Electrochemistry, Volume 2B, Electrodics in Chemistry, Engineering, Biology and Environmental Science*; Kluwer Academic/Plenum Publishers: New York, 1998.
- [43] Waltmana, R. J.; Diaz, F.; Bargon, J. *J. Phys. Chem.* **1984**, *88*, 4343.
- [44] Diaz, A. *Chem. Scr.* **1981**, *17*, 145.
- [45] Tourillon, G.; Garnier, F. *J. Electroanal. Chem.* **1982**, *135*, 173.
- [46] Bargon, J.; Mohmand, S.; Waltman, R. J. *J. Res. Dev.* **1983**, *27*, 330.

- [47] Karyakin, A. A.; Karyakina, E. E.; Schmidt, H. L. *Electroanalysis* **1999**, *11*, 149.
- [48] MacDiarmid, A. G.; Chiang, J. C.; Richter, A. G.; Epstein, A. *Synth. Met.* **1987**, *18*, 285.
- [49] Mazeikiene, R.; Niaura, G.; Eicher-Lorka, O.; Malinauskas, A. *Vib. Spectrosc.* **2008**, *47*, 105.
- [50] Atta, N. F.; Galal, A.; Karagozler, A. E.; Zimmer, H.; Rubinson, J. F.; Mark, H. B. *J. Chem. Soc. Chem. Commun.* **1990**, *19*, 1347.
- [51] Bauldreay, J. M.; Archer, M. D. *Electrochim. Acta* **1983**, *28*, 1515.
- [52] Hawn, D. D.; Armstrong, N. R. *J. Phys. Chem.* **1978**, *82*, 1288.
- [53] Osa, T.; Fujihira, M. *Nature* **1976**, *264*, 349.
- [54] Shepard Jr. V. R.; Armstrong, N. R. *J. Phys. Chem.* **1979**, *83*, 1268.
- [55] Fujihira, M.; Ohishi, N.; Osa, T. *Nature* **1977**, *268*, 226.
- [56] Fujihira, M.; Osa, T.; Hursh, D.; Kuwana, T. *J. Electroanal. Chem.* **1978**, *88*, 285.
- [57] Morishima, Y.; Isono, M.; Itoh, Y.; Nozakura, S. *Chem. Lett.* **1981**, *8*, 1149.
- [58] Tamilarasan, R.; Natarajan, P. *Nature* **1981**, *292*, 224.
- [59] Mesmaeker, K. D.; Dewitt, R. *Electrochim. Acta* **1981**, *26*, 297.
- [60] Albery, W. J.; Foulds, A. W.; Hall, K. J.; Hillman, A. R.; Egdell, R. G.; Orchard, A. F. *Nature* **1979**, *282*, 793.
- [61] Albery, W. J.; Foulds, A. W.; Hall, K. J.; Hillman, A. R. *J. Electrochem. Soc.* **1980**, *127*, 654.
- [62] Albery, W. J.; Bowen, W. R.; Fisher, F. S.; Foulds, A. W.; Hall, K. J.; Hilhnan, A. R.; Egdell, R. G.; Orchard, A. F. *J. Electroanal. Chem.* **1980**, *107*, 37.

- [63] Albery, W. J. *Phil. Trans. R. Soc. Ser. A* **1981**, 302, 221.
- [64] Albery, W. J.; Boutelle, M. G.; Colby, P. J.; Hillman, A. R. *J. Electroanal. Chem.* **1982**, 133, 135.
- [65] Albery, W. J.; Bartlett, P. N.; Davies, J. P.; Foulds, A. W.; Hillman, A. R.; Bachiller, S. F. *Faraday Disc. Chem. Soc.* **1981**, 70, 341.
- [66] Archer, M. D.; Ferreira, M. I. C.; Albery, W. J.; Hillman, A. R. *J. Electroanal. Chem.* **1980**, 111, 295.
- [67] Bowen, W. R. *Acta Chem. Scand. A* **1980**, 34, 437.
- [68] Haas, O.; Zumbrennen, H. R. *Helv. Chim. Acta* **1981**, 64, 854.
- [69] Torstensson, A.; Gorton, L. *J. Electroanal. Chem.* **1981**, 130, 199.
- [70] Biesaga, M.; Pyrzyńska, K.; Trojanowicz, M. *Talanta* **2000**, 51, 209.
- [71] Wang, J.; Golden, T. *Anal. Chim. Acta* **1989**, 217, 343.
- [72] Huang, S. S.; Tang, H.; Li, B. F. *Microchim. Acta* **1998**, 128, 37.
- [73] Ren, J.; Zhang, H.; Ren, Q.; Xia, C.; Wan, J.; Qin, Z. *J. Electroanal. Chem.* **2001**, 504, 59.
- [74] Gong, F. C.; Zhang, X. B.; Guo, C. C.; Shen, G. L.; Yu, R. Q. *Sensors* **2003**, 3, 91.
- [75] Jeong, H.; Kim, H.; Jeon, S. *Microchem. Journal* **2004**, 78, 181.
- [76] Wang, Y.; Kang, J.; Wu, H.; Xue, Z.; Lu, X. *Anal. Lett.* **2005**, 37, 575.
- [77] Ozoemena, K. I.; Zhao, Z.; Nyokong, T. *Electrochem. Commun.* **2005**, 7, 679.
- [78] Yang, D. W.; Gong, F. C.; Cao, Z. *Sensor Actuat. B-Chem.* **2006**, 114, 152.
- [79] Li, C. X.; Zeng, Y. L.; Liu, Y. J.; Tang, C. R. *Anal. Sci.* **2006**, 22, 393.
- [80] Gong, F. C.; Xiao, Z. D.; Cao, Z.; Wu, D. X. *Talanta* **2007**, 72, 1453.

- [81] Batista, I. V.; Lanza, M. R. V.; Dias, I. L. T.; Tanaka, S. M. C. N.; Tanaka, A. A.; Sotomayor, M. D. P. T. *Analyst* **2008**, *133*, 1692.
- [82] Kurzatowska, K.; Shpakovsky, D.; Radecki, J.; Radecka, H.; Jingwei, Z.; Milaeva, E. *Talanta* **2009**, *78*, 126.
- [83] Joseph, R.; Girish Kumar, K. *Anal. Lett.* **2009**, *42*, 2309.
- [84] Joseph, R.; Girish Kumar, K. *Drug Test. Analysis* **2010**, *2*, 278.
- [85] Kang, J.; Wang, Y.; Lu, X. *J. Solid State Electrochem.* **2003**, *7*, 694.
- [86] Xue, Z.; Yang, J.; Zhi, F.; Wang, W.; Liu, X.; Lu, X. *Anal. Lett.* **2009**, *42*, 668.
- [87] Fang, C.; Tang, X.; Zhou, X. *Anal. Sci.* **1999**, *15*, 41.
- [88] Chen, W.; Lin, X.; Huang, L.; Luo, H. *Microchim. Acta* **2005**, *151*, 101.
- [89] Ming, S. D.; Fang, L. Y. *Analytical Laboratory* **2005**, *13*, 302.
- [90] Wan, Q.; Wang, X.; Wang, X.; Yang, N. *Polymer* **2006**, *47*, 7684.
- [91] Yang, N.; Wang, X. *Electrochim. Acta* **2007**, *52*, 6962.
- [92] Wang, C.; Wang, F.; Li, C.; Xu, X.; Li, T.; Wang, C. *Dyes & Pigments* **2007**, *75*, 213.
- [93] Huang, K. J.; Xu, C. X.; Xie, W. Z. *Bull. Korean Chem. Soc.* **2008**, *29*, 988.
- [94] Huo, H. Y.; Luo, H. Q.; Li, N. B. *Microchim. Acta* **2009**, *167*, 195.
- [95] Huang, K. J.; Xu, C.X.; Sun, J. Y.; Xie, W. X.; Peng, L. *Anal. Lett.* **2010**, *43*, 176.
- [96] Ensafi, A. A.; Taei, M.; Khayamian, T. *Colloids and Surfaces B: Biointerfaces* **2010**, *79*, 480.
- [97] Kul, D.; Brett, C. M. A. *International Journal of Electrochemistry* **2011**, *2011*, 406.

- [98] Na, W.; Ruo, Y.; Ya-qin, C.; Ling-yan, Z.; Ying, Z.; Ying, Z.; Xue-lian, L.; Qiang, Z. *Analytical Laboratory* **2005**, *12*, 226.
- [99] Li, X.; Niu, Q.; Li, G.; Zhan, T.; Sun, W. *J. Braz. Chem. Soc.* **2011**, *22*, 422.
- [100] Xu, C. X.; Huang, K. J.; Fan, Y.; Wu, Z. W.; Li, J. *Journal of Molecular Liquids* **2012**, *16*, 532.
- [101] Yao, H.; Sun, Y.; Lin, X.; Tang, Y.; Huang, L. *Electrochim. Acta* **2007**, *52*, 6165.
- [102] Chandra, U.; Kumara Swamy, B. E.; Gilbert, O.; Sherigara, B. S. *Int. J. Electrochem. Sci.* **2010**, *5*, 1475.
- [103] Chandra, U.; Kumara Swamy, B. E.; Gilbert, O.; Reddy, S.; Sherigara, B. S. *American Journal of Analytical Chemistry* **2011**, *2*, 262.
- [104] Yao, H.; Sun, Y.; Lin, X.; Tang, Y.; Liu, A.; Li, G.; Li, W.; Zhang, S. *Anal. Sci.* **2007**, *23*, 677.
- [105] Girish Kumar, K.; Jayashree, R. *J. Pharm. Biomed. Anal.* **1993**, *11*, 165.
- [106] Girish Kumar, K.; Karpagaselvi, L. *Analyst* **1994**, *119*, 1375.
- [107] Girish Kumar, K.; Letha, R. *J. Pharm. Biomed. Anal.* **1997**, *15*, 1725.
- [108] Rao, G. D.; Girish Kumar, K.; Chowdary, K. P. R. *J. Indian Council of Chemists* **2000**, *17*, 32.
- [109] Rao, G. D.; Girish Kumar, K.; Chowdary, K. P. R. *Indian J. Pharm. Sci.* **2001**, *63*, 161.
- [110] Girish Kumar, K.; John, S.; Poduval, R.; Augustine, P. *The Chinese Pharm. Jour.* **2005**, *57*, 29.
- [111] Girish Kumar, K.; Augustine, P.; Poduval, R.; John, S. *Pharmazie* **2006**, *61*, 291.
- [112] Girish Kumar, K.; Augustine, P.; John, S. *Port. Electrochim. Acta* **2007**, *25*, 375.

- [113] Girish Kumar, K.; John, S.; Augustine, P.; Poduval, R.; Saraswathyamma, B. *Anal. Sci.* **2007**, *23*, 291.
- [114] Girish Kumar, K.; Augustine, P.; John, S.; Radecki, J.; Radecka, H. *Anal. Lett.* **2008**, *41*, 1144..
- [115] Saraswathyamma, B.; Pajak, M.; Radecki, J.; Maes, W.; Dehaen, W.; Girish Kumar, K.; Radecka, H. *Electroanalysis* **2008**, *20*, 2009.
- [116] Saraswathyamma, B.; Grzybowska, I.; Cz. Orlewska; Radecki, J.; Dehaen, W.; Girish Kumar, K.; Radecka, H. *Electroanalysis* **2008**, *20*, 2317.
- [117] Issac, S.; Girish Kumar, K. *Anal. Methods* **2010**, *2*, 1484.
- [118] Joseph, R.; Girish Kumar, K. *Anal. Sci.* **2011**, *27*, 67.
- [119] Lonappan, L.; Issac, S.; Joseph, R. Thomas, D.; Girish Kumar, K. *Micro & Nano Letters* **2011**, *6*, 867.
- [120] Lonappan, L.; Girish Kumar, K. *Sensor Lett.* **2011**, *9*, 541.
- [121] <http://www.home.fuse.net>
- [122] <http://www.egr.msu.edu>
- [123] <http://www.en.wikipedia.org/wiki/Trimethoprim>
- [124] El-Ansary, A. L.; Issa, Y. M.; Selim, W. *Anal. Lett.* **1999**, *32*, 955.
- [125] Polas ek, M.; Jambor, M. *Talanta* **2002**, *58*, 1253.
- [126] Brooks, M. A.; de Silva, J. A. F.; Arconte, L. M. D. *Anal. Chem.* **1973**, *45*, 263.
- [127] Carapuca, H. M.; Cabral, D. J.; Rocha, L. S. *J. Pharm. Biomed. Anal.* **2005**, *38*, 364.
- [128] Weinfeld, R. E.; Macaseib, T. C. *J. Chromatogr. B* **1979**, *164*, 73.
- [129] Adler, A. D.; Longo, F. R.; Finarelli, J. D.; Goldmacher, J.; Assour, J. *J. Org. Chem.* **1967**, *32*, 476.

- [130] Gaughan, R. R.; Shriver, D. F.; Boucher, L. J. *Proc. Nat. Acad. Sci. USA* **1975**, *72*, 433.
- [131] Laviron, E. *J. Electroanal. Chem.* **1974**, *52*, 355.
- [132] Goyal, R. N.; Kumar, A. *Electroanalysis* **1990**, *2*, 539.
- [133] *The United States Pharmacopoeia Rockville*: United States Pharmacopoeia Convention INC, 2005.
- [134] <http://www.en.wikipedia.org/wiki/Ambroxol>
- [135] Nobilis, M.; Pasters, J.; Svoboda, D.; Kvetina, J. *J. Chromatogr. Biomed. Appl.* **1992**, *581*, 251.
- [136] Koundourellis, J. E.; Malliou, E. T.; Broussali, T. A. *J. Pharm. Biomed. Anal.* **2000**, *23*, 469.
- [137] Indrayanto, G.; Handayani, R. *J. Pharm. Biomed. Anal.* **1993**, *11*, 781.
- [138] Dincer, Z.; Basan, H.; Goger, N. G. *J. Pharm. Biomed. Anal.* **2003**, *31*, 867.
- [139] Perez-Ruiz, T.; Martinez-Lozano, C.; Sanz, A.; Miguel, M. T. S. *Talanta* **1996**, *43*, 1029.
- [140] Pospisilova, M.; Polasek, M.; Jokl, V. *J. Pharm. Biomed. Anal.* **2001**, *24*, 421.
- [141] Satinsky, D.; Santos, L. M. L. D.; Sklenarova, H.; Solich, P.; Montenegro, M. C. B. S. M.; Araujo, A. N. *Talanta* **2005**, *68*, 214.
- [142] Perez-Ruiz, T.; Martinez-Lozano, C.; Sanz, A.; Bravo, E. *J. Chromatogr. B* **2000**, *742*, 205.
- [143] Kim, H.; Yoo, J. Y.; Han, S. B.; Lee, H. J.; Lee, K. R. *J. Pharm. Biomed. Anal.* **2003**, *32*, 209.
- [144] Schmid, J. *J. Chromatogr. Biomed. Appl.* **1987**, *414*, 65.
- [145] Bazylak, G.; Nagels, L. J. *J. Pharm. Biomed. Anal.* **2003**, *32*, 887.

- [146] Demircigil, B. T.; Uslu, B.; Ozkan, Y.; Ozkan, S. A.; Senturk, Z. *Electroanalysis* **2003**, *15*, 230.
- [147] Habib, I. H. I.; Zayed, S. I. M. *Die Pharmazie* **2005**, *60*, 193.
- [148] İssac, S. *Fabrication of electrochemical sensors for various pharmaceuticals* (Ph.D thesis), 2011.
- [149] Felix, F. S.; Brett, C. M. A.; Angnes, L. *Talanta* **2008**, *76*, 128.
- [150] Mc Grath, G. J.; Kane, E. O.; Smyth, W. F.; Tagliaro, F. *Anal. Chim. Acta* **1996**, *322*, 159.
- [151] Moane, S.; Rodriguez, J. R. B.; Ordieres, A. J. M.; Blanco, P. T.; Smyth, M. R. *J. Pharm. Biomed. Anal.* **1995**, *14*, 57.
- [152] *European Pharmacopoeia*, Directorate for the quality of medicines of the Council of Europe, France, 2003.
- [153] <http://www.en.wikipedia.org/wiki/Sulfamethoxazole>
- [154] Girish Kumar, K.; Indrasenan, P. *Analyst* **1988**, *113*, 1369.
- [155] Pereira, V.; Cass, Q. B. *J. Chromatogr. B* **2005**, *826*, 139.
- [156] Vrcea, T. B.; van der Ven, A. J. A. M.; Verwey-van Wissena, C. P. W. G. M.; van Ewijk-Beneken Kolmer, E. W. J.; Swolfs, A. E. M.; van Galen, P. M.; Amadajais-Groenen, H. *J. Chromatogr. B* **1994**, *658*, 327.
- [157] Amini, H.; Ahmadiani, A. *J. Pharm. Biomed. Anal.* **2007**, *43*, 1146.
- [158] Kulikov, U.; Verushkin, A. G.; Loginova, L. P. *Chromatographia* **2005**, *61*, 455.
- [159] Hassouna, M. E. M. *Anal. Lett.* **1997**, *30*, 2341.
- [160] Nagaraja, P.; Naik, S. D.; Shreshta, A. K.; Shivakumar, A. *Acta Pharm.* **2007**, *57*, 333.
- [161] De Cordova, M. L. F.; Barrales, P. O.; Torne, G. R.; Diaz, A. M. *J. Pharm. Biomed. Anal.* **2003**, *31*, 669.

- [162] Fan, J.; Chen, Y.; Feng, S.; Ye, C.; Wang, J. *Anal. Sci.* **2003**, *19*, 419.
- [163] Erroz, C. L.; Vistas, P.; Cordoba, M. H. *Talanta* **1994**, *41*, 2159.
- [164] Teshima, D.; Otsubo, K.; Makino, K.; Itoh, Y.; Oishi, R. *Biomed. Chromatogr.* **2004**, *18*, 51.
- [165] You, T.; Yang, X.; Wang, E. *Analyst* **1998**, *123*, 2357.
- [166] Zhang, Z. L.; Zhou, J. L. *J. Chromatogr. A* **2007**, *1154*, 205.
- [167] Andrade, L. S.; Rocha-Filho, R. C.; Cass, Q. B.; Fatibello-Filho, O. *Electroanalysis* **2009**, *21*, 1475.
- [168] Souza, C. D.; Braga, O. C.; Vieira, I. C.; Spinelli, A. *Sensor Actuat. B-Chem.* **2008**, *135*, 66.
- [169] Msagati, T. A. M.; Ngila, J. C. *Talanta* **2002**, *58*, 605.
- [170] Sun, Y. Q.; You, W.; Gao, Z. N. *Yao Xue Xue Bao* **2008**, *43*, 396.
- [171] Ozkorucuklu, S. P.; Sahin, Y.; Alsancak, G. *Sensors* **2008**, *8*, 8463.
- [172] Aravand, M.; Ansari, R.; Heydari, L. *Mater. Sci. Eng. C* **2011**, *31*, 1819.
- [173] Kotoucek, M.; Skopalova, J.; Michalkova, D. *Anal. Chim. Acta* **1997**, *353*, 61.
- [174] Rao, T. N.; Sarada, B. V.; Tryk, D. A.; Fujishima, A. *J. Electroanal. Chem.* **2000**, *491*, 175.
- [175] Astrid, M. V.; Maria, E.; Carrera, B.; Von Baer, D.; Carlos, B. F.; Malcolm, R. S. *Anal. Chim. Acta* **1984**, *159*, 119.
- [176] <http://en.wikipedia.org/wiki/Domperidone>
- [177] Shindler, J. S.; Finnerty, G. T.; Towlson, K.; Dolan, A. L.; Davies, C. L.; Parkes, J. D. *British Journal of Clinical Pharmacology* **1984**, *18*, 959.
- [178] Rossi, S. *Australian Medicines Handbook*; Adelaide, 2006.
- [179] Silvers, D.; Kipnes, M.; Broadstone, V. *Clinical therapeutics* **1998**, *20*, 438.

- [180] Rajendraprasad, Y.; Rajasekhar, K. K.; Shankarananth, V.; Yaminikrishna, H. V.; Saikumar, S.; Venkataraghavreddy, P. *Journal of Pharmacy Research* **2009**, *2*, 1593.
- [181] Al-Khamis, K. I.; Hagga, M. E. M.; Al-Khamis, H. A.; Al-Awadi, M. *Anal. Lett.* **1990**, *23*, 451.
- [182] Amin, A. S.; Ragab, G. H. *Anal. Sci.* **2003**, *19*, 747.
- [183] Sherje, A. P.; Kasture, A. V.; Gujar, K. N.; Yeole, P. G. *Indian J. Pharm. Sci.* **2008**, *70*, 102.
- [184] Salem, M. Y.; El-Bardicy, M. G.; El-Tarras, M. F.; El-Zanfally, E. S. *J. Pharm. Biomed. Anal.* **2002**, *30*, 21.
- [185] Prabu, S. L.; Shirwaikar, A.; Dinesh Kumar, C.; Joseph, A.; Kumar, R. *Indian J. Pharm. Sci.* **2008**, *70*, 128.
- [186] Baeyens, W.; Moerloose, P. D. *Anal. Chim. Acta* **1979**, *110*, 261.
- [187] Walash, M. I.; Belal, F.; El-Enany, N.; Abdelal, A. A. *J. Fluoresc.* **2008**, *18*, 61.
- [188] Shu, W. M.; Ling, G.; Hui, C. X.; Guang, G. W. *Acta Pharmacol Sin* **2002**, *3*, 285.
- [189] Smit, M. J.; Sutherland, F. C. W.; Hundt, H. K. L.; Swart, K. J.; Hundt, A. F.; Els, J. *J. Chromatogr. A* **2002**, *949*, 65.
- [190] Li, Z.; Yao, J.; Zhang, Z.; Zhang, L. *Journal of Chromatographic Science* **2008**, *47*, 883.
- [191] Kobylinska, M.; Kobylinska, K. *J. Chromatogr. B* **2000**, *744*, 207.
- [192] Zavitsanos, A. P.; MacDonald, C.; Bassoo, E.; Gopaul, D. *J. Chromatogr. B* **1999**, *730*, 9.
- [193] Ali, M. S.; Ghori, M.; Khatri, A. R. *J. Pharm. Biomed. Anal.* **2006**, *41*, 358.
- [194] Sivakumar, T.; Manavalan, R.; Muralidharan, C.; Valliappan, K. *J. Pharm. Biomed. Anal.* **2007**, *43*, 1842.

- [195] Patel, B. H.; Patel, M. M.; Patel, J. R.; Suhagia, B. N. *Journal of Liquid Chromatography & Related Technologies* **2007**, *30*, 439.
- [196] Ali, I.; Gupta, V. K.; Singh, P.; Pant, H. V. *Talanta* **2006**, *68*, 928.
- [197] Sivasubramanian, L.; Anilkumar, V. *Indian J. Pharm. Sci.* **2007**, *69*, 674.
- [198] Yamamoto, K.; Hagino, M.; Kotaki, H.; Iga, T. *J. Chromatogr. B* **1998**, *720*, 251.
- [199] Michaud, V.; Simard, C.; Turgeon, J. *J. of Chromatogr. B* **2007**, *852*, 611.
- [200] Sivakumar, T.; Manavalan, R.; Valliappan, K. *Acta Chromatographica* **2007**, *18*, 130.
- [201] Patel, B.; Dedania, Z.; Dedania, R.; Ramolia, C.; Vidya Sagar, G.; Mehta, R. S. *Asian J. Research Chem.* **2009**, *2*, 210.
- [202] Sabnis; Sadanand, S.; Dhavale, D. N.; Jadhav, Y. V.; Gandhi, V. S. *Journal of AOAC* **2008**, *91*, 344.
- [203] Jain, D.; Kachave, R. N.; Bhadane, R. N. *Journal of Liquid Chromatography and Related Technologies* **2010**, *33*, 786.
- [204] Girish Kumar, K.; Augustine, P.; John, S. *J. Appl. Electrochem.* **2010**, *40*, 65.
- [205] El-Shahawi, M. S.; Bahaffi, S. O.; El-Mogy, T. *Anal. Bioanal. Chem.* **2007**, *387*, 719.
- [206] Wahdan, T.; El- Ghany, N.A. *Il Farmaco* **2005**, *60*, 830.
- [207] [http://en.wikipedia.org/wiki/Methyl\\_red](http://en.wikipedia.org/wiki/Methyl_red)
- [208] <http://en.wikipedia.org/wiki/Tinidazole>
- [209] [www.nlm.nih.gov/medlineplus/druginfo/meds](http://www.nlm.nih.gov/medlineplus/druginfo/meds)
- [210] Adegoke, O. A.; Umoh, O. E.; Soyinka, J. O. *J. Iran. Chem. Soc.* **2010**, *7*, 359.
- [211] Lopez-Martinez, L.; Luna-Vazquez, F. J.; Lopez-de-Alba, P. L. *Anal. Chim. Acta* **1997**, *340*, 241.

- [212] Nagaraja, P.; Sunitha, K. R.; Vasantha, R. A.; Yathirajan, H. S. *J. Pharm. Biomed. Anal.* **2002**, *28*, 527.
- [213] Dinesh. N. D.; Nagaraja, P.; Rangappa, K. S. *Turk. J. Chem.* **2004**, *28*, 335.
- [214] Adegoke. O. A.; Umoh, O. E. *Acta Pharm.* **2009**, *59*, 407.
- [215] Prasad, C. V. N.; Sripriya, V.; Saha, R. N.; Parimoo, P. *J. Pharm. Biomed. Anal.* **1999**, *21*, 961.
- [216] Rajnarayana, K.; Chaluvadi, M. R.; Alapati, V. R.; Mada, S. R.; Jayasagar, G.; Krishna, D. R. *Pharmazie* **2002**, *57*, 535.
- [217] Ouyang, L. Q.; Wu, H. L.; Liu, Y. J.; Wang, J. Y.; Yu, Y. J.; Zou, H. Y.; Yu, R. Q. *Chin. Chem. Lett.* **2010**, *21*, 1223.
- [218] Venkateshwaran, T. G.; Stewart, J. T. *J. Chromatogr. B* **1995**, *672*, 300.
- [219] Sebaiy, M. M.; El-Shanawany, A. A.; El-Adl, S. M.; Abdel-Aziz, L. M.; Hashem, H. A. *Asian J. Pharm. Ana.* **2011**, *1*, 79.
- [220] Dharuman, J.; Vasudevan, M.; Somasekaran, K. N.; Dhandapania, B.; Ghodea, P. D.; Thiagarajan, M. *International Journal of PharmTech Research* **2009**, *1*, 121.
- [221] Alnajjar, A.; AbuSeada, H. H.; Idris, A. M. *Talanta* **2007**, *72*, 842.
- [222] Zhang. I.; Zhang. Z.; Wu, K. *J. Pharm. Biomed. Anal.* **2006**, *41*, 1453.
- [223] Habel, D.; Guermouche, S.; Guermouche, M. H. *Biomed. Chromatography* **1997**, *11*, 16.
- [224] Gui, Y.; Ni, Y. N.; Kokot, S. *Chin. Chem. Lett.* **2011**, *22*, 591.
- [225] Salvi, V. S.; Sathe, P. A.; Rege, P. V. *Journal of Analytical and Bioanalytical Techniques* **2010**, *1*, 110.
- [226] Jain, R.; Rather, J. A. *Colloids and Surfaces A: Physicochem. Eng. Aspects* **2011**, *378*, 27.
- [227] Shahrokhian, S.; Rastgar, S. *Electrochim. Acta* **2012**, *78*, 422.

- [228] Zuhri, A. Z. A.; Al-Khalil, S.; Shubietah, R. M.; El-Hroub, I. *J. Pharm. Biomed. Anal.* **1999**, *21*, 881.
- [229] Wang, C.; Wang, F.; Li, C.; Xu, X.; Li, T.; Wang, C. *J. Pharm. Biomed. Anal.* **2006**, *41*, 1396.
- [230] Yang, C. *Anal. Sci.* **2004**, *20*, 821.
- [231] Lin, L.; Chen, J.; Lin, Q.; Chen, W.; Chen, J.; Yao, H.; Liu, A.; Lin, X.; Chen, Y. *Talanta* **2010**, *80*, 2113.
- [232] Geng, M.; Xu, J.; Hu, S. *Reactive & Functional Polymers* **2008**, *68*, 1253.
- [233] Gilbert, O.; Kumara Swamy, B. E.; Chandra, U.; Sherigara, B. S. *Int. J. Electrochem. Sci.* **2009**, *4*, 582.
- [234] Chandra, U.; Kumara Swamy, B. E.; Gilbert, O.; Sherigara, B. S. *Int. J. Electrochem. Sci.* **2010**, *5*, 1475.
- [235] Chandra, U.; Kumara Swamy, B. E.; Gilbert, O.; Reddy, S.; Sherigara, B. S. *American Journal of Analytical Chemistry* **2011**, *2*, 262.
- [236] Yao, H.; Sun, Y.; Lin, X.; Tang, Y.; Huang, L. *Electrochim. Acta* **2007**, *52*, 6165.
- [237] Liu, X.; Luo, L.; Ding, Y.; Kang, Z.; Ye, D. *Bioelectrochem.* **2012**, *86*, 38.
- [238] Yao, H.; Sun, Y.; Lin, X.; Tang, Y.; Liu, A.; Li, G.; Li, W.; Zhang, S. *Anal. Sci.* **2007**, *23*, 677.
- [239] Liu, X.; Luo, L.; Ding, Y.; Kang, Z.; Ye, D. *Bioelectrochem.* **2012**, *86*, 38.
- [240] Fonseca, J. M. L.; Rivera, M. C. G.; Monteagudo, J. C. G.; Uriarti, E. *J. Electroanal. Chem.* **1993**, *347*, 277.
- [241] Levine, I.R. *Quantum Chemistry*; 4<sup>th</sup> Edition, Prentice Hall, 2002.
- [242] McQuarrie, D. A. *Quantum Chemistry*; Viva Books Private Limited, 2005.
- [243] Cramer, C. J. *Essentials of Computational Chemistry*; John Wiley & Sons, 2002.

- [244] Leach, A. R. *Molecular modelling-Principles and applications*; 2<sup>nd</sup> Edition, Prentice Hall, 2001.
- [245] Lowe, J. P.; Peterson, K.A. *Quantum Chemistry*; 3<sup>rd</sup> Edition, Elsevier, 2009.
- [246] Becke, A. D. *J. Chem. Phys.* **1993**, *98*, 1372.
- [247] Kim, K.; Jordan, K. D. *J. Phys. Chem.* **1994**, *98*, 10089.
- [248] Stephens, P. J.; Devlin, F. J.; Chabalowski C. F.; Frisch, M. J. *J. Phys. Chem.* **1994**, *98*, 11623.
- [249] Becke, A. D. *Phys. Rev. A* **1988**, *38*, 3098.
- [250] Lee, C.; Yang, W.; Parr, R. G. *Phys. Rev. B* **1988**, *37*, 785.
- [251] Vosko, S. H.; Wilk, L.; Nusair, M. *Can. J. Phys.* **1980**, *58*, 1200.
- [252] Kim, K.; Jordan, K. D. *J. Phys. Chem.* **1994**, *98*, 10089.
- [253] Zotti, L. A.; Teobaldi, G.; Hofer, W. A.; Auwarter, W.; Weber- Bargioni, A.; Barth, J. V. *Surf. Sci.* **2007**, *601*, 2409.
- [254] Shubina, T. E.; Marbach, H.; Flechtner, K.; Kretschmann, A.; Jux, N.; Buchner, F.; Steinrck, H.-P.; Clark, T.; Gottfried, J. M. *J. Am.Chem. Soc.* **2007**, *129*, 9476.
- [255] Karr, P. A.; Zandler, M. E.; Beck, M.; Jaeger, J. D.; Mc Carty, A. L.; Smith, P. M.; D'Souza, F. *J. Mol. Struct. (THEOCHEM)* **2006**, *765*, 91.
- [256] Xu, T.; He, H.; Wang, Q.; Dubey, M.; Galipeau, D.; Ropp, M. *Proceeding of 33<sup>rd</sup> IEEE Photovoltaic Specialist Conference*, San Diego, May 11-16, **2008**.
- [257] Mathew, S.; Iijima, H.; Toude, Y.; Umeyama, T.; Matano, Y.; Ito, S.; Tkachenko, N. V.; Lemmetyinen, H.; Imahori, H. *J. Phys. Chem. C* **2011**, *115*, 14415.
- [258] Bader, R. F. W. *Atoms in Molecules-A Quantum Theory*; Oxford Science: Oxford, 1990.

- [259] Bader, R. F. W. *Chem. Rev.* **1991**, *91*, 893.
- [260] Carroll, M. T.; Chang, C.; Bader, R. F. W. *Mol. Phys.* **1988**, *63*, 387.
- [261] Carroll, M. T.; Bader, R. F. W. *Mol. Phys.* **1988**, *65*, 695.
- [262] Bone, R. G. A.; Bader, R. F. W. *J. Phys. Chem.* **1996**, *100*, 10892.
- [263] Alkorta, I.; Rozas, I.; Elguero, J. *Theor. Chem. Acc.* **1998**, *99*, 116.
- [264] Calhorda, M. J.; Lopes, P. E. M. *J. Organomet. Chem.* **2000**, *609*, 53.
- [265] Weinhold, F.; Landis, C. R. *Chem. Educ. Res. Pract. Eur.* **2001**, *2*, 91.
- [266] Frisch, M. J. et al. *Gaussian 03*; Gaussian, Inc.: Wallingford, CT, **2003**.
- [267] Becke, A. D. *J. Chem. Phys.* **1993**, *98*, 5648.
- [268] Hehre, W. J.; Radom, L.; Schleyer, P. V. R.; Pople, J. A. *Ab Initio Molecular Orbital Theory*; Wiley: New York, **1998**.
- [269] Jissy, A. K.; Datta, A. *J. Phys. Chem. B* **2010**, *114*, 15311.
- [270] Stevens, W. J.; Krauss, M.; Basch, H.; Jasien, P. G. *Can. J. Chem.* **1992**, *70*, 612.
- [271] Stevens, W.; Basch, H.; Krauss, J. *J. Chem. Phys.* **1984**, *81*, 6026.
- [272] Hay, P. J.; Wadt, W. R. *J. Chem. Phys.* **1985**, *82*, 299.
- [273] Jissy, A. K.; Ashik, U. P. M.; Datta, A. *J. Phys. Chem. C* **2011**, *115*, 12530.
- [274] Mendkovich, A. S.; Syroeshkin, M. A.; Mikhalchenko, L. V.; Mikhailov, M. N.; Rusakov, A. I.; Gul'tyai, V. P.; Wadhawan, J. D. *Int. J. Electrochem.* **2011**, *34*, 6043.
- [275] Kovacic, P.; Somanathan, R. *Med. Chem. Commun.* **2011**, *2*, 106.
- [276] Wheeler, J. F.; Lunte, C.; Zimmer, H.; Heinamani, W. R. *J. Pharm. Biomed. Anal.* **1999**, *8*, 143.

..........

## ***List of Publications***

### **Research papers published in International Journals**

---

- [1] Leena Rajith, Krishnapillai Girish Kumar, Electroanalysis of trimethoprim on metalloporphyrin incorporated glassy carbon electrode, *Drug Testing and Analysis* **2010**, 2, 436.
- [2] Leena Rajith, Jissy, A.K. Krishnapillai Girish Kumar, Ayan Datta, Mechanistic study of the facile oxidation of trimethoprim on a manganese porphyrin incorporated glassy carbon electrode, *Journal of Physical Chemistry C* **2011**, 115, 21858.
- [3] Divya Thomas, Leena Rajith, Laina Lonappan, Sindhu Issac, Krishnapillai Girish Kumar, Sensitive determination of nitrite in food samples using voltammetry, *Food Analytical Methods* **2012**, 5, 752.
- [4] Theresa Jos, Sindhu Issac, Renjini Joseph, Leena Rajith, Krishnapillai Girish Kumar, Electrocatalysis and determination of pyridine-2-aldoxime methochloride using carbon nanotube-modified gold electrode, *Micro and Nano Letters* **2012**, 7, 854.
- [5] Anuja, E.V. Zafna Rasheed, Leena Rajith, Laina Lonappan, Krishnapillai Girish Kumar, MWCNT–modified gold electrode sensor for the determination of propyl gallate in vegetable oils, *Food Analytical Methods* **2012** (Published online)

**Papers presented in National/International Conferences**

---

- [1] Electrocatalytic oxidation of trimethoprim at [5,10,15,20-tetrakis(4-methoxyphenyl)porphyrinato]manganese(III)chloride modified glassy carbon electrode and its analytical applications (International Conference on Frontiers in Chemical Research, Mangalore University, Karnataka, India, December 2008).
- [2] Differential pulse voltammetric determination of trimethoprim using metalloporphyrin based glassy carbon electrode (National seminar on Emerging Trends in Pharmaceutical Analysis, Kommareddy Venkata Sadasivarao Siddhartha College of Pharmaceutical Sciences, Vijayawada, Andhra Pradesh, India, February 2009).
- [3] Determination of ambroxol on metalloporphyrin modified glassy carbon electrode using various voltammetric techniques (International Conference on Materials for the New Millenium, Cochin University of Science and Technology, Kochi, Kerala, India, January 2010).
- [4] Electrochemical behaviour of sulfamethoxazole on a poly(malachite green) based glassy carbon electrode (Fifteenth National Convention of Electrochemists, VIT University, Vellore, Tamilnadu, India, February 2010).

.....*SR*.....